

Copyright 2010 Snehal Patel

SPLICEOSOMAL SMALL NUCLEAR RIBONUCLEOPROTEIN PARTICLE  
TRAFFICKING AND MATURATION IN THE NUCLEAR COMPARTMENT

BY

SNEHAL B. PATEL

DISSERTATION

Submitted in partial fulfillment of the requirements  
for the degree of Doctor of Philosophy in Biochemistry  
in the Graduate College of the  
University of Illinois at Urbana-Champaign, 2010

Urbana, Illinois

Doctoral Committee:

Associate Professor Michel Bellini, Chair  
Professor Robert Gennis  
Assistant Professor Prasanth Kannanganattu  
Associate Professor Satish Nair  
Professor David Shapiro

## ABSTRACT

We show for the first time that upon injection into the cytoplasm of the oocyte, fluorescein-labeled spliceosomal snRNAs, in the context of functional snRNPs, are targeted to elongating pre-mRNAs. This finding presents us with a novel assay with which to dissect the mechanism by which snRNPs are targeted to nascent pre-mRNA transcripts. Two critical advantages offered by this system are immediately evident. First, it allows us to investigate the mechanisms employed to recruit snRNPs as it actually transpires within the realm of the cell nucleus. Second, it allows a genome-wide analysis of snRNP recruitment to nascent transcripts, and, hence, the conclusions drawn from these studies do not depend on the sequence of any particular promoter or pre-mRNA. Indeed, it is with this assay that we have stumbled upon a most unanticipated discovery: Contrary to the current paradigm, the co-transcriptional recruitment of splicing snRNPs to nascent transcripts is not contingent on their role in splicing *in vivo*. Based on these and other data, we have constructed a two-step recruitment-loading model wherein snRNPs are first recruited to pre-mRNA transcripts and only then loaded directly onto cis-acting sequences on nascent pre-mRNA.

While conducting studies on snRNP trafficking, a new discovery was made. We found that the lampbrush chromosomes could be visualized by light microscopy *in vivo*, and that these chromosomes have an architecture that is identical with those in formaldehyde treated nuclear spread preparations. Importantly, we now have the first system with which we can examine the dynamic interactions of macromolecules with specific RNA polymerase II transcriptional units in the live nucleus.

## ACKNOWLEDGEMENTS

Many have contributed to my progress in graduate school and to this work specifically. Whether in good times or in bad, I have had the extra-ordinary fortune of having extra-ordinary friends. I thank all of you. In Brent Beenders and Chris Austin, I found camaraderie and a sense of unity. You have experienced with me the struggles and pleasures of graduate school. To my loving mother, I am forever indebted. Without you, I am lost. Should I have dedication and determination in me, it surely comes from you, my father. Your wisdom guides me always. My stern sister, while in our youth, you were my fierce combatant, today, you have become my faithful confidant and the source of my inspiration. My illustrious advisor, Dr. Michel Bellini, I thank you last because there is so much say. The question came to my mind as to what my most memorable moments were in graduate school. While an accumulation of infinite moments seem to have passed by in just six years, I will always think back to our excursions to Espresso Royale, when we could sit face to face over your cappuccinos and my lattes and talk Science in the way that only scientists do. These were most memorable, and for these, I thank you. In you, I found someone who shares my passion for understanding Nature, the way that she works, and the way that she is built. In you, I found an advisor, a mentor, and a friend. For all of these things, for all of the opportunities you have provided, and for much, much more, you have my eternal gratitude and utmost respect.

To Vibhaben & Bhikhubhai

## TABLE OF CONTENTS

LIST OF FIGURES .....	vi
LIST OF TABLES.....	viii
LIST OF ABBREVIATIONS.....	ix
CHAPTER I: INTRODUCTION.....	1
History, Significance, and Goals .....	1
Notes and Clarifications.....	3
The Structure of Spliceosomal snRNPs.....	4
The Biogenesis of Spliceosomal snRNPs.....	6
The Functions of Spliceosomal snRNPs.....	23
The <i>Xenopus laevis</i> Oocyte.....	26
CHAPTER II: A NEW SYSTEM FOR EXAMINING CO-TRANSCRIPTIONAL SNRNP RECRUITMENT AND SPLICING.....	33
Introduction.....	33
Results.....	33
Discussion.....	37
CHAPTER III: SPLICING INDEPENDENT RECRUITMENT OF SPLICEOSOMAL SNRNPs TO NASCENT RNAPII TRANSCRIPTS.....	48
Introduction.....	48
Results.....	49
Discussion.....	53
CHAPTER IV: LIVE IMAGES OF RNA POLYMERASE II TRANSCRIPTIONAL UNITS.....	63
Introduction.....	63
Results.....	65
Discussion.....	68
CHAPTER V: EXPERIMENTAL PROCEDURES.....	78
CHAPTER VI: CONCLUSIONS AND FUTURE DIRECTIONS.....	99
Conclusions.....	99
Future Directions .....	103
REFERENCES .....	110
CURRICULUM VITAE.....	126

## LIST OF FIGURES

Figure 1: The Sm snRNP assembly and maturation pathway .....	29
Figure 2: The U6 snRNP assembly and maturation pathway.....	30
Figure 3: Phase contrast (PC) images show Cajal bodies (CB), Nucleoli (N), and Splicing Factor Compartments (SFCs). .....	31
Figure 4: Montage of nuclear spread.....	32
Figure 5: Newly assembled spliceosomal snRNPs associate rapidly with CBs and SFCs. ....	40
Figure 6: Association of newly made fluorescent spliceosomal snRNPs with active transcriptional units. ....	41
Figure 7: Newly assembled snRNPs associate with RNAPII but not RNAPIII nascent transcripts. ....	43
Figure 8: Depletion of the U2 snRNA inhibits U2B'' targeting to chromosomal loops. ....	44
Figure 9: Newly formed fluorescent U2 snRNP rescues the association of U2B'' with nascent transcripts and SFCs in U2-depleted oocytes. ....	45
Figure 10: Y14 is not recruited to nascent transcripts in the absence of the U2 snRNA. ....	46
Figure 11: Mutant U1 and U2 snRNAs that cannot engage splicing are still recruited to active transcriptional units. ....	58
Figure 12: The first stem loop of the U1 snRNA is necessary and sufficient for its association with SFCs and nascent RNP fibrils. ....	59
Figure 13: A non-functional U2 snRNP targets nascent RNP fibrils.....	60
Figure 14: Spliceosomal U1, U4, and U5 snRNPs target LBC.....	61
Figure 15: The oil-isolation procedure does not affect chromosome architecture. ....	71
Figure 16: Lampbrush chromosomes in oil-isolated nuclei .....	73

Figure 17: DIC images of individual RNAPII transcription units in oil-isolated nuclei.....	75
Figure 18: LBC structure in oil-isolated nuclei after actinomycin D treatment.....	76
Figure 19: Steady-state dynamics of chromosomal YFP-MCD1.....	77
Figure 20: U snRNA secondary structure and antisense oligonucleotides.....	98
Figure 21: The recruitment-loading model.....	106
Figure 22: Co-transcriptional assembly of an export competent mRNP.....	107
Figure 23: Deletion mutants of the U1 snRNA.....	108
Figure 24: Deletion mutants of the U2 snRNA.....	109



## LIST OF TABLES

Table 1: The composition of major mature spliceosomal snRNPs in <i>H. sapiens</i> .....	28
Table 2: Complementary DNA oligonucleotides for U snRNA depletion .....	97

## LIST OF ABBREVIATIONS

aDMA	<u>a</u> symmetric <u>d</u> imethyl <u>a</u> rginine
AdML RNA	<u>a</u> denovirus <u>m</u> ajor <u>l</u> ate <u>m</u> RNA
AMD	<u>a</u> ctin <u>o</u> mycin <u>D</u>
BLAST	<u>b</u> asic <u>l</u> ocal <u>a</u> lignment <u>s</u> earch <u>t</u> ool
BPS	<u>b</u> ran <u>ch</u> <u>p</u> oint <u>s</u> equence
CAB box	<u>C</u> ajal <u>b</u> ody <u>b</u> ox
CARM5	<u>c</u> oactivator- <u>a</u> ssociated <u>a</u> rginine <u>m</u> ethyltransferase <u>5</u>
CAS	<u>c</u> ellular <u>a</u> poptosis <u>s</u> usceptibility protein
CB	<u>C</u> ajal <u>b</u> ody
CBC	<u>c</u> ap <u>b</u> inding <u>c</u> omplex
CBP	<u>c</u> ap <u>b</u> inding protein
CK2	<u>c</u> asein <u>k</u> inase <u>2</u>
cNLS	<u>c</u> lassical <u>n</u> uclear <u>l</u> ocalization <u>s</u> equence
2', 3' cP <sub>i</sub>	<u>2</u> ', <u>3</u> ' cyclic phosphate
CPSF	<u>c</u> leavage and <u>p</u> olyadenylation <u>s</u> pecificity <u>f</u> actor
CRM1	<u>c</u> hromosome <u>r</u> egion <u>m</u> aintenance <u>1</u>
CTD	<u>c</u> arboxy- <u>t</u> erminal <u>d</u> omain of the RPB1 subunit of RNAP II
DSE	<u>d</u> istal <u>s</u> equence <u>e</u> lement
eIF4E	<u>e</u> karyotic translation <u>i</u> nitiation <u>f</u> actor <u>4E</u>
EJC	<u>e</u> xon <u>j</u> unction <u>c</u> omplex
FISH	<u>f</u> luorescence <u>i</u> n <u>s</u> itu hybridization

fluo	<u>fluorescein</u>
g.g.	<i><u>Gallus gallus</u></i>
hnRNP	<u>heterogeneous nuclear ribonucleoprotein</u>
h.s.	<i><u>Homo sapiens</u></i>
IGC	<u>interchromatin granule cluster</u>
IBB	<u>importin <math>\beta</math> binding domain</u>
Imp $\alpha$	<u>importin <math>\alpha</math></u>
Imp $\beta$	<u>importin <math>\beta</math></u>
ISG20	<u>interferon-stimulated gene product of 20kDa</u>
JBP1	<u>Janus kinase binding protein 1</u>
LBC	<u>lampbrush chromosome</u>
LSm	<u>Like Sm</u>
m	<u>methyl</u>
$\gamma$ -m-P <sub>3</sub>	<u><math>\gamma</math>-methyl triphosphate</u>
m <sub>1</sub> G	5' to 5'-linked N7- <u>methyl</u> guanosine
m <sub>3</sub> G	2, 2, 7-trimethy <u>guanosine</u>
mRNP	<u>messenger ribonucleoprotein</u>
N	<u>nucleolus</u>
NLS	<u>nuclear localization sequence</u>
NoLe	<u>nucleolar localization element</u>
NPC	<u>nuclear pore complex</u>
Nup	<u>nucleoporin</u>
PBP	<u>proximal sequence element binding protein</u>

PHAX	phosphorylated adapter for RNA export
pre-mRNA	precursor-messenger RNA
PRMT	protein arginine methyltransferase
Prp	pre-RNA processing
PSE	proximal sequence element
PTF	proximal sequence element binding transcription factor
Ran	Ras-like nuclear protein
RanBP	Ran binding protein
RanGAP	Ran GTPase activating protein
rDNA	ribosomal DNA
RG	arginine-glycine rich
RNP	ribonucleoprotein
RNAPI	RNA polymerase I
RNAPII	RNA polymerase II
RNAPIII	RNA polymerase III
rRNA	ribosomal RNA
scaRNA	small Cajal body-specific RNA
sDMA	symmetric dimethyl arginine
SFC	splicing factor compartments
SL1	stem loop I
SmIR	Sm import receptor
SMA	spinal muscular atrophy
SMN	survival of motor neurons

SNAPc	<u>s</u> mall <u>n</u> uclear RNA gene <u>a</u> ctivating <u>p</u> rotein <u>c</u> omplex
snoRNA	<u>s</u> mall <u>n</u> ucleolar <u>R</u> NA
SNP1	<u>s</u> nurportin-1
snRNA	<u>s</u> mall <u>n</u> uclear <u>R</u> NA
snRNP	<u>s</u> mall <u>n</u> uclear <u>r</u> ibonucleoprotein particle
SR	<u>s</u> erine- <u>a</u> rginine rich
3'-SS	<u>3</u> '- <u>s</u> plice <u>s</u> ite
5'-SS	<u>5</u> '- <u>s</u> plice <u>s</u> ite
SSR	<u>5</u> '- <u>s</u> plice <u>s</u> ite <u>r</u> ecognition sequence
SSm	<u>s</u> pecific spliceosomal <u>S</u> m proteins
TAF	<u>T</u> ATA box binding protein <u>a</u> ssociated <u>f</u> actor
TBP	<u>T</u> ATA box <u>b</u> inding <u>p</u> rotein
Tgs1	<u>t</u> rimethyl <u>g</u> uanosine <u>s</u> ynthase <u>1</u>
TMG	2, 2, 7- <u>t</u> rimethyl <u>g</u> uanosine
tRNA	<u>t</u> ransfer <u>R</u> NA
TU	<u>t</u> ranscriptional <u>u</u> nit
U snRNA	<u>U</u> ridine-rich <u>s</u> mall <u>n</u> uclear <u>R</u> NA
U6 TuTase	<u>U</u> 6 <u>t</u> erminal <u>u</u> ridyl <u>t</u> ransferase
WD	Tryptophan-aspartate
x.l.	<i><u>X</u>enopus <u>l</u>aevis</i>
Xpo1	<u>E</u> xportin <u>1</u>
x.t.	<i><u>X</u>enopus <u>t</u>ropicalis</i>
Ψ	Pseudouridine

# CHAPTER I

## INTRODUCTION

### **History, Significance, and Goals**

Prior to the 1970's, the nucleic acid sequence of eukaryotic genes was believed to be colinear with the amino acid sequence of their encoded proteins, an assumption extrapolated from extensive studies on prokaryotic gene structure. During that decade, however, studies on several genes by independent groups working on diverse eukaryotic systems and their viral pathogens unveiled the rather enigmatic presence of split-genes<sup>1</sup> or genes interrupted by non-coding segments [1]. The most compelling evidence for intervening sequences came, fortuitously, from R-loop mapping studies of polyribosome-associated adenovirus major late mRNA (AdML RNA) isolated from infected cells. When this mRNA hybridized to the template strand of its cognate gene, regions of RNA-DNA duplex were observed, as anticipated. Surprisingly, however, these duplex regions were interrupted by long loops of single stranded DNA. The realization that the duplex regions correspond to the expressed sequences or exons and that the looped regions correspond to the intervening sequences or introns soon followed [2-4]. It was for this work that Phillip A. Sharp shared the 1993 Nobel Prize for Physiology or Medicine with Richard M. Roberts for their discovery<sup>2</sup> of split-genes [3, 5]. Several mechanistic explanations were offered to explain the presence of introns in eukaryotic genes and their precursor messenger RNAs (pre-mRNAs) but their absence in mature, cytoplasmic mRNAs. Now, it is well established that RNA splicing, the process wherein introns are removed and

---

<sup>1</sup> This term is no longer *en vogue* as most protein-coding genes in higher eukaryotes bear these non-coding segments; in essence, the “split” nature of genes appears to be the norm. Rather, it is more common today to denote genes that do not contain these intervening segments as intronless genes.

<sup>2</sup> Importantly, however, several other groups contributed significantly to this discovery and whether these two gentlemen were the “first” to discover split-genes is debatable.

exons are ligated, is the process at work and is the critical event that ensures the production of a mature mRNA to direct the translation of the correct protein. It may be grandiose but nonetheless accurate to say that the discovery of split-genes and the phenomenon of RNA splicing revolutionized the molecular view of eukaryotic gene regulation and demanded a revision of the definition of the corpuscular unit of heredity, which we have come to call the Gene [1].

The last quarter century has been prolific in new and exciting findings in the world of pre-mRNA splicing and the magnificently intricate machine that catalyzes this reaction, the spliceosome. Although not the immediate topic of this work, a humble fraction of these is mentioned below to underscore the importance—in all sub-disciplines of biology and medicine—of understanding splicing and spliced genes. First, alternative splicing, wherein an intron can be retained as an exon (intron retention mode) or an exon can be removed as an intron (exon cassette mode), enhances a genome's coding capacity while augmenting proteome diversity and contributes to differential gene expression [6]. Second, introns are no longer discarded as being “junk” selfish genetic elements [7]. Indeed, many introns encode RNAs with important cellular functions, such as the small nucleolar (sno) and small Cajal body specific (sca) RNAs [8] and even functional mRNAs [9]. Furthermore, as discussed above, some introns serve a dual role as exons [8, 10]. Third, as exons often code for independently folding and functioning regions of a protein called domains, exon shuffling via chromosomal recombination or mobile genetic elements provides an evolutionary account for the presence of tandemly repeated, divergent domains in a given protein or the homology between certain domains in two, otherwise, heterologous proteins [11, 12]. Indeed, proteins with novel functions can evolve simply by combinatorial exchanges of already existing exon modules followed by divergence. A

testament to her great economy, Nature has generated a remarkably diverse proteome from only a handful of structural domains, reflecting an underlying unity to the extraordinary diversity of life. Finally, aberrant pre-mRNA splicing is the molecular basis for many hereditary diseases in humans [13, 14]. In spite of these and a myriad of other findings, much remains to be understood and many controversies remain: This work quite generally aims to understand the trafficking and maturation of essential splicing factors called small nuclear ribonucleoprotein particles (snRNPs) within the complex environment of the nuclear compartment.

### **Notes and Clarifications**

Important specifications regarding this work are in order. First, as in common practice, wherever the term “splicing” is used in this text, it will refer to RNA splicing, not protein splicing [15]. Second, splicing is in no way unique to protein-coding RNAs or the eukaryotic world. Indeed, the process is universal in that it has been observed in all three major classes of RNA and in all three domains of life [16]. This work, however, will focus exclusively on pre-mRNA splicing. Third, unlike most other post/co-transcriptional steps in regulating the expression of genes, such as ribosomal frame shifting or RNA editing, pre-mRNA splicing in advanced eukaryotes appears to be the rule rather than the exception [17]. As such, we turn our attention to the oocyte of a vertebrate species, the African clawed frog *Xenopus laevis*, which has allowed us to examine splicing *in vivo* on a genome-wide scale. Fourth, introns have been categorized according to their mode of removal. The most abundant class of introns in pre-mRNA, the so-called spliceosomal introns—which are unique to eukaryotes, will be the prime feature here. Fifth, a low abundance, evolutionarily divergent class of spliceosomal introns,



referred to as the U12-type or AT-AC<sup>3</sup> introns exists [17]. Although this type of intron and its machinery will come to bear in this work, we will largely focus on the abundant U2-type or AG-GU<sup>4</sup> introns. Finally, the author is well aware of the existence of trans-spliceosomal splicing, wherein exons from two independent RNA molecules are ligated [18]. However, only cis-spliceosomal splicing will be considered here.

### **The Structure of Spliceosomal snRNPs**

The removal of the most abundant class of introns requires the five major spliceosomal snRNPs (U1, U2, U4, U5, U6 snRNPs). Each snRNP consists of a modified uridylic acid-rich small nuclear RNA (U1, U2, U4, U5, U6 snRNAs) and a cortege of associated proteins (Table 1) [19-22]. The 2, 2, 7-trimethyl guanosine (m<sub>3</sub>G) capped U1, U2, U4, and U5 snRNAs (Sm snRNAs) contain an Sm site (RAU<sub>3-6</sub>GR, where R is a purine) flanked by stem-loops, which collectively constitute domain A [23]. Sm<sup>5</sup> proteins (B/B', D1, D2, D3, E, F, G) assemble into a heteroheptameric ring around the Sm site to form the core of the snRNP particle. Similarly, the  $\gamma$ -methyl triphosphate ( $\gamma$ -m-P<sub>3</sub>) capped U6 snRNA acquires a heteroheptameric ring of LSm proteins (Like Sm 2-8), with its terminal U<sub>4</sub>-2', 3' cyclic phosphate (2', 3' cP<sub>i</sub>) tail serving as the 7-fold axis [24-28]. Proteins of the L/Sm lineage share an ancient signature motif, the Sm fold. Indeed, orthologs are ubiquitous in all three domains of life and participate in a multiplicity of RNA processing events [29-32]. In addition to the core proteins, each snRNP is decorated with an ensemble of proteins unique to a given snRNP, the snRNP-specific proteins [22].

---

<sup>3</sup> The latter term stemmed from the initial observation in the first few introns discovered in this category that begin with AT and end in AC dinucleotides. A more comprehensive analysis of these introns demonstrated the AT-AC rule to be erroneous; hence, the nomenclature has largely lost its favor.

<sup>4</sup> Again, the latter nomenclature is outmoded as U2- and U12-type introns were both found to be flanked by AG and GU consensus dinucleotides.

<sup>5</sup> "Sm" is derived from Smith, a systemic lupus erythromatosis patient whose autoimmune serum detected methylRG epitopes in a subset of Sm proteins.

There are three variations in the Sm core structure worthy of mention here. First, SmB and SmB' proteins are produced from an alternatively spliced transcript in mammals, but the single yeast ortholog (Smb1) does not have splice variants [21, 33-35]. Second, mammalian SmN is a paternally expressed paralog (deleted in Prader-Willi Syndrome) of SmB/B' for which it substitutes in brain and heart tissue [36-38]. Finally, in the unicellular protist, *Trypanosoma brucei*, U2 and U4 snRNAs associate with Specific spliceosomal Sm proteins<sup>6</sup> (SSm) as well as a subset of canonical Sm proteins [38].

The mono-snRNPs just described do not represent their *in vivo* functional forms; rather, they are organized into higher order particles. The U4, U5, and U6 snRNPs exist largely in their functional form as a U4/U6.U5<sup>7</sup> tri-snRNP [39, 40]. The same holds true of the U4atac, U5<sup>8</sup>, and U6atac snRNPs, which form the minor spliceosomal U4atac/U6atac.U5 tri-snRNP [41]. Surprisingly, minor spliceosomal counterparts of the U1 and U2 snRNPs, the U11 and U12 snRNPs, respectively, are known to assemble into the minor spliceosomal U11/U12 di-snRNP [41-43]. Furthermore, penta-snRNP complexes, which consist of all five major splicing snRNPs and may represent a sort of splicing “holoenzyme”, have been shown to exist in both yeast and humans [44-46]. Although the physiological relevance of the penta-snRNP remains controversial, the fact that there is some degree of preassembly of the splicing machinery is well accepted [47, 48].

The snRNPs, along with over 300 other splicing factors, assemble onto pre-mRNA to form the spliceosome, and it is this dynamic macromolecular machine that orchestrates the

---

<sup>6</sup> Although the authors stated that this is the first of such snRNA-specific association of Sm proteins identified, this claim rightfully belongs to the SmN protein, which was shown to differ in its interactions with the U1 and U2 snRNAs in a concentration- and cell type-dependent fashion over a decade beforehand.

<sup>7</sup> The solidus represents strong interactions between the U4 and U6 snRNPs, including extensive hybridization between their respective snRNAs. The point represents weaker snRNP interactions between the U4 and U5 snRNPs.

<sup>8</sup> The U5 snRNP is a component of both spliceosomes. Otherwise, the machineries are incompatible for the splicing of their respective introns.

excision of introns and the ligation of exons through two successive trans-esterification reactions [17, 49]. Prior to participating in splicing, however, snRNPs must be assembled through a series of intricate steps that, in all organisms, begins in the nuclear compartment. In *animalia*, *protista*, and *plantae*, a brief transit to the cytoplasm is essential for the assembly of Sm snRNPs, but the assembly of the U6 snRNP is uninterrupted by a cytoplasmic phase [50, 51]. In contrast, the assembly of all snRNPs in *fungi* may very well proceed entirely within the nucleus [51]. In the discussion to follow, we describe the trafficking and maturation of spliceosomal snRNPs in vertebrates<sup>9</sup>, where this process is best understood, as well as the roles of three discrete nuclear organelles, Cajal bodies<sup>10</sup> (CBs) [22, 52-57], splicing factor compartments<sup>11</sup> (SFCs) [58-60], and nucleoli [61, 62], and the newly discovered cytoplasmic organelles, the U bodies [63]. Ultimately, we return to the cellular function of snRNPs in pre-mRNA splicing.

### **The Biogenesis of Spliceosomal snRNPs**

As mentioned, the assembly of Sm snRNPs and the U6 snRNP follow distinct pathways. A schematic of these pathways is provided (Figures 1 and 2). The assembly of all spliceosomal snRNPs begins with the transcription of a U snRNA. The genes for the U snRNAs reside in the nuclear genome and are transcribed by either RNA polymerase (RNAP) II or III [64-66].

Interestingly, while there has been significant divergence in the length and sequence of the

---

<sup>9</sup> Most work on snRNP biogenesis has been done in amphibian oocytes and transformed cell lines of humans and mice.

<sup>10</sup> The term Cajal body was adopted in 2003 to celebrate the centennial of its discovery, to honor its discoverer Santiago Ramon y Cajal, and to acknowledge the homology of these organelles in different organisms and different cell types. Previously, they were referred to as nucleolar accessory bodies (Purkinje cells), coiled bodies (HeLa cells), C snurposomes (amphibian oocytes), and binnenkorpor (insect oocytes).

<sup>11</sup> Unlike CBs, the naming of these organelles has not been unified despite their homology. As such, they are referred to as SC35 domains, splicing factor compartments (SFCs), speckles, interchromatin granule clusters (IGCs, electron microscopy), or B snurposomes (amphibian oocytes) in different systems and/or by different investigators. I have discarded the term B snurposomes (in spite of our amphibian model system) and adopted SFCs to reflect their molecular composition and putative function in storage of splicing factors.

coding portion of Sm snRNAs from primitive eukaryotes to eumetazoans, both have been well-conserved for the U6 snRNA [67]. During evolution, multiple copies (20-100) of U1, U2, U4, and U5 genes have arisen by gene duplication; however, the U6 gene is present only in ~5 functional copies in the haploid human genome [68-72]. Major clusters of the human U1 and U2 genes are present on chromosomes 1 and 17, respectively [69, 70], whereas the U6 genes are scattered throughout the genome [72]. The relative sparseness of U6 genes, along with the essential role the U6 snRNA is believed to play in catalysis and the numerous interactions that occur along most of its length with other snRNAs and their substrate pre-mRNA, explain the relatively high degree of conservation of its primary sequence [67]. While the Sm snRNA genes were free to diverge with little consequence to the fitness of the organism, most changes to the U6 snRNA sequence would have proved deleterious.

Notably, the studies that resulted in the above estimates of the number of the U snRNA genes were conducted either by Southern blot analysis or with basic local alignment search tool (BLAST) searches on incompletely sequenced genomes. Furthermore, BLAST hits that did not conform exactly to the most abundant form (the only one known at the time) of the U snRNA were discarded. Thus, genes that encode developmentally expressed or rare forms of the U snRNAs were not taken into account. Interestingly, my own preliminary BLAST results on the completed human genome suggest that we may have underestimated the number and chromosomal dispersion of U snRNA genes. Empirical approaches coupled with bioinformatics studies that use completed genomic databases and take into consideration transcription regulatory elements and polymorphic variations should provide new insights into the chromosomal organization and phylogeny of U snRNA genes and pseudogenes.

## Sm snRNP biogenesis

### *Synthesis of pre-snRNAs by RNAPII.*

The Sm snRNAs are transcribed as 3'-extended (2-10nt longer) precursors by RNAPII, and like all other RNAPII transcripts, they co-transcriptionally acquire a 5' to 5'-linked N7-methyl guanosine (m<sub>1</sub>G) cap [73, 74]. Although it has not been formally demonstrated, the nuclear cap binding complex (CBC) likely associates with m<sub>1</sub>G capped U snRNAs co-transcriptionally, as it does with m<sub>1</sub>G capped pre-mRNAs [75, 76]. Sm snRNA genes contain an snRNA-specific TATA-less core promoter, the proximal sequence element (PSE, -55nt), that drives basal levels of transcription [77]. The PSE helps define the +1 transcription start site [78] and recruits the snRNA-specific general transcription factor, PSE binding transcription factor<sup>12</sup> (PTF) [79]. High levels of transcription require an upstream enhancer region, the distal sequence element (DSE, -220nt), which consists of an OCT site and one or more closely positioned SPH sites, which recruit the POU domain-containing Oct-1 [77, 80] and Zn finger-containing Sp1/Staf [81, 82] transcriptional activators, respectively. Since different U snRNA variants are present in different tissues and during development, clearly other regulatory elements, yet to be identified, are responsible for their expression [83-85].

The 3'-ends of the pre-snRNAs are generated by an RNA processing event obligately coupled to PSE directed transcription, rather than by a transcriptional termination event [86-88]. A conserved 3'-box (GTTTN<sub>0-3</sub>AAAPuNNAGA, N = any nucleotide, Pu = purine) marks the cleavage site which resides ~10nt upstream [89-91], and a heterododecameric metallo β-lactamase complex (Integrator<sup>13</sup>) contains the enzymatic activity for 3' end formation [92]. The

---

<sup>12</sup> PTF is also called PSE binding protein (PBP) or small nuclear RNA gene activating protein complex (SNAPc). It consists of five subunits: SNAP190, SNAP50, SNAP45, SNAP43, and SNAP19.

<sup>13</sup> The name reflects its function in "integrating" the CTD of RPB1 with 3' end processing of Sm snRNAs. The subunits are named Int1-Int12. The catalytic subunit was identified to be Int11.

Integrator was identified as a component of RNAPII holoenzymes and was found to associate with the C-terminal domain (CTD) of its largest subunit, RPB1 [92]. Consistently, 3' end cleavage was inhibited when the phosphorylation status of the CTD was altered [93-95]. Interestingly, two subunits of the Integrator are paralogous to components of the cleavage and polyadenylation specificity factor (CPSF) complex [92]. Indeed, many similarities exist between 3' end formation in pre-snRNAs and pre-mRNAs. More recently, phosphorylation of serine 7 of the CTD was shown to be specifically required for the expression of Sm snRNAs and the recruitment of the integrator complex [96].

### ***Are CBs involved in regulating pre-snRNA synthesis?***

CBs have been observed to associate with a specific set of gene loci in *diptera*, amphibians, and humans with high frequency. Included in this group are the cell-cycle dependent histone genes [97-100], intron-encoded [101] and dedicated [102] snoRNA genes, and U snRNA genes [99, 103, 104]. In HeLa cells, roughly 45% of U2 loci and 25% of U1 loci examined associated with CBs [104]. U4 and the minor splicing U11 and U12 snRNA genes also associated with CBs although with reduced frequency, but the U6 locus showed no preference for CB association [105]. It remains to be examined as to whether the U5, U4atac, and U6atac loci associate with CBs.

Although it is unlikely that the association of CBs with gene loci is merely fortuitous given the specificity and frequency of interactions, the physiological relevance of this association is not immediately clear. It has been proposed, however, to be important for CB genesis and/or transcriptional regulation of the associated gene locus [101, 103-105]. These associated gene loci may serve as “CB organizing centers” much in the same way that rDNA loci serve as

nucleolar organizing centers. However, the absence of DNA within CBs and the mobility of CBs within the nucleus would indicate that the gene loci are not required for the maintenance of CB structure. This, however, does not rule out the formal possibility that the loci may have a role in nucleating CB formation. This would be in sharp contrast to the fundamental role of rDNA as an integral component of the fibrillar center of the nucleolus, which both establishes and maintains the structure of the nucleolus [106]. The observation that CBs are frequently observed in close association and sometimes “budding” off of nucleoli<sup>14</sup>, however, suggests that CBs most likely derive from nucleoli, rather than gene loci [107].

Alternatively, CBs may participate in the regulation of transcription at these loci and/or the processing and export of their transcripts. Investigations into the requirement for transcription and nascent snRNA at the U2 locus have resulted in conflicting conclusions. In HeLa cells, it was found that the frequency of association of CBs with artificial arrays of U1 and U2 genes was proportional to the level of transcription and dependent on the coding sequence of the U2 snRNA [108, 109]. This is consistent with the fact that CBs associate with the cell cycle dependent histone genes during S phase when the loci are actively transcribed [110]; however, it is inconsistent with the fact that the frequency of CB association does not correlate with the transcriptional activity at various histone loci [111]. This group proposed that CBs may play a role in feedback inhibition to maintain set point snRNA levels [108, 109]. Alternatively, CBs may be positive regulators of snRNA transcription since active RNAPII, TATA box binding protein (TBP), and PTF $\gamma$ /SNAP43 were found in domains associated/overlapping with both CBs and U2 DNA loci [112]. However, due to high levels of nucleoplasmic U2 snRNA, RNA FISH was not performed to test for the presence of nascent U2 snRNA transcripts and, therefore, the

---

<sup>14</sup> CBs were first described in Purkinje neurons of the cerebellum by Santiago Ramon y Cajal in 1903. He called them *cuervo accessorio* or the nucleolar accessory body based on their frequent association with nucleoli.

transcriptional activity at the U2 locus. In another study, also conducted in HeLa cells, it was found that the frequency with which CBs associated with the endogenous U2 gene locus was independent of the presence of a U2 RNA focus, the presumptive collection nascent U2 snRNAs<sup>15</sup> [104]. Furthermore, the CB appeared to associate with the U2 DNA locus rather than the U2 RNA focus. These results suggested that neither transcription nor nascent U2 snRNA is required for the association of CBs. Further investigations will be needed to elucidate the precise nature of the U2 RNA focus given the dubious observation that these foci were found both associated with U2 gene loci and as independent structures<sup>16</sup>. If the RNA FISH probe indeed detected nascent U2 snRNA, it would be interesting to examine its relationship to the domain that contains active RNAPII, TBP, and PTF.

In spite of the increasing possibilities, there are a few correlations worthy of mention [105]. First, the frequency of association of CBs with gene loci appears to be proportional to the copy number at that locus. Second, to date, all gene loci which associate with CBs are transcribed by RNAP II. Finally, the RNAs transcribed from these loci neither contain introns nor acquire poly(A) tails, except for the intron-encoded snoRNAs.

### ***The nuclear export of pre-snRNAs.***

The newly transcribed pre-snRNAs must be transported to the cytoplasm to continue their maturation, necessitating the assembly of an export competent complex [50, 113]. To this effect, the nuclear CBC, consisting of CBP20<sup>17</sup> and CBP80, first associates with the m<sub>1</sub>G cap of the

---

<sup>15</sup> In this study, nascent U2 snRNA was detected with RNA probe that targets the read through transcript, not the coding portion of the U2 snRNA. This method allowed the investigator to avoid the detection of the highly concentrated U2 snRNP free in the nucleoplasm.

<sup>16</sup> It is quite possible that a locus was present but escaped detection. This possibility stems from the fact that only the major U2 cluster was detected by their approach. Single copy and minor clusters of U2 genes did not seem to generate any signal.

<sup>17</sup> CBP20 and CBP80 are cap binding proteins of 20 and 80kDa, respectively.



RNA [114, 115]. Next, the phosphorylated adaptor for RNA export (PHAX) binds the CBC-RNA complex [116, 117]. The export receptor, exportin 1<sup>18</sup> (Xpo1), recognizes the export adaptor, PHAX, in its phosphorylated form bound to its CBC/pre-snRNA cargo and binds to this complex together with RanGTP<sup>19</sup> [116, 117]. While all of the above interactions are individually quite weak, cooperative binding ensures the formation of a stable export complex. After assembly, the entire complex translocates through the nuclear pore complex (NPC).

The possibility that CBs may participate in the formation of an export competent pre-snRNA has been suggested by the finding that RNA FISH probes are able to detect pre-U2 snRNA in CBs [104] and that immunofluorescence demonstrates the presence of PHAX and Xpo1 [104, 118-120] in the CBs. In addition, fluorescently labeled U2 snRNAs injected into the nucleus of the *Xenopus laevis* oocytes accumulate in CBs prior to export [121]. The specificity of the detection of pre-U2 snRNA is questionable as BrUTP (our data) and P-32 UTP [122] is not detected in CBs until after long incubations even though pre-U2 is detected in the cytoplasm as early as 4min [123]. This could, however, reflect an increased sensitivity of RNA FISH. The detection of pre-U2 snRNA in all CBs, including those that are not associated with U2 gene loci, suggests that unassociated CBs were once associated with U2 DNA loci or that locus association is not required for the accumulation of the pre-U2 snRNA. The latter would indicate that CB association with gene loci is not required for the assembly of an export competent pre-snRNA complex. It remains to be seen whether other pre-U snRNAs are found in CBs.

This work and others have shown that the assembly of an export competent mRNA begins at the transcriptional unit [48, 124]. It will be interesting to see if symmetry exists

---

<sup>18</sup> Also called chromosome region maintenance 1 protein (CRM1), Xpo1 is typically known for its role in exporting classical nuclear localization sequence (cNLS) containing proteins.

<sup>19</sup> Ran (Ras-like nuclear protein) belongs to the superfamily of monomeric G proteins. The RanGTP/RanGDP gradient between the nucleus and cytoplasm is essential for unidirectional trafficking.

between RNAPII transcribed coding and non-coding RNAs. In particular, the co-transcriptional recruitment of PHAX to snRNA gene loci would suggest that the assembly of an export competent pre-snRNA also begins co-transcriptionally. If so, these results would collectively suggest that the differences in the transcriptional machinery may account for the differences in the export pathways for U snRNAs and mRNAs. In essence, the fate of the RNA is governed by its promoter structure.

Radiolabeling experiments have demonstrated the presence labeled pre-snRNAs in the cytoplasm within 4min after a pulse of P-32 UTP [73, 125, 126]. Therefore, their transcription, 3'-end formation, assembly into an export complex, putative transit through CBs, and translocation through the NPC must all occur quite rapidly. Passage through the NPC marks the beginning of the cytoplasmic phase of snRNP biogenesis.

### ***The Cytoplasmic Phase: Assembly of Core Sm snRNPs.***

Immediately upon cytoplasmic entry, RanGTP's hydrolytic activity is accelerated by RanGTPase Activating Proteins (RanGAPs) and Ran binding proteins (RanBP1/RanBP2) on the cytoplasmic filaments of the NPC, and PHAX is dephosphorylated by protein phosphatase 2A [116, 117, 127]. These two events result in the dissociation of RanGDP and Xpo1 and, together, ensure unidirectional transport of the pre-snRNA cargo. Dephosphorylated PHAX remains associated<sup>20</sup> with the CBC/pre-snRNA complex, presumably until the m<sub>1</sub>G cap is hypermethylated [117, 127]. This association may potentially prevent an illicit association

---

<sup>20</sup> Although its presence was not tested, one might infer that CBC, too, remains associated based on the fact that it serves as a bridge between PHAX and the m<sub>1</sub>G capped RNA. Alternatively, since PHAX is an RNA binding protein *in vitro*, the interaction of dephosphorylated PHAX with the pre-Sm snRNA may have changed such that CBC is no longer required.

with the cytoplasmic cap binding protein<sup>21</sup>, which would target the RNA for translation. CBC and PHAX are independently recycled to the nucleus, where the latter is phosphorylated by casein kinase 2 (CK2) to initiate another round of pre-snRNA export [127].

The remainder of the cytoplasmic phase of maturation is orchestrated by a large 20S assembly called the SMN complex, consisting of the survival of motor neurons protein (SMN), 7 distinct gemin proteins (gemin 2-8), and several other factors [128-130]. Mutations in the telomeric SMN gene (*SMN1*) in humans results in spinal muscular atrophy (SMA), an autosomal recessive condition characterized by the degeneration of the motor unit. A discussion of SMA, its etiology, and its selective influence on the motor unit can be found elsewhere [131-133].

The SMN complex participates in all three snRNP maturation events in the cytoplasm: *1) the assembly of an Sm ring onto the Sm site, 2) the hypermethylation of the m<sub>1</sub>G cap, and 3) the trimming of the pre-snRNA's 3' end.* Indeed, the SMN complex associates with a distinct set of snRNP populations, each representing different stages in their cytoplasmic maturation: a disassembled export complex, the core Sm snRNP, and an import complex [134]. Furthermore, SMN may very well serve as an adaptor for re-import of the snRNA into the nucleus [135].

**1)** The assembly of the core snRNP begins with the formation of the Sm ring around the Sm site. Although the Sm proteins do not form rings in the absence of the snRNA, they exist as dimers (B/B'-D3, D1-D2) or trimers (E-F-G) [136]. First, the SMN complex facilitates the formation of a semi-stable open ring complex consisting of D1-D2-E-F-G proteins around the Sm site of pre-U snRNAs [136, 137]. Then, the SMN complex completes the formation of a 7-membered ring (-D3-B/B'-D1-D2-E-F-G-) upon integration of the B/B'-D3 heterodimer [136,

---

<sup>21</sup> This factor is also referred to as the eukaryotic translation initiation factor 4E (eIF4E).

137]. While the Sm core can be assembled *in vitro* on essentially any RNA with a short stretch of uridines, the SMN complex likely serves as a specificity factor—in addition to an assembly factor—that ensures the assembly of the Sm ring only on RNAs with the appropriate snRNP code [138]. The WD repeat containing subunit of the SMN complex, Gemin 5, recognizes this code on the snRNA, which consists of the Sm site and parts of the adjacent stem-loop structure(s) [139]. The U1 snRNA is distinct in that its code consists of stem-loop I (SL1) [129, 140]. SL1, however, is not a strict requirement as a SL1-deleted U1 snRNA still acquires its Sm complement and is recruited to the nucleus [48].

While the process by which the Sm proteins are assembled onto the Sm site is poorly understood, several proposals have been generated. SMN itself binds with high affinity to symmetric dimethyl arginines (sDMA) in the arginine-glycine rich (RG) motif of B/B', D1, and D3 through its tudor domain [141-145]. SMN may, thus, directly transfer Sm subcomplexes onto the Sm site [141-145]. Gemin 6 and 7 contain a non-canonical Sm fold and form a heterodimer [146]. A seductive hypothesis was that the dimer serves as a surrogate to B/B'-D3 in order to stabilize the open ring intermediate [146]. Given that all components of the SMN complex, with the exception of Gemin2, associate with Sm proteins, [129] how the SMN complex contributes to the assembly of the Sm ring onto an Sm site is open to many possibilities. Crystal structures of SMN subcomplexes [143, 144, 146] and interaction maps of the SMN complex [147] will surely facilitate future studies.

Recently, there have been new developments in our understanding of Sm protein methylations. Symmetric dimethylation of the RG motif was long thought to be catalyzed by a Type II protein arginine methyltransferases (PRMT), PRMT5/Janus Kinase Binding Protein 1 (JBP1) exclusively [148-150]. While this appears to be true in *Drosophila* [151], more recently, a

new set of PRMTs, PRMT7 [152, 153] and PRMT9 [154], have been shown to symmetrically dimethylate Sm proteins in humans. Curiously, PRMT5 and PRMT7 were shown to function in a non-redundant and non-additive fashion [152]. While sDMA were detected on both nuclear and cytoplasmic Sm proteins, asymmetric DMA (aDMA) were only detected in nuclear Sm proteins [155]. The aDMA are formed by Type I PRMTs; however, they can also be formed by all three Type II PRMTs to some extent *in vitro*. PRMT4/Coactivator-associated arginine methyltransferase (CARM1) but not other Type I PRMTs was shown to asymmetrically dimethylate Sm proteins [156]. Which enzyme(s) are involved in the synthesis of aDMA on nuclear Sm proteins remains to be determined. In the nucleus, aDMA may serve a role in the targeting of snRNPs to various compartments or to regulate alternative splicing [156]. In the cytoplasm, sDMA may be important for core snRNP assembly [152, 157]; however, methylation mutants of SmD3 were shown to assemble into Sm rings around snRNAs in the cytoplasm and nucleus [158].

2) The trimethyl guanosine synthase 1 (Tgs1), an SMN complex-associated methyltransferase, recognizes SmB/B' in the context of an Sm core as well as the m<sub>1</sub>G cap on the snRNA and subsequently transfers two methyl groups to position 2 of the m<sub>1</sub>G cap forming the m<sub>3</sub>G<sup>22</sup> cap [159, 160]. Since the addition of B/B'-D3 heterodimer completes the assembly of the Sm ring, the association of Tgs1 with B/B', in the context of an Sm ring, ensures that only snRNAs with fully assembled Sm rings are hypermethylated.

3) Nucleolytic trimming of the 3' end of the pre-snRNA generates the mature length snRNA. Sm core assembly is required for 3' end trimming [161, 162]. However, whether 3' end

---

<sup>22</sup> Neither CBC nor eIF4E can associate with this type of cap structure.

trimming is required for nuclear import remains debatable [74, 163-165], and the factor(s) responsible for this 3' end maturation event has yet to be identified in metazoans. However, the presence of a ladder of m<sub>3</sub>G capped RNAs spaced 1nt apart from the pre-snRNA to the mature snRNA in the cytoplasm suggests that the enzyme is primarily a cytoplasmic 3' to 5' exonuclease [74, 166, 167]. In addition, several endonucleases are required to generate the mature 3' end of U snRNAs in yeast [168, 169] and possibly in mammals [170]. Interestingly, smaller ladders have also been observed in the nucleus, suggesting that 3' end maturation is completed in the nucleus [74, 167, 171]. Supporting this idea is the finding that the interferon-stimulated gene product of 20kDa (ISG20), a 3' to 5' exonuclease component of the exosome, co-immunoprecipitates with the SMN complex and several U snRNAs in nuclear fractions [172]. In addition, the nuclear exosome is known to be required for the maturation of U snRNAs in yeast [168].

### ***Are U bodies involved in cytoplasmic maturation of snRNPs?***

While the molecular mechanisms regulating the cytoplasmic maturation events of snRNAs have been extensively studied, the spatial arrangement of these events within the cytoplasm remains poorly documented. A recent study suggests that snRNP maturation might partly occur in discrete cytoplasmic bodies [63]. These organelles were named the “U bodies” because they contain the major U snRNPs. While they were described for the first time in *Drosophila* oocytes, U bodies were also found in many other cell types, including cultured human and amphibian cells [63] and, thus, are likely to be universal organelles. Importantly, the enrichment of SMN within the U bodies and their association with P bodies directly implicates them in snRNP maturation.

### ***The nuclear entry of assembled snRNPs.***

The core snRNP must be brought into the nucleus to continue its maturation and, afterwards, participate in splicing. The requirements for nuclear import vary depending on the particular snRNP and on the cell system [173]. In general, however, the m<sub>3</sub>G cap and the Sm core [174] are considered to be nuclear localization signals (NLS). The m<sub>3</sub>G cap dependent and Sm core dependent pathways utilize the same import receptor importin  $\beta$  (Imp  $\beta$ ) but distinct import adaptors [175]. The m<sub>3</sub>G cap dependent pathway is well characterized and was shown to use snurportin-1 (SNP1) as its import adaptor (excellently reviewed in [176]). As SNP1 remains associated with the NPC subunit, nucleoporin 214 (Nup214), and its exporter Xpo1 upon recycling to the cytoplasm, core snRNPs are, thus, thought to first engage SNP1 on the cytoplasmic filaments of the NPC. Once in the nucleus, the SNP1/Imp  $\beta$ /m<sub>3</sub>G cargo complex is disassembled in a Ran and energy independent fashion [177, 178]. The Sm core dependent pathway is less understood, but recent evidence implicates the SMN complex as the likely import adaptor [135, 179]. It has been proposed, however, that the release of cargo is mediated by the CB signature protein coilin as it was shown to associate with SmB and compete with SMN *in vitro* [180]. Indeed, coilin has been proposed to target snRNPs to CBs [181-183].

Pulse-chase experiments have shown that cytoplasmic pre-snRNAs complete maturation and are re-imported into the nucleus as core Sm snRNPs with a half-life of ~10 minutes [73, 125]. Thus, export complex disassembly, Sm core assembly, cap hypermethylation, 3' end trimming, import complex assembly, and translocation through the NPC occur quite rapidly. The latter marks the beginning of the nuclear phase of snRNP biogenesis.

### ***The Nuclear Phase: formation of mature snRNPs.***

The nuclear phase is the least understood part of the entire snRNP biogenesis pathway, and it involves a multiplicity of processes and factors, as well as trafficking to several subnuclear domains. In particular, extensive internal modifications of the U snRNAs by 2'-O-methylation and pseudouridylation, represent a critical step in the making of a fully functional snRNP. The requirement of such modifications was especially well demonstrated for the assembly of the 17S U2 snRNP [184]. Several domains such as CBs [50], the nucleolus [121], and the nucleoplasm [185], were directly implicated in the regulation of these internal modifications. CBs appear to play a predominant role as they were shown to contain a novel class of guide RNAs called scaRNAs, which direct the 2'-O-methylation and pseudouridylation of the Sm snRNAs [161]. In addition, CBs may also be the site where snRNP-specific proteins are acquired [186]. Finally, the assembly U4/U6 di-snRNP and U4/U6.U5 tri-snRNP may occur in or be facilitated by CBs [187-189]. Eventually, snRNPs are thought to be recruited to SFCs where further packaging and/or storage together with other splicing factors may occur and are subsequently released when required for spliceosomal assembly (reviewed in [58]).

### **U6 snRNP biogenesis**

#### ***Synthesis of pre-U6 snRNA by RNAPIII.***

Like the biogenesis of Sm snRNPs, the biogenesis of the U6 snRNP begins with the synthesis of its RNA component. The transcription of the pre-U6 snRNA is directed by many of the same cis-acting sequences as the Sm type RNA genes. In particular, U6 snRNA genes contain a PSE and DSE that are structurally similar and functionally interchangeable with that of the Sm snRNA genes [190-192]. A major difference, however, resides in the presence of a



TATA box within the U6 gene promoter, and while the molecular mechanisms are not yet understood, the PSE, DSE, and TATA box of the U6 gene presumably act in concert to specify the recruitment of RNAPIII. Indeed, when the TATA box is deleted from the U6 snRNA gene, transcription is directed by RNAPII. Reciprocally, when the U6 TATA box is placed within the promoter of the Sm snRNA genes, they switch polymerase specificity to RNAPIII. While both Sm and U6 snRNA genes require TBP for their transcription, each requires a TBP-associated factor (TAF) that is distinct from each other and from other RNAPII and III genes, respectively [193]. The TBP-TAFs complex for U6 genes has been identified as TFIIB- $\alpha$  [194]. The promoter for the U6 snRNA genes is referred to as a Type III RNAPIII promoter and is shared by other small metabolically stable RNA genes (U6atac and 7SK, for example) (reviewed in [64, 195]). Type III promoters represent an unusual class of RNAPIII promoters in that they are extragenic sequences, whereas Type I (box A and box B, 5S rRNA genes) and Type II (box C, tRNA genes) promoters are both intragenic control elements.

Unlike that for Sm snRNAs, the formation of the 3' end of the pre-U6 snRNA is a transcription termination event, rather than an RNA processing event. The terminal poly(U) sequence serves as a transcription termination signal, which is the general mechanism encountered for all RNAPIII genes [64]. After pre-U6 snRNA is transcribed, it undergoes many of the same maturation events that pre-Sm snRNAs undergo. In the case of the pre-U6 snRNA, however, it is thought that maturation is confined exclusively to the nucleus. Interestingly, U6 snRNP was demonstrated in the cytoplasm of yeast heterokaryons [196], in mouse fibroblast cell lines [197] and more recently within the cytoplasmic U bodies of *Drosophila* oocytes [63]. Whether the cytoplasmic phase of U6 snRNP is required for its maturation or bears a new functional significance is not known.

### ***U6 snRNP maturation.***

After the transcription of the pre-U6 snRNA, the La autoantigen binds both its 5' and 3' end. La binds the 5' triphosphate cap through its Walker A box [198] and the 3' U<sub>4</sub> through its winged-helix motif [199]. The association of the La protein is believed to protect a subset of RNAPIII transcripts from ribonuclease degradation and to target them to nucleoli [200]. A poly(U) polymerase (U6 Terminal Uridyl Transferase, U6-TuTase) [201-203], enriched in nucleoli, and an U6 specific 3'-exonuclease [204] extend and trim, respectively, the 3' tail of the pre-U6 snRNA to form the mature length U6 snRNA. The mature 3' end is eventually generated by the formation of a 2', 3' cP<sub>i</sub> [205]. However, the factor(s) responsible for the required enzymatic activity have yet to be identified. A specific 130kDa methyltransferase catalyzes the addition of a methyl group to the 5' triphosphate cap to form the mature 5' end, a  $\gamma$ -m-P<sub>3</sub> cap [206]. The formation of  $\gamma$ -m-P<sub>1</sub> cap and 2', 3' cP<sub>i</sub> tail precludes the association of the La protein [198, 207]. However, the LSm proteins are able to associate with this modified 3' end to form the core domain of the U6 snRNP [25]. Unlike the Sm proteins, the LSm proteins form a heteroheptameric ring complex in the absence of RNA [25]. Thus, LSm core assembly may very well be a single step process. Like the Sm snRNAs, the U6 snRNA is 2'-O-methylated and pseudouridylated. However, these modifications are guided by snoRNAs, rather than scaRNAs [208, 209]. It is well-established that the U6 snRNA transiently localizes to nucleoli after its transcription and prior to accumulating in CBs [210]. The snoRNA and U6-TuTase directed modifications of the U6 snRNA most likely occur within the nucleolus [201, 209]. Given that the U6 snRNP also localizes to CBs, it is still possible that some modifications also occur in this compartment. The order and compartmentalization of U6 snRNA metabolism remains an active area of investigation.

### ***Beyond mono-snRNPs***

The U4, U5, and U6 snRNPs are known to assemble into a U4/U6.U5 tri-snRNP prior to engaging their pre-mRNA substrates. The formation of the U4/U6 di-snRNP occurs through the extensive base pairing of the U4 and U6 snRNAs followed by the addition of di-snRNP specific proteins [211]. Tri-snRNP assembly follows with the incorporation of the U5 snRNP into the U4/U6 di-snRNP and the association of tri-snRNP specific proteins [211].

The only known U6 snRNP-specific protein is SART3/p110/Prp24p [212]. The absence of SART3 in the U4/U6 di-snRNP and the enhanced formation of di-snRNPs in the presence of SART3 suggest that it is a di-snRNP assembly factor [212, 213]. Consistent with their role in snRNP maturation, CBs are enriched in SART3 [188]. Furthermore, the U4/U6 di-snRNP accumulates in CBs when hPrp31 is knocked down, suggesting that the U4/U6.U5 tri-snRNP may also be assembled in CBs [187]. In contrast, however, others have shown that a U6 snRNA mutant that lacks a nucleolar localization element/Cajal body box (NoLe/CAB box) and, thus, fails to target both the nucleolus and CB still assembles into a U4/U6 di-snRNP [214]. These differences may be due to differences in somatic cell line/oocyte differences or organismal variations. Finally, the discovery of the penta-snRNP supports a model in which all five major spliceosomal snRNPs would be pre-assembled, possibly within CBs [215], prior engaging pre-mRNAs [45].

### ***The past, present, and future of snRNP biogenesis***

The last decade was rich in providing new insights into the molecular processes involved in the biogenesis of fully functional splicing snRNPs and the regulation of their nucleocytoplasmic exchanges. The intra-nuclear trafficking of snRNPs was also well documented, in

particular with respect to several organelles, such as CBs, nucleoli, and SFCs, which are currently thought to orchestrate several aspects of their maturation, assembly, and storage. Similarly, the recently discovered U bodies are potential structures organizing the cytoplasmic maturation phase of snRNPs. How the trafficking of snRNPs within these various discrete cellular structures is regulated and how it influences pre-mRNA splicing are two fundamental and related questions that remain to be answered.

### **The functions of spliceosomal snRNPs**

After the maturation of spliceosomal snRNPs is complete, they participate in a critical step in the expression of genes, pre-mRNA splicing (reviewed in [17]). They are involved in the recognition of cis-acting elements in pre-mRNA: the 5' splice site (5'-SS), 3' splice site (3'-SS), and the branchpoint sequence (BPS). In addition to their role in substrate recognition, they participate in the catalytic steps themselves. In fact, it is believed that the spliceosome is a ribozyme where the snRNA moieties provide the catalytic residues (reviewed in [216, 217]). This theme is parallel to that of another macromolecular ribozyme, the ribosome.

Unlike the ribosome, however, the spliceosome has not been crystallized due to its complex conformational gymnastics and transiently interacting components. Nonetheless, crystal and NMR structures of partially assembled snRNPs and electron microscopy on purified snRNPs and spliceosomes have contributed significantly to our understanding of pre-mRNA splicing (reviewed in [218]). In addition, indirect structural evidence comes from *in vitro* cross-linking studies and yeast genetics [219-226].

### ***Step-wise assembly and preassembly models of spliceosome assembly.***

The canonical model of splicing (reviewed in [17]) maintains that pre-mRNA serves as a template for the sequential recruitment of the splicing snRNPs and that this recruitment is strictly dependent on the hybridization of cis-acting sequences on pre-mRNA and recognition sequences on snRNAs: First, the spliceosomal E complex<sup>23</sup> is formed upon recognition of the 5'-SS by the snRNA component of the U1 snRNP. Next, the spliceosomal A complex is formed upon recognition of the BPS by the RNA component of the U2 snRNP. Finally, the spliceosomal B complex is formed after the recruitment of a U4/U6.U5 tri-snRNP complex. After several rearrangements in RNA-RNA, RNA-protein, and protein-protein interactions and two-sequential transesterification reactions, the intron is removed as a lariat, and its delimiting exons are joined together.

This so-called stepwise model originally devised on the basis of *in vitro* order of addition experiments has faced several challenges in the past decade. First, it would appear that the U2 snRNP is required for the formation of the spliceosomal E complex, which suggests a role for the U2 snRNP even before the U1 snRNP engages the 5'-SS [136, 227]. Second, a penta-snRNP particle, consisting of all five splicing snRNPs in equal stoichiometric abundance, retaining U4/U6 base pairing interactions uncharacteristic of a spliceosome, and void of pre-mRNA, was purified in yeast [45, 46]. When supplemented with snRNP depleted extract, this particle was competent to splice synthetic splicing substrates as a unitary particle, providing evidence for a preassembly model of splicing wherein all five snRNPs engage the pre-mRNA in a single step as a single complex. The penta-snRNP was recently examined by cryo-electron microscopy and was shown to contain a channel that would accommodate pre-mRNA [228]. Finally, the human penta-snRNP was shown to engage a small RNA that consisted exclusively of the 5'-SS,

---

<sup>23</sup> In yeast, the E complex is referred to as the commitment complex.

indicating that the BPS and 3'-SS are not required for the recruitment of the U2 snRNP or the tri-snRNP [44].

There is currently heated controversy over these two models in the splicing field. The differences in the observations may be attributed to the diversity in the systems various groups are using: in vitro vs. in vivo, yeast vs. human cells, differences in splicing reporters, differences in extract source and preparation. It will be interesting to see how this complex reaction occurs within the cell nucleus.

### ***Splicing is co-transcriptional.***

Much like other pre-mRNA processing, most pre-mRNA splicing in metazoans appears to be a co-transcriptional event, which is to say that introns are being removed as the nascent transcript is being extended (reviewed in [229]). Moreover, it has been proposed that the temporal simultaneity and spatial congruency of transcription and splicing are direct consequences of the structural and functional coupling of their respective machineries (reviewed in [230]). Accordingly, elongating RNAPII transcripts were previously shown to recruit splicing factors, such as the snRNPs and SR proteins, and more recently, the exon junction complexes (EJCs), which mark the ultimate products of splicing, exon-exon junctions (reviewed in [231]). Furthermore, although these transcripts generally increase in length along the contour of a transcriptional unit, there are RNAs that have internal loops that bring together splice sites or are shorter than the RNAs upstream indicating the formation of lariats and the excision of introns, respectively [232]. Finally, intron-containing RNAs transcribed by a RNAPII with a mutant CTD of RPB1 are successfully capped but fail to recruit snRNPs to transcriptional units and fail

to mature into mRNA, suggesting a more direct role for the transcription machinery in recruiting the splicing machinery [233].

### **The *Xenopus laevis* oocyte**

The *Xenopus laevis* oocyte, our system of choice, has been used extensively to study the maturation and trafficking of splicing snRNPs and splicing itself. Indeed, much of what we know about these processes comes from work using these prophase I arrested cells. The utility of this system resides in several aspects unique to the oocyte. First, because of the large size of the oocyte (~1mm diameter) and its nucleus (~0.4mm diameter) in comparison to typical somatic cells (~10µm diameter), large volumes may be injected into the cytoplasm (50nL) or nucleus (10nL) to introduce exogenous molecules [234]. Second, *Xenopus* oocytes like all oocytes store a large pool of maternal factors in preparation for the cleavage stage that follows fertilization<sup>24</sup>. As such, there is a large pool of Sm proteins in the cytoplasm of the oocyte, a fact that several groups have exploited to examine core snRNP assembly on snRNAs injected into the cytoplasm. Third, the nuclear structures to which the snRNPs traffic are much more abundant and much larger in amphibian oocytes than those in somatic cells, thus, providing a level of cytological resolution offered by few other systems (reviewed in [235]).

The lampbrush chromosomes (LBCs) of amphibian oocytes exhibit unique structural characteristics that make it possible to study the recruitment of snRNPs to nascent transcripts in vivo. In particular, these extended diplotene bivalent chromosomes display numerous lateral loops of chromatin that correspond to regions of intense transcriptional activity by RNAPII (for review see [236]). The chromosomal loops are composed of two distinct domains: the first

---

<sup>24</sup> During the cleavage stage, synchronous cell division occurs rapidly without any cell growth; thus, essential maternal factors must be stored in high abundance to ensure an equal distribution to progeny cells.

domain corresponds to a decondensed euchromatin axis that can be demonstrated using antibodies against the RNAPII transcriptional machinery or various chromatin components [215]. The second domain corresponds to nascent RNP fibrils, which are formed from nascent pre-mRNAs associated with a cortege of factors involved in their maturation. These RNP fibrils create a dense RNP matrix around the loop axis that is readily observable by phase contrast or differential interference contrast (DIC) microscopy. Indeed, the elongation of transcripts along the axis is reflected in a characteristic thin to thick morphology of the loops ([215, 237]; for review see [238]).

The contents of the nucleus can be observed in two distinct ways: nuclear spread preparations (Figure 3 and 4) and mineral oil isolated nuclei. In the former preparation, the nucleus is dissected from the oocyte in aqueous buffer, the nuclear envelope is removed, and the structures in the nucleus are allowed to “spread” on the plane of the slide. In the latter preparation, the nucleus is isolated in a mineral oil medium and transferred along with some mineral oil to a microscope slide for observation. It has been shown previously, that nuclei isolated in this way retain all nuclear functions, including splicing and transcription, for up to 24hrs. Whereas CBs, SFCs, and nucleoli were observed in both nuclear spread preparations and mineral oil isolated nuclei, LBCs were only detected in spread preparations. We now have devised a method for preparing oil-isolated nuclei that allows observation of LBCs and their active RNAPII transcriptional units.



snRNP	12S U1	17S U2	25S U4/U6.U5		
<b>snRNA</b>	<b>U1</b>	<b>U2</b>	<b>U4</b>	<b>U5</b>	<b>U6</b>
length (nt)	164	186	142	116	106
RNAP	II	II	II	II	III
Type	Sm	Sm	Sm	Sm	LSm
5' Cap	m <sub>3</sub> G	m <sub>3</sub> G	m <sub>3</sub> G	m <sub>3</sub> G	γ-m-P <sub>3</sub>
3' end	3'OH	3'OH	3'OH	3'OH	U <sub>4</sub> -cP <sub>i</sub>
m <sup>6</sup> A	0	1	0	0	1
m <sup>2</sup> G	0	0	0	0	1
2'-O-m	3	10	4	5	8
Ψ	2	13	3	3	3
<b>Heptameric Core/Ring Proteins</b>	B/B'	B/B'	B/B'	B/B'	Lsm2
	D1	D1	D1	D1	Lsm3
	D2	D2	D2	D2	Lsm4
	D3	D3	D3	D3	Lsm5
	E	E	E	E	Lsm6
	F	F	F	F	Lsm7
	G	G	G	G	Lsm8
<b>Specific Proteins</b>	U1-A	U2-A'	15.5K	15K	
	U1-C	U2-B''	61K	40K	
	U1-70K	SF3a		100K	
		SF3b		102K	
		P14		116K	
		SF2/ASF		200K	
		hPrp5p		220K	
		hPrp43			
		SR140		27K <sup>t</sup>	20K <sup>d</sup>
		CHERP		65K <sup>t</sup>	90K <sup>d</sup>
		U2AF		110K <sup>t</sup>	60K <sup>d</sup>
		Hsp60			
		Hsp75			
		PUF60			
	SPF45				
	SPF31				
	BRAF35				

**Table 1: The composition of major mature spliceosomal snRNPs in *H. sapiens*.** Details regarding the small nuclear RNA are indicated, as well as the RNA polymerase responsible for its synthesis. m<sub>3</sub>G = 5' to 5' linked 2, 2, 7-trimethyl guanosine triphosphate cap. γ-m-P<sub>3</sub> = γ-methyl triphosphate cap. U<sub>4</sub>-cP<sub>i</sub> = U<sub>4</sub>-2', 3'-cyclic phosphate tail. m<sup>6</sup>A and m<sup>2</sup>G = methylation of exocyclic amine on A or G bases. 2'-O-m = 2'-O-methylated ribose. Ψ = pseudouridine. d = U4/U6 di-snRNP specific. t = tri-snRNP specific.

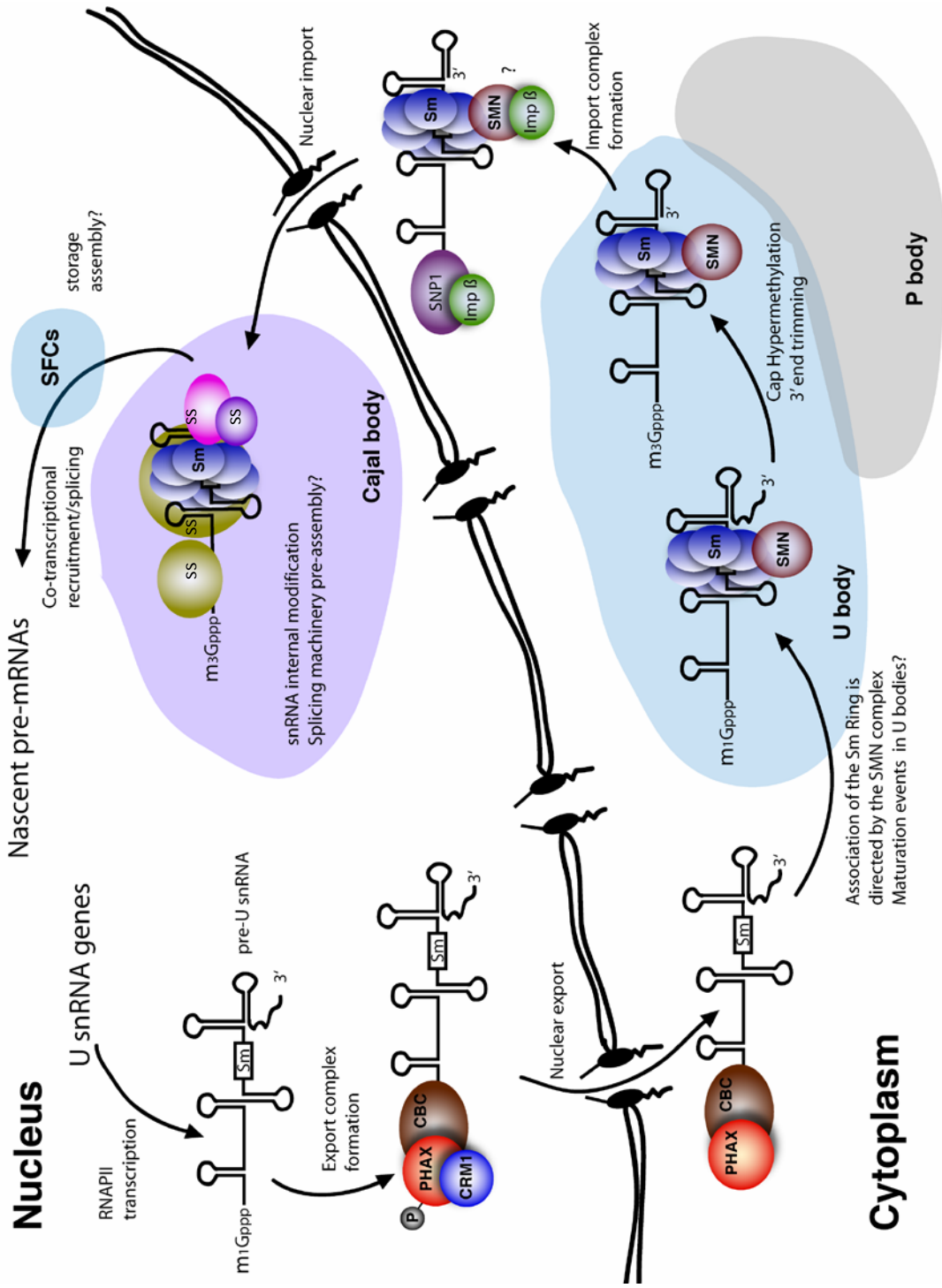


**Figure 1. The Sm snRNP assembly and maturation pathway.** The U2 snRNA was used here as a representative member of the RNAPII transcribed U snRNAs. ss = snRNP-specific proteins

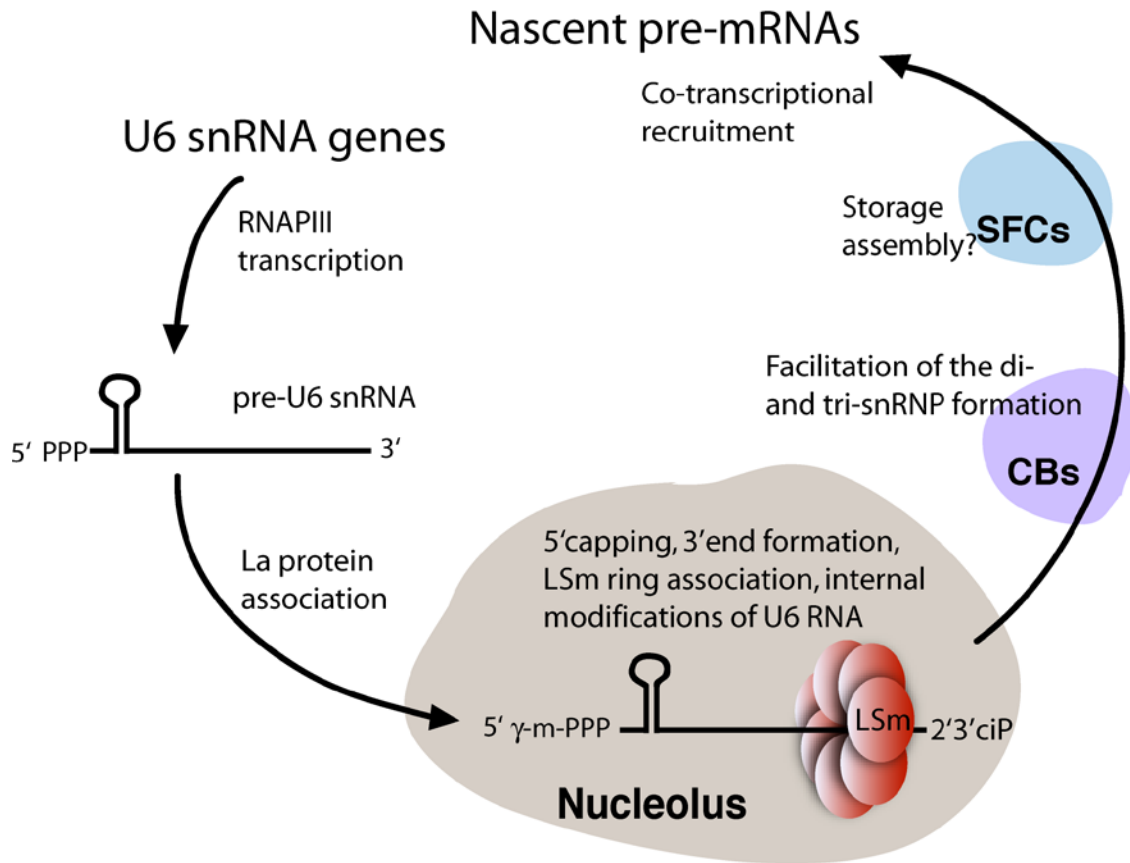
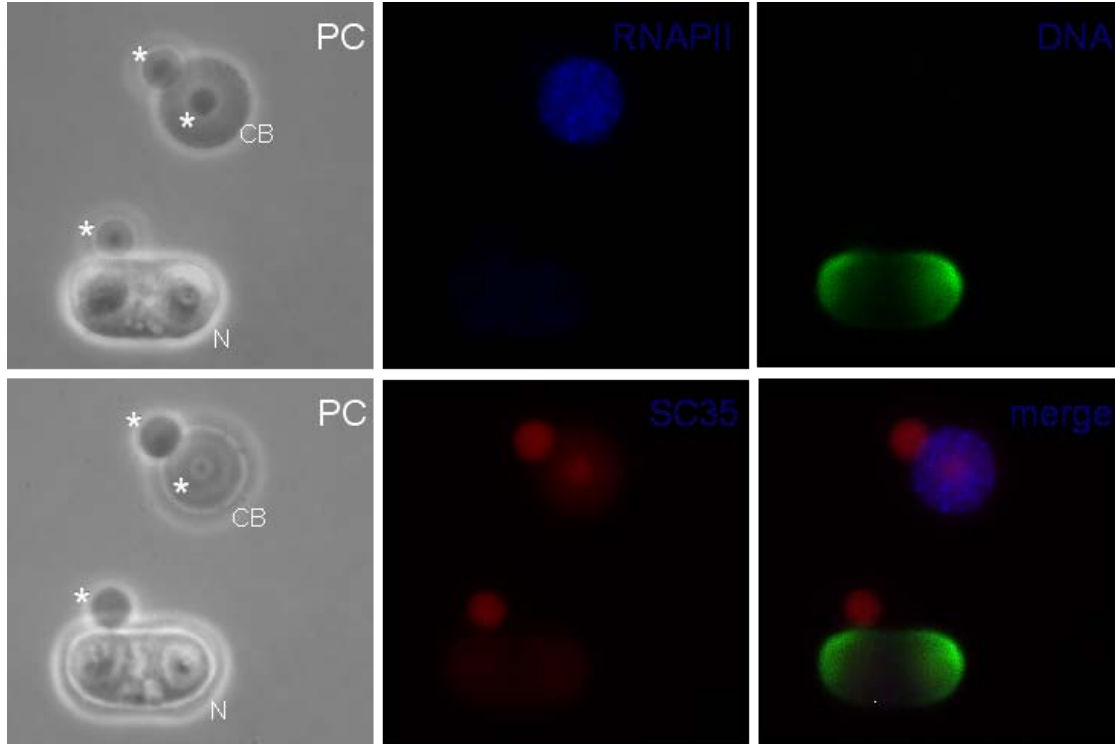


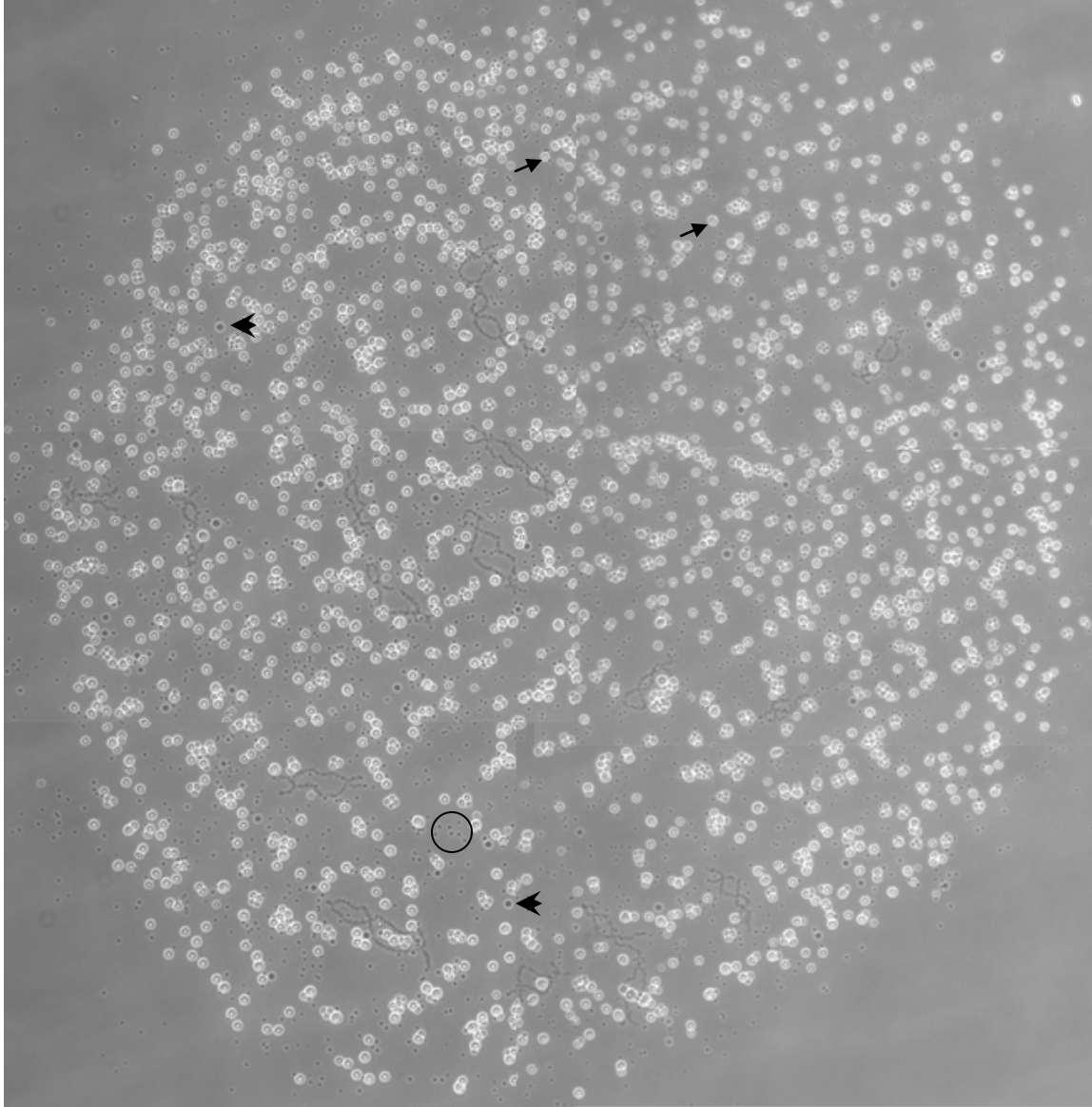
**Figure 2. The U6 snRNP assembly and maturation pathway.**




---

**Figure 3: Phase contrast (PC) images show Cajal bodies (CB), Nucleoli (N), and Splicing Factor Compartments (SFCs, \*).** The top PC image focuses on the nucleolus, Cajal body, and its included SFC. The plane of the lower PC image is closer to the slide to place the SFC associated with the surface of the Cajal body and the SFC close to the nucleolus in focus. In the *Xenopus* oocyte system, these three bodies are readily distinguishable by phase contrast microscopy alone through comparison of their density, size, shape, associations, and surface features (see text). Fluorescence images show specific labeling of these structures with probes that target their signature molecules: the Cajal body with  $\alpha$ -RNAPII antibody, SFCs with  $\alpha$ -SC35 antibody, and the nucleolus with the DNA-specific dye YOYO-1.

---



---

**Figure 4: Montage of nuclear spread.** Nuclear spread shows 16 of 18 diplotene bivalent LBCs, ~1000 nucleoli (arrow), ~50 CBs (arrow head), and >1000 SFCs (encircled).

---

## CHAPTER II

### A NEW SYSTEM FOR EXAMINING CO-TRANSCRIPTIONAL snRNP RECRUITMENT AND SPLICING

#### **Introduction**

At steady state, spliceosomal snRNPs are distributed diffusely in the interchromatin space and are highly enriched in SFCs and on LBCs, and to a lesser extent in CBs [215]. To examine the intra-nuclear trafficking pathway of snRNPs, several groups have exploited the fact that when fluorescently labeled snRNAs are injected into the cytoplasm of the oocyte, they ultimately form functional snRNPs. Curiously, these fluorescent snRNPs were highly enriched in CBs and only poorly targeted to SFCs [215]. Furthermore, their association with nascent transcripts on pre-mRNAs was never documented. Here, we show for the first time that fluorescent spliceosomal snRNAs, in the context of snRNP particles, are recruited to elongating RNAPII transcripts on the loops of the LBCs and that they are actively engaged in co-transcriptional splicing. We discuss the potential of this assay to dissect *in vivo* the molecular mechanisms of snRNP recruitment to nascent pre-mRNAs.

#### **Results**

##### ***Newly assembled fluorescent snRNPs target chromosomal loops.***

Chromosomal loops are likely sites of pre-mRNA processing and since injected synthetic spliceosomal RNAs can rescue splicing in oocytes depleted of the corresponding endogenous snRNA [239, 240], our hypothesis was that injected fluorescent snRNAs do associate with chromosomal loops but at a concentration too low to be detected without amplification. To test

that idea, fluorescein-conjugated U1, U2, U4, and U5 snRNAs were synthesized, injected into the cytoplasm of *Xenopus* oocytes, and their fate monitored over time on fixed nuclear spreads. A two-antibody detection system was used to enhance the fluorescent signals, and as expected, all four snRNAs entered the nucleus and associated with CBs. Figure 5 shows the targeting of the U1 snRNP to both CBs and SFCs only 1 hour after cytoplasmic injection. The same result was obtained with U2, U4, and U5 snRNAs. In contrast, the non-spliceosomal U7 snRNP (discussed below), used here as a negative control, did not associate with SFCs but strongly targeted CBs. In addition and for the first time, we were able to demonstrate their association with the active transcriptional units (Figure 6). Unlike previous reports, we found that fluorescent snRNPs target the chromosomal loops rapidly after injection since a weak but specific signal was also detected in these nuclear domains as soon as 1 hour after injection. Detailed analyses of the loop staining using laser scanning confocal microscopy revealed an association of the fluorescent snRNPs with the nascent RNPs rather than with the axial chromatin (Figure 6B inset). This loop distribution is identical to that of the endogenous snRNPs as previously determined by *in situ* hybridization [241]. Importantly, the labeling of the loops cannot be attributed to an incorporation of free fluorescent UTP (possibly produced by degradation of the injected snRNAs) into nascent transcripts since the injection of 200 pmol of fluorescent UTP fails to generate any detectable signal (data not shown). Instead, the staining of the loops is most likely due to the association of the snRNAs in their snRNP conformation.

***The U7 snRNP is not recruited to chromosomal loops.***

To test whether the presence of the fluorescent snRNPs on chromosomes was the result of a genuine recruitment rather than that of random binding, we analyzed the subnuclear

distribution of a synthetic fluorescent U7 snRNA after cytoplasmic injections. Just like the spliceosomal snRNAs, the U7 snRNA assembles into a snRNP that is subsequently recruited to the nucleus [242-245]. The nuclear U7 snRNP comprises part of the processing machinery responsible for the maturation of histone pre-mRNAs [246-250], and it was previously shown by *in situ* hybridization that more than 90% of the nuclear U7 snRNA associates with CBs and is absent from chromosomes [244, 245]. The U7 snRNP is, thus, not expected to interact with chromosomal loops. Figures 5 and 6C show that the newly made fluorescent U7 snRNP was efficiently targeted to CBs but not to chromosomes.

***The chromosomal targeting of fluorescent snRNPs requires RNAPII transcripts.***

To further test whether snRNPs are recruited to active sites of transcription, oocytes were treated with the transcription inhibitor actinomycin D (AMD) prior to nuclear spread preparation. Such treatment results in a complete loss of chromosomal signal, as shown in Figure 7A for the U1 snRNP. This data further supports the conclusion that the association of the fluorescent snRNPs with chromosomes depends on the presence of nascent transcripts. While there is no RNAPI activity on lampbrush chromosomes, both RNAPII and RNAPIII are actively engaged in transcription. The sites of RNAPIII transcription have been mapped to ~ 90 distinct chromosomal loci [251]. These sites are not visible by light microscopy because they lack the density of an RNP matrix but are readily detected by immunofluorescence using anti-RNAPIII antibodies [251]. An antibody directed against one of the specific subunits of RNAPIII, RPC53, was used in Figure 7B to show that a newly assembled fluorescent U1 snRNP does not associate with RNAPIII transcriptional units. This result is in agreement with the fact that RNAPIII



transcripts are not substrates of the spliceosome. Identical results were obtained with the U2 snRNP (data not shown).

Taken together, these data demonstrate that the association of newly made U1, U2, U4, and U5 snRNPs with chromosomal loops reflects physiologically relevant interactions between these snRNPs and the elongating RNAPII transcripts. They also establish a new cytological system to determine *in vivo* which characteristic(s) of a spliceosomal snRNP is essential to regulate its recruitment to the active RNAPII transcriptional units of the amphibian oocyte.

### ***Are splicing factors present on chromosomal loops functional in splicing?***

While spliceosomal snRNPs and SR proteins have long been known to associate with chromosomal loops, whether splicing is actually occurring at these loci was never formally demonstrated. To this effect, we first showed that the depletion of the U2 snRNA results in the loss of the U2 snRNP-specific protein U2B'' from the chromosomal loops (Figure 8).

Interestingly, U2B'' was found to re-localize from chromosomes, SFCs, and CBs to nucleoli.

The significance of U2B'' re-localization is not known, but we used it subsequently in all our experiments as a cytological indicator of successful U2 snRNA depletions. Because micro-

injected DNA oligonucleotides are short-lived, we were able to show that newly injected U2

snRNA could re-establish the normal distribution pattern of U2B'' in U2-depleted oocytes

(Figure 9). This result further validates our previous conclusion that the association of

fluorescent snRNAs with the chromosomal loops reflects the targeting of fully mature snRNPs.

We then asked whether pre-mRNA splicing occurs on the chromosomal loops and if it is prevented by the depletion of the U2 snRNA. During pre-mRNA splicing, the spliceosome stably deposits a large proteinaceous complex, named the exon junction complex (EJC),

approximately 20 nucleotides upstream of exon-exon junctions (reviewed in [252]). Such EJCs influence the cellular fate of spliced mRNAs with which they remain associated during nuclear export and until they are displaced by translating ribosomes. One of the EJC core subunits, Y14 [253, 254], is deposited after exon-exon ligation [255]. Importantly, then, deposition of Y14 on nascent transcripts is a reliable indication of splicing activity. To test whether EJCs are present on chromosomal loops, Y14 was expressed in fusion with an HA tag and its subcellular distribution was analyzed using the anti-HA antibody mAb 3F10. Figure 10A shows that, upon injection of HA-Y14 transcripts into the cytoplasm of stage V oocytes, a protein with the expected molecular weight of ~24 kDa is synthesized and efficiently recruited to the nucleus. There, it associates with CBs, SFCs as previously reported in somatic nuclei [256], and to a lesser extent with nucleoli. In addition and in agreement with the fact that pre-mRNA splicing occurs co-transcriptionally, Y14 also associates with nascent transcripts. Remarkably, the depletion of U2 snRNA results in a complete loss of Y14 from chromosomal loops (Figure 10B), indicating a lack of spliceosomal activity on nascent RNP fibrils. Finally, a cytoplasmic injection of fluorescently labeled U2 snRNAs restores the presence of the U2 snRNP and Y14 on chromosomal loops (Figures 9 and 10B). Together, these data show that pre-mRNA splicing occurs on the chromosomal loops in the presence, but not in the absence of U2 snRNP.

## **Discussion**

### ***The trafficking of snRNPs to CBs, SFCs, and LBC loops.***

The trafficking of snRNPs has been examined by several groups using the *Xenopus* oocyte system. However, as newly formed fluorescent snRNPs were never demonstrated to associate with nascent transcripts, interesting questions regarding which snRNA sequences are

required to recruit snRNPs to elongating pre-mRNAs were intractable. Here we have demonstrated that the failure to detect fluorescent snRNPs to LBC loops was merely the result of a lack of sensitivity of detection. In the next chapter, we describe how we have exploited this assay, to examine snRNA sequence requirements for recruiting the U1 and U2 snRNPs to CBs, SFCs, and LBC loops.

***The first system to examine co-transcriptional splicing on a genome wide scale in vivo.***

While splicing assays have existed for two decades now, they all use a single reporter transcript, such as the AdML RNA or  $\beta$  globin transcript. Furthermore, many of these assays are performed in nuclear extracts. Indeed, the use of different splicing reporters and *in vitro* systems have resulted in conflicting requirements for splicing *in vivo*. In this work, we have used Y14 recruitment as a marker for examining co-transcriptional splicing on the numerous loops of the LBCs; thus, the results of this assay do not depend on any particular transgene.

***EJCs associate with the active RNAPII transcriptional units of the lampbrush chromosomes.***

In the course of our study, we used the deposition of EJCs onto nascent transcripts as an indication of splicing, as it allows the simultaneous monitoring on nuclear spreads of all RNAPII transcriptional units in the same oocyte. EJCs are recruited co-transcriptionally by the spliceosome to mark exon-exon junctions after intron removal (reviewed in [252]), and accordingly, we demonstrate here that Y14, a subunit of the EJC, targets the numerous LBC lateral loops. In the absence of the U2 snRNA, spliceosomal assembly and hence pre-mRNA splicing is inhibited [240, 257, 258], which is illustrated on nuclear spreads by the loss of Y14 from LBCs. Thus, while the association of splicing factors with chromosomal loops is well-

established, this work validates the functionality of these interactions. Interestingly, we recently obtained evidence that Magoh, another EJC subunit, distributes similarly to Y14 in the oocyte. This result was expected as Y14 and Magoh were shown previously to interact [253, 254]. We are now currently using the advantageous spatial resolution offered by LBCs, together with the fact that these chromosomes can now be visualized in *in vivo*-like conditions (Patel and Bellini, in preparation), to characterize the kinetics of association of Y14, Magoh and splicing factors with the active transcriptional units.

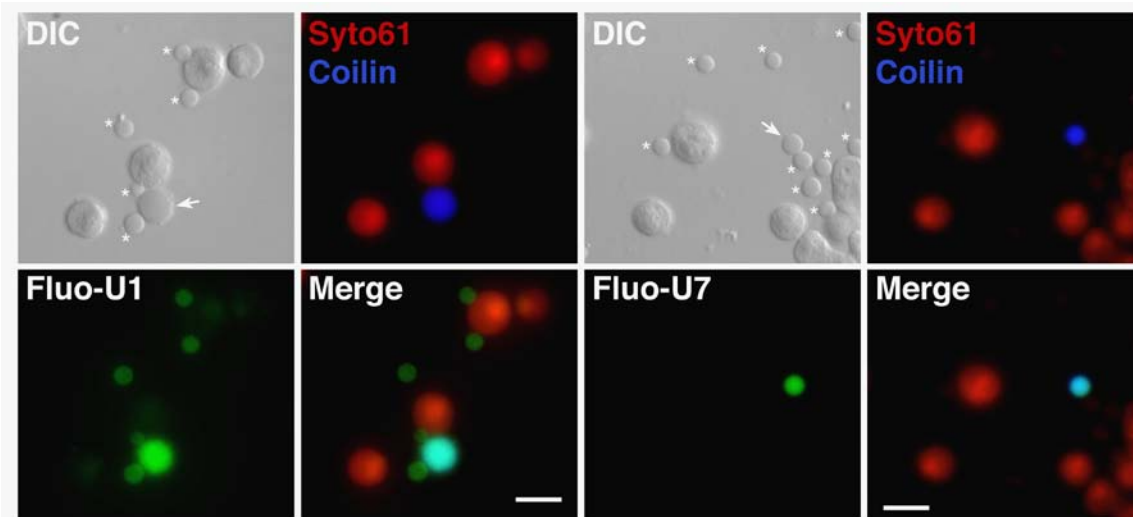


**Figure 5. Newly assembled spliceosomal snRNPs associate rapidly with CBs and SFCs.** Differential Interference Contrast (DIC) and corresponding fluorescent micrographs of nuclear spreads from oocytes injected with fluorescent U1 or U7 snRNAs, respectively (green). Organelles are readily distinguished by their morphology with DIC and specific probes. Here, the DNA specific dye Syto61 was used to label nucleoli (red), while the anti-coilin antibody (mAb H1) was used to label CBs (blue, arrows). Newly made fluorescent U1 snRNP is detected in both CBs and SFCs (asterisks) as early as 1 hour after cytoplasmic injection of fluorescent U1 snRNA. In contrast, a newly assembled fluorescent U7 snRNP, which is not involved in splicing, accumulates exclusively within CBs. In both cases nucleoli are negative. Scale bars are 5  $\mu\text{m}$ .

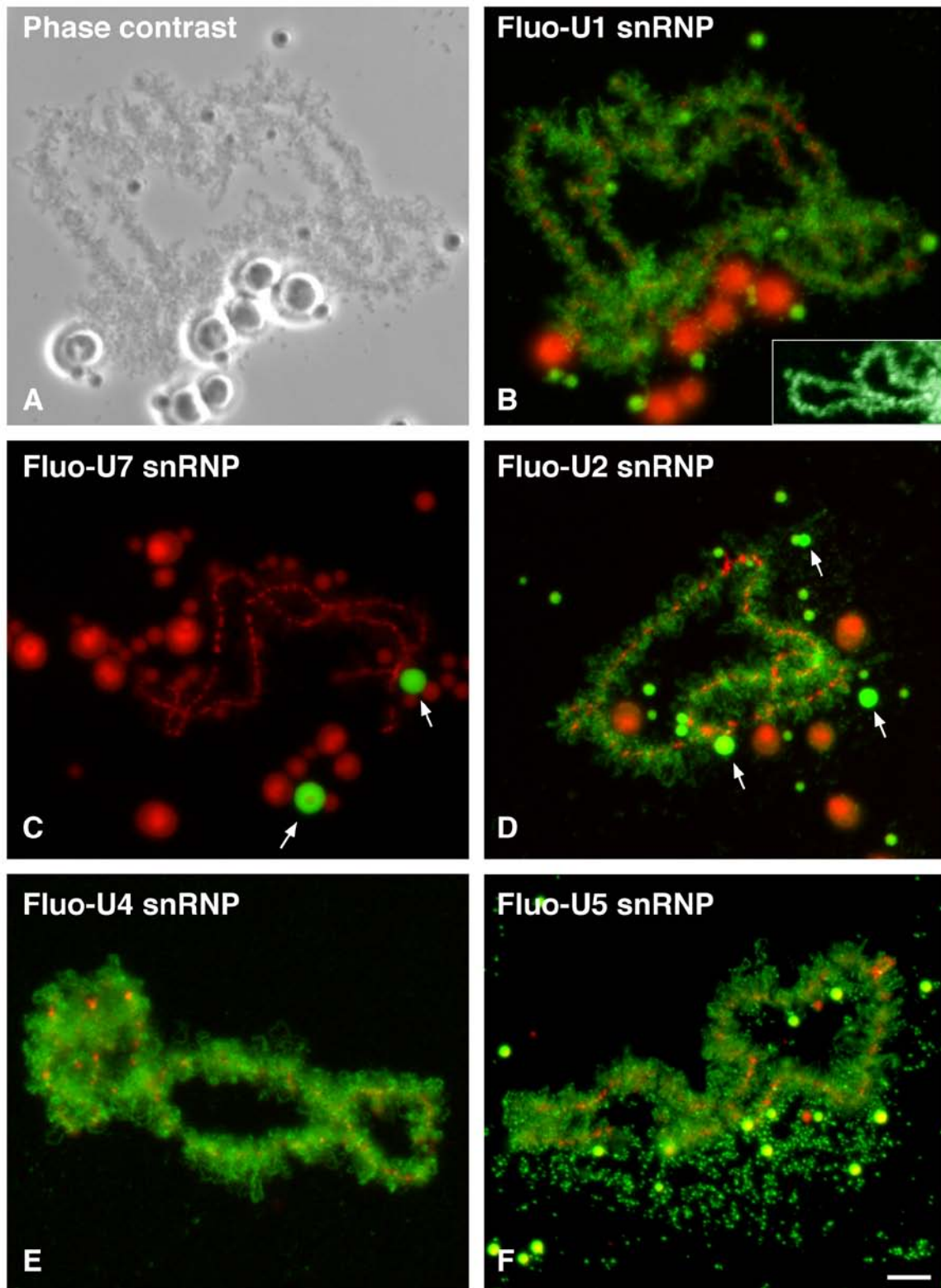
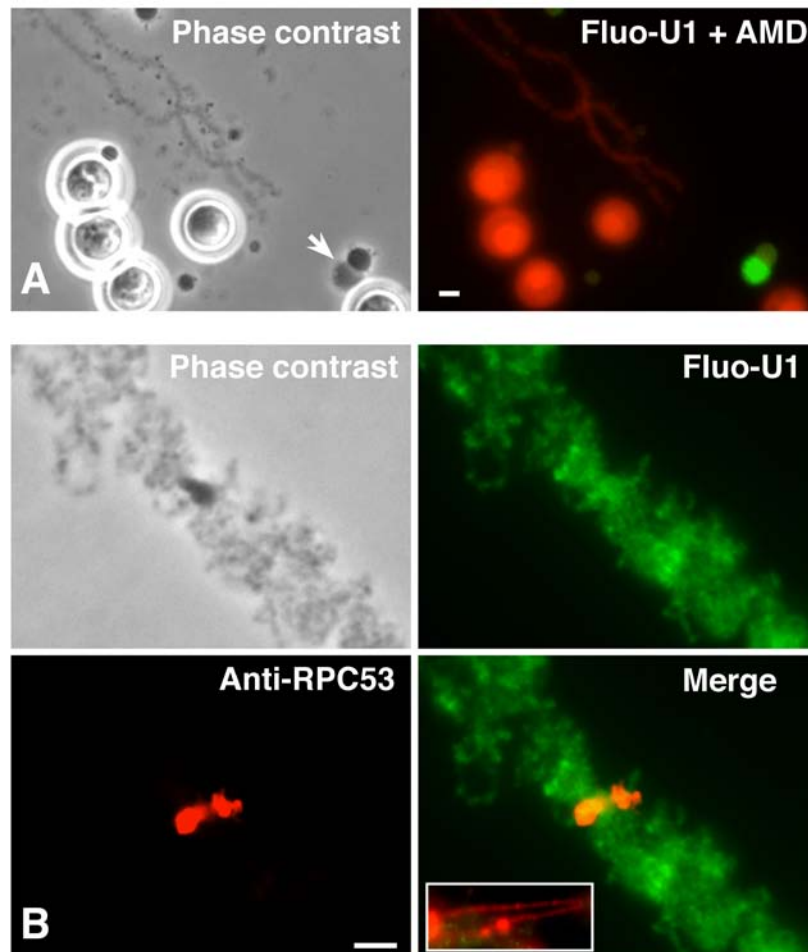


Figure 6 (cont. on next page)

---

**Figure 6. Association of newly made fluorescent spliceosomal snRNPs with active transcriptional units.** *In vitro* transcribed snRNAs were injected into the cytoplasm of stage V oocytes, and nuclear spreads were prepared 18 hours later. In all preparations, the DNA was counterstained with DAPI, pseudo-colored here in red. The fluorescent snRNA signal is shown in green. **A and B)** A phase contrast image and its corresponding fluorescent image are presented for the U1 snRNP. **C-F)** Fluorescent images are shown for U7, U2, U4 and U5 snRNPs. Consistent with the distribution of the endogenous splicing snRNPs, the newly assembled U1, U2, U4 and U5 snRNPs were detected in SFCs, CBs (arrows), and on the loops of the LBCs. The inset in **B** corresponds to a laser scanning confocal image of several chromosomal loops showing the association of the U1 snRNP with the nascent RNP fibrils. **C)** The non-spliceosomal U7 snRNP accumulated in CBs but was absent from SFCs and the chromosomal loops. Note that DAPI labels well Nucleoli and to a lesser extent SFCs (most likely because of their high content in RNAs), which are structures of  $\sim 1 \mu\text{m}$  in diameter. DAPI also labels well the chromosomal axes, which correspond to transcriptionally inactive domains. Scale bar is  $10 \mu\text{m}$ .

---



**Figure 7. Newly assembled snRNPs associate with RNAPII but not RNAPIII nascent transcripts.** Phase contrast and corresponding fluorescent micrographs of nuclear spreads from oocytes injected 18 hours earlier with fluorescent U1 snRNA (green). **A)** Oocytes were treated with actinomycin D (AMD) for 1 hour before nuclear spread preparation. Phase contrast shows one of the 18 LBCs, which are devoid of lateral loops as a result of transcription inhibition. Fluorescent U1 snRNP associates with CBs (arrow) and SFCs but fails to target chromosomes. The chromosomal axis and nucleoli are counterstained with DAPI (pseudo-colored in red). **B)** An anti-RPC53 antibody was used to identify the ~90 RNAPIII transcriptional sites. One such RNAPIII locus is shown here (red) to illustrate the fact that newly assembled fluorescent U1 snRNPs are not recruited there. Note that this locus is not visible by phase contrast. If many RNAPIII loci appear as rather amorphous structures like the one presented here, several others tend to display long lateral loops. One such loop is presented in the inset at the same magnification. Notice that no green signal is associated with the loop. Scale bars are 5  $\mu\text{m}$ .



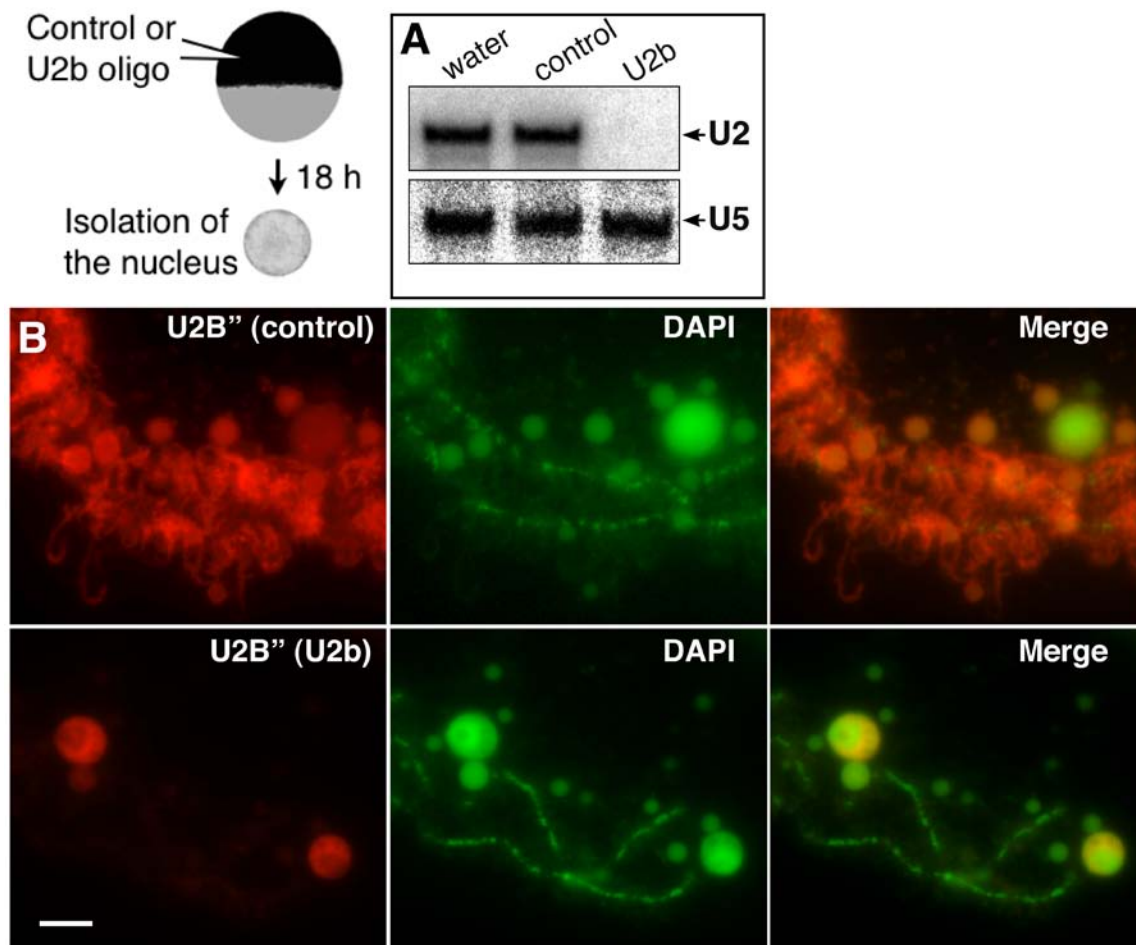


**Figure 8. Depletion of the U2 snRNA inhibits U2B'' targeting to chromosomal loops.** **A)** Northern blot analysis indicates that U2 snRNA is completely depleted in U2b oligonucleotide injected oocytes but is unaffected in control oocytes that were injected with the Control oligonucleotide or just water. Each lane was loaded with the total RNA fraction of one nucleus isolated 18 hours after injection. U5 snRNA was used here as a loading control. **B)** Fluorescent micrographs of nuclear spreads prepared 18 hours after injection with either the U2b or the C oligonucleotide. The U2 specific protein U2B'' was detected using mAb 4G8 (green). In control oocytes, U2B'' is found associated with the nascent transcripts of the chromosomal loops as well as with SFCs. Nucleoli are also weakly stained. In U2b injected oocytes, U2B'' is no longer detected on the chromosomal loops or the SFCs. Instead the granular region of nucleoli is brightly labeled. DAPI is pseudo-colored in red. Scale bar is 5  $\mu$ m.

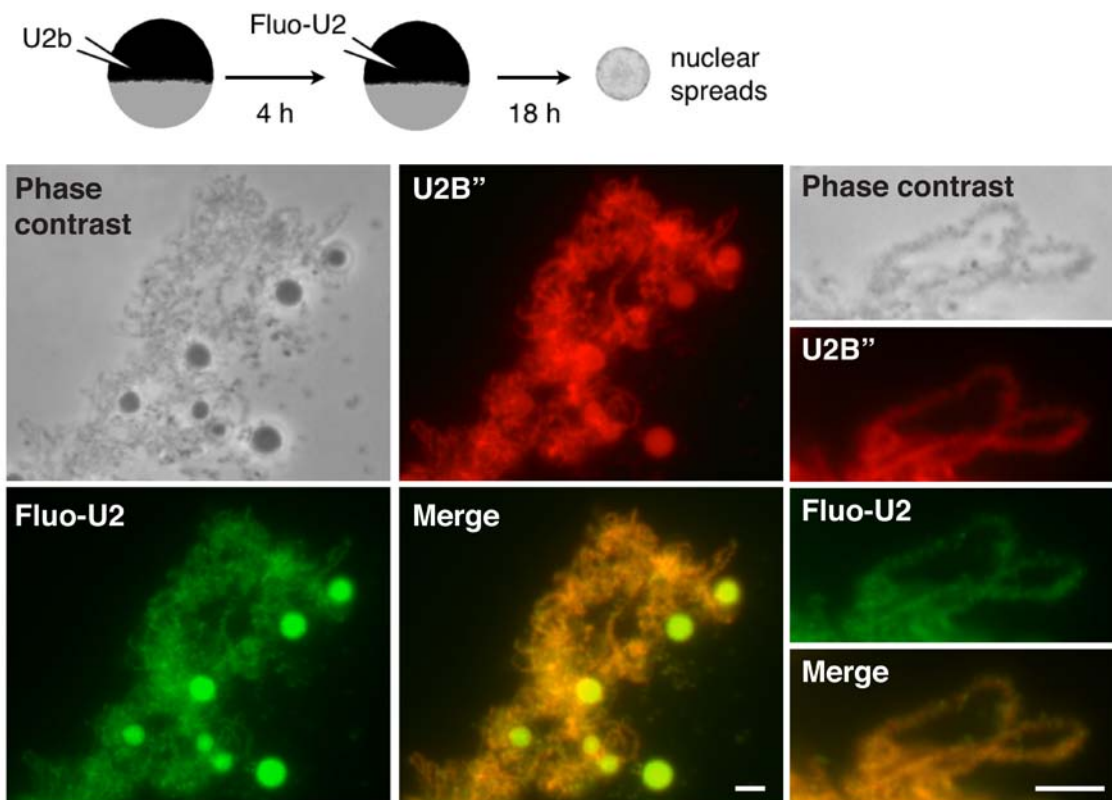


**Figure 9. Newly formed fluorescent U2 snRNP rescues the association of U2B'' with nascent transcripts and SFCs in U2-depleted oocytes.** Phase contrast and corresponding fluorescent micrographs of nuclear spreads from oocytes injected with U2b and fluorescent U2 snRNA as indicated in the diagram. U2B'' was detected using mAb 4G8 (red) and displays an extensive colocalization with fluorescent U2 snRNA (green) on both chromosomal loops and SFCs. Scale bars are 2  $\mu$ m.

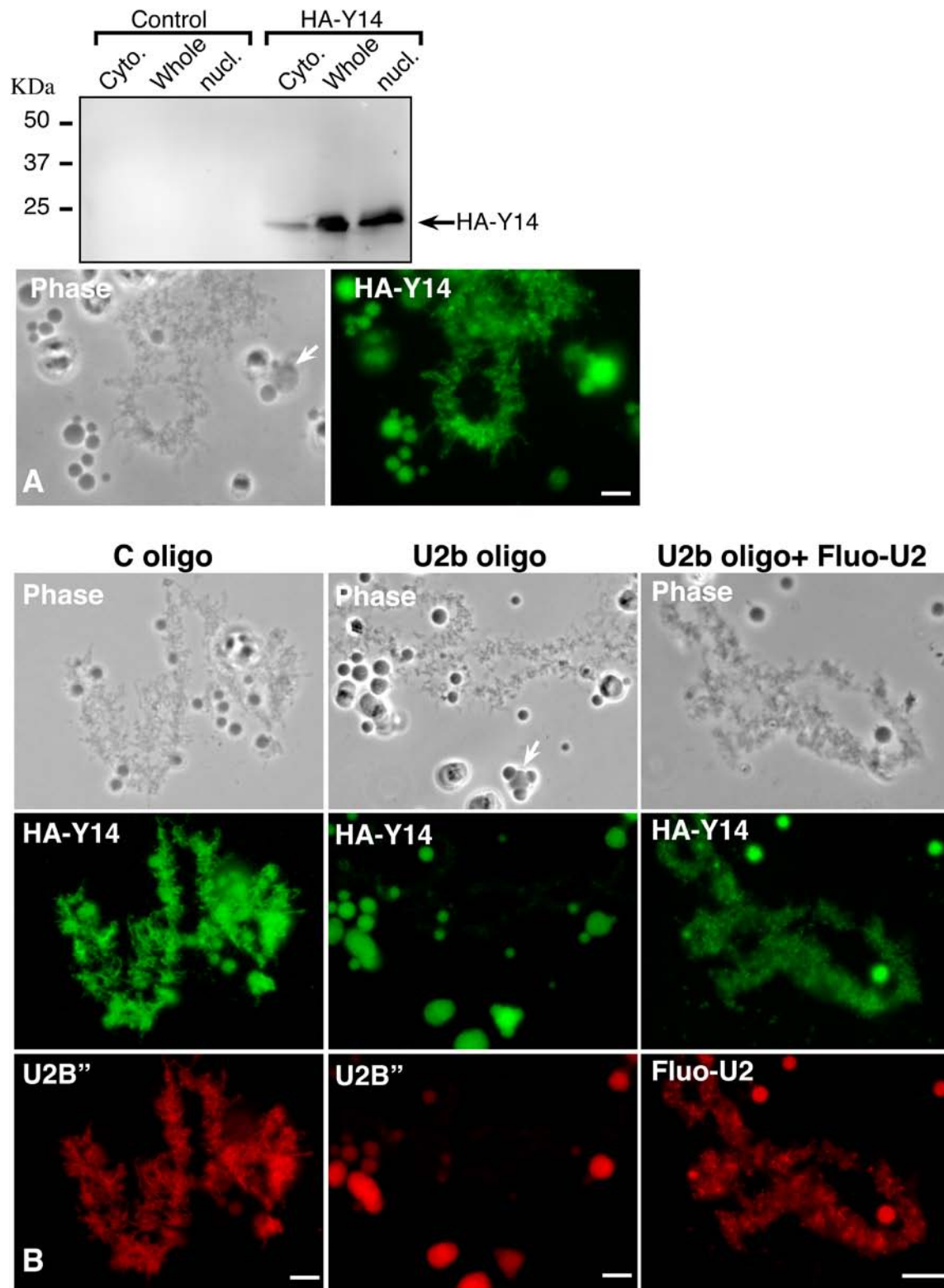


Figure 10 (cont. on next page)

---

**Figure 10. Y14 is not recruited to nascent transcripts in the absence of the U2 snRNA. A)** The fate of newly expressed HA-Y14 was followed in stage V oocytes using the anti-HA antibody mAb 3F10, 48 hours after the injection of its corresponding transcript. A single band of ~24 KDa, which is primarily nuclear, is detected on immunoblots. On nuclear spreads, HA-Y14 (green) associates strongly with CBs (arrow) as well as with the nascent transcripts on chromosomal loops. SFCs and the dense fibrillar region of nucleoli are weakly stained. **B)** Phase contrast and corresponding fluorescent micrographs of nuclear spreads from oocytes co-injected with HA-Y14 transcripts and either the C oligo or the U2b oligo. In the rescue experiment, fluorescent U2 snRNA was injected 18 hours later. All nuclear spreads were prepared 48 hours after the initial injections. The distribution of HA-Y14 (green) and U2B<sup>''</sup> (red) were defined using mAb 3F10 and mAb 4G8 respectively. In U2 snRNA depleted oocytes (U2b injected), HA-Y14 is still found within CBs (arrow), SFCs, and nucleoli, but it is absent from chromosomal loops. In these oocytes, U2B<sup>''</sup> accumulates within nucleoli. Remarkably, the chromosomal association of HA-Y14 is rescued by fluorescent the U2 snRNA (pseudo-colored in red). Scale bars are 5  $\mu$ m.

---

## CHAPTER III

### SPLICING INDEPENDENT RECRUITMENT OF SPLICEOSOMAL snRNPS TO NASCENT RNAPII TRANSCRIPTS

#### **Introduction**

While data on the spatial and temporal recruitment of splicing factors onto a template pre-mRNA abound, very little is still known about the essential characteristics of a spliceosomal snRNP that contribute *in vivo* to its association with nascent transcripts. Previous work on U1 and U2 snRNPs highlighted the importance of the base pairing of their RNA moieties to cis-acting sequences on pre-mRNAs, the intronic 5' splice site (5'-SS) and the branch point sequence (BPS), respectively [259-262]. In the case of the U1 snRNP, however, it was shown that the base pairing of its 5' end with 5'-SS is only one of several interactions that contribute to the formation of a U1 snRNP/pre-mRNA complex [263] and occurs after an initial recruitment of the U1 snRNP [264]. Interestingly, the cleavage of the 5' end of the U1 snRNA has no effect on the rate of association of the U1 snRNP with a consensus 5' SS RNA oligonucleotide *in vitro* [265]. Rather, the recognition of the 5'-SS by the U1 snRNP appears to be driven by its overall protein complement. Which of the several U1 snRNP proteins and which sequence element(s) of the U1 snRNA are critical for its targeting to nascent transcripts is still unclear, however. The same question also remains unanswered for the other spliceosomal snRNPs, and in light of their complex intranuclear trafficking prior to engaging pre-mRNA splicing (reviewed in [50]), it cannot be addressed directly using *in vitro* systems.

With our new targeting assay, we demonstrated that non-functional forms of U1 and U2 snRNAs still associate with the active transcriptional units. In particular, we showed that their

association with nascent RNP fibrils is independent of their base pairing with pre-mRNAs. Additionally, stem loop I of the U1 snRNA was identified as a discrete domain that is both necessary and sufficient for association with nascent transcripts. Finally, in oocytes deficient in splicing, the recruitment of U1, U4, and U5 snRNPs to transcriptional units was not affected. Taken together, these data indicate that the recruitment of snRNPs to nascent transcripts and the assembly of the spliceosome are uncoupled events.

## **Results**

### ***Non-functional U1 and U2 snRNPs are still recruited to nascent transcripts.***

U1 and U2 snRNPs are thought to be involved early in the stepwise formation of the spliceosome onto a target pre-mRNA, and they both display a short sequence that hybridizes to the 5' splice site (5'-SS) or the branch point sequence (BPS) of an intron, respectively (reviewed in [266]). In the case of the U1 snRNA, the 5'-SS recognition sequence (SSR) lies within its first 20 nucleotides. To test whether the recruitment of the U1 snRNP to transcriptional units requires its hybridization with pre-mRNAs, a fluorescent U1 snRNA truncated from its first 20 residues, U1( $\Delta$ SSR) snRNA, was synthesized and injected into the cytoplasm of *Xenopus* oocytes. It was established that the removal of these residues of the U1 snRNA does not prevent the assembly of a U1( $\Delta$ SSR) snRNP with its full protein complement [263, 265], and as expected, the newly made U1( $\Delta$ SSR) snRNP was rapidly recruited to the nucleus. Interestingly, in addition to accumulating within CBs and SFCs, the U1( $\Delta$ SSR) snRNP targeted the chromosomal loops just as well as the full length U1 snRNP (Figure 11). A similar deletion analysis was carried out for the U2 snRNP, in which the BPS recognition sequence (BPR) was removed. Such a U2( $\Delta$ BPR) snRNA can no longer engage splicing by hybridizing with an intronic BPS, yet the newly formed

U2( $\Delta$ BPR) snRNP associates with chromosomal loops as well as with CBs and SFCs, identically to wild-type U2 snRNP (Figure 11). Together, these data demonstrate that the recruitment of U1 and U2 snRNPs to nascent transcripts is not directed by the hybridization of their snRNA moieties to cis-acting signals on pre-mRNAs. Importantly, they also highlight the fact that the association of U1 and U2 snRNPs with elongating transcripts can be uncoupled from their function in splicing.

In the case of the U2 snRNP, its splicing activity depends greatly on the modification of the U2 snRNA by 2'-O-methylation and pseudouridylation [227, 240]. In particular, the modification of several residues within the first 29 nucleotides of the U2 snRNA is critical for the formation of a mature 17S snRNP particle [240]. Thus, we produced a fluorescently labeled U2 snRNA deleted of these residues, U2( $\Delta$ 29) snRNA, injected it into the cytoplasm of stage V oocytes, and analyzed its nuclear distribution 18 hours later on nuclear spreads. Figure 13 shows that the newly assembled U2( $\Delta$ 29) snRNP associates well with the chromosomal loops, further supporting the idea that the association of snRNPs with active RNAPII transcriptional units is independent of their ability to engage splicing. In addition, SFCs are brightly labeled, but surprisingly, CBs appear to be only weakly stained (see white arrow in Figure 13), especially when the fluorescent signal is compared to that of the full length U2 snRNP (see Figure 6). Since CBs are implicated in the internal modification of the spliceosomal snRNAs, one possible explanation is that the lack of the first 29 residues, among which many are modified, renders the U2( $\Delta$ 29) snRNA a poor substrate for the modification machinery and as a result reduces its overall residence time within CBs.

***Targeting of U1 snRNP to nascent transcripts and SFCs is directed by stem loop I.***

Three proteins are known to be specific for the U1 snRNP: U1A, U1C, and U1-70K. Both U1-70K and U1A bind directly to the U1 snRNA through stem loop I and II, respectively, while U1C interacts with U1-70K [267, 268]. Because U1C was previously implicated in the association of the U1 snRNP with pre-mRNAs *in vitro* [269], we tested whether the deletion of stem loop I would impact on the subnuclear distribution of the U1 snRNP. The first 47 residues of U1 were deleted, and the resulting mutant U1( $\Delta$ 47) snRNA was injected into the cytoplasm of stage V oocytes. Nuclear spreads were prepared 18 hours later. Figure 12A shows that U1( $\Delta$ 47) snRNP accumulates in CBs but fails to associate with both SFCs and the nascent transcripts on chromosomal loops. Since the removal of the first 20 residues of the U1 snRNA does not disrupt its chromosomal targeting (Figure 11), we concluded that stem loop I is the structure present within the first 47 nucleotides that is critical for the association of the U1 snRNP with nascent transcripts. To test that idea, we constructed a chimeric RNA by fusing stem loop I to the 3' end of the U7 snRNA, which is exclusively found associated with CBs (Figures 5 and 6). The resulting U7/U1(I) snRNA was injected into stage V oocytes and its subnuclear distribution analyzed on nuclear spreads (Figure 12B). Remarkably, stem loop I alone is sufficient to promote the targeting of the U7 snRNP to chromosomal loops and SFCs. Surprisingly, CBs are only weakly labeled (white arrows). This result was unexpected as the U7 snRNP is known to accumulate in CBs at very high concentrations [245, 270] and suggests that stem loop I is important to regulate the kinetics of U1 snRNP exchange between CBs and the nucleoplasm.



***Spliceosomal assembly on nascent transcripts is not required to recruit snRNPs.***

The observation that several mutant U1 and U2 snRNPs, which cannot participate in the assembly of the spliceosome, still target chromosomal loops prompted us to ask whether the association of snRNPs with active transcriptional units could be uncoupled from the splicing reaction itself. An efficient way to inhibit pre-mRNA splicing is to deplete the oocyte of U2 snRNAs using an antisense oligonucleotide-RNase H degradation strategy [240, 271]. In absence of the U2 snRNP, the formation of the A complex (a spliceosomal intermediate containing both U1 and U2 snRNPs) and, hence, splicing itself is inhibited [240, 257, 258]. Importantly, splicing can be rescued by a cytoplasmic injection of *in vitro* made U2 snRNAs [239, 240].

Finally, we tested whether U1, U4, and U5 snRNPs could still be recruited to transcriptional sites in absence of any splicing activity. It was shown previously that the presence of a fully functional U1 snRNP is critical to transcription and, hence, to the maintenance of chromosomal loops in amphibian oocytes [271]. As expected, we found that the U1 snRNP still associates with the nascent transcripts of the chromosomal loops in U2 snRNA-depleted oocytes (Figure 14). This result is also consistent with an early recruitment of the U1 snRNP to the pre-mRNA template as it would be in the canonical model of splicing, which proposes a stepwise assembly of the spliceosome. In such a model, the U4/U6.U5 tri snRNP is recruited only after the formation of the A complex. While the U5 snRNP is commonly used as a representative member of the U4/U6.U5 tri-snRNP, it is present in both the major (U2-type) and the minor (U12-type) spliceosomes. Thus, the U4 snRNP, a specific member of the U2-type spliceosome, was also used here as a marker of the U4/U6.U5 tri-snRNP. Surprisingly, in the

absence of the U2 snRNP, the U4/U6.U5 tri-snRNP is still recruited to nascent transcripts (Figure 14), indicating that the A complex is not required. Together, these data demonstrate that the splicing activity present on the chromosomal loops does not direct the association of snRNPs with nascent RNP fibrils.

## **Discussion**

### ***The recruitment of U1 and U2 snRNPs to nascent RNP fibrils is independent of their base-pairing with pre-mRNAs.***

The removal of most introns requires a conserved 5'-SS, a BPS followed by a polypyrimidine tract, and a 3' splice site (3'-SS). While current models propose that the spliceosome assembles onto the target pre-mRNA in an ordered process, it is still unclear which early intermediate complexes form *in vivo* and in which order. The establishment of one of these intermediates, the A complex, involves base pairing of the U1 and U2 snRNAs to the 5'-SS and BPS, respectively. Whether the removal of the 5'-SS recognition sequence on U1 snRNA results in a non-functional U1 snRNP is difficult to assess as the requirement of the U1 snRNA itself for intron removal *in vitro* depends on the pre-mRNA template as well as the concentration of SR proteins in the chosen splicing extract [272, 273]. In addition, while some reports indicate a strict requirement of the 5' end of the U1 snRNA for intron removal [259], others present the hybridization of U1 snRNA 5' end to pre-mRNA as a non-essential stabilizing force [263] that might influence the transition between spliceosomal intermediate complexes [274]. In the case of the U2 snRNA, however, the requirement of the BPS recognition sequence for efficient pre-mRNA splicing has been well established [260-262]. Interestingly, we have shown here that U1( $\Delta$ SSR) and U2( $\Delta$ BPR) snRNAs, which cannot hybridize to introns, are assembled into

snRNPs and target the nascent transcripts on chromosomal loops. One interpretation is that the respective base pairing of U1 and U2 snRNAs with the 5'-SS and BPS is not essential for their association with nascent transcripts *in vivo*. This is in agreement with a previous work showing that the initial recruitment of the U1 snRNP to pre-mRNAs appears to be mediated by U1 snRNP proteins in a 5'-SS independent manner [265, 275]. In addition, *in vitro* studies showed that the hybridization of the U1 snRNA to target pre-mRNAs is dispensable for early intermediate formation and intron removal [275]. In particular, the U1 snRNP was recently shown to be co-transcriptionally recruited to pre-mRNAs with mutations in the 5'-SS that abolish hybridization with the U1 snRNA [264] suggesting that the 5'-SS/U1 snRNA base pairing occurs after an initial recruitment phase [263, 274]. Another possibility stems from the structural organization of the chromosomal loops. In amphibian oocytes, the RNAPII loops are readily visible by light microscopy because of their dense ribonucleoprotein matrix, which is composed of the nascent RNAPII transcripts and associated maturation factors. Surprisingly, some of these factors, such as the 3' end processing factor CstF77, are only involved in the late steps of pre-mRNA maturation [276]. The presence of CstF77 over the entire length of the loops [277], therefore, suggests that some pre-mRNA processing factors might associate with nascent RNP particles but remain inactive until the occurrence of their corresponding cis-acting RNA elements. The efficient recruitment of U1( $\Delta$ SSR) and U2( $\Delta$ BPR) snRNPs to nascent transcripts could, thus, be the result of a staging event in which snRNPs would first be recruited to the nascent RNP fibrils and be maintained there until spliceosomal assembly could occur. In this model, the initial recruitment of snRNPs would rely in part on already associated hnRNPs, such as the SR proteins, whose presence was previously shown to require intronic sequences on the pre-mRNA [278].

***U1 snRNP intra-nuclear trafficking depends on stem loop I.***

We show here that the deletion of the first 47 nucleotides of U1 snRNA, which contain both the 5'-SS recognition sequence and stem loop I, has a dramatic effect on its subnuclear distribution. The resulting U1( $\Delta$ 47) snRNP still accumulates strongly within CBs, but it fails to target SFCs and the chromosomal loops. While these data demonstrate that a discrete region of U1 snRNA is critical for its intranuclear trafficking, it also raises the question of how stem loop I regulates the association of the U1 snRNP with two subnuclear domains that are distinct in structure and functions. The lack of association of the U1( $\Delta$ 47) snRNP with nascent RNP fibrils could be due in part to the fact that the U1C protein cannot associate with the U1( $\Delta$ 47) snRNA in the absence of stem loop I [269]. U1C was previously implicated in the binding of pre-mRNAs by the U1 snRNP [265, 279, 280], and its absence from a U1( $\Delta$ 47) snRNP could, thus, result in the loss of chromosomal targeting. There is no pre-mRNA splicing activity occurring in SFCs, however. Instead, one demonstrated function of these nuclear bodies is to serve as reservoirs for RNAPII maturation factors, which are subsequently recruited to active transcriptional sites [281]. In light of the current model in which newly assembled snRNPs transit through CBs for modification and assembly prior to their association with SFCs [22, 50, 277], an attractive possibility is, then, that stem loop I is essential to regulate kinetic exchanges of the U1 snRNP between CBs and the nucleoplasm. In particular, stem loop I might be essential for U1 snRNP to exit CBs. Interestingly, we showed that stem loop I is not only sufficient to direct the association of the non-spliceosomal U7 snRNP to nascent transcripts and SFCs, but it also modifies the association of the U7snRNP with CBs. Indeed, while the normal fluorescent U7 snRNP accumulates greatly in CBs, this association is dramatically reduced by its fusion with stem loop I. Importantly, the chromosomal association of chimeric U7/U1(I) snRNP

demonstrates that a snRNP, which cannot participate in splicing, can be targeted to nascent transcripts. In agreement with this idea, we find that both U2( $\Delta$ BPR) and U2( $\Delta$ 29) snRNPs, which are non-functional [240, 260-262], are recruited efficiently to nascent transcripts.

***The recruitment of snRNPs onto nascent transcripts is splicing independent.***

A model in which the recruitment of snRNPs and spliceosomal assembly are uncoupled *in vivo* is further supported by our finding that the U1 snRNP and the U4/U6.U5 tri-snRNP still associate with the chromosomal loops when pre-mRNA splicing is inhibited by the depletion of the U2 snRNA. Because current paradigms for spliceosome assembly command a stable binding of the U2 snRNP to the BPS prior to the engagement of the U4/U6.U5 tri-snRNP, a likely explanation to these data is that the U4/U6.U5 tri-snRNP targets the nascent transcripts but does not engage in splicing even when the cis-acting RNA elements become available during transcription elongation, yet one cannot exclude two other interesting possibilities. The first one is that the U4/U6.U5 tri-snRNP was previously shown to recognize the 5'-SS in the absence of the U2 snRNP *in vitro* [282]. In addition, the U5 snRNP was demonstrated to interact with the 5'-SS before the start of splicing [283], and more recently, the U4/U6.U5 tri-snRNP, together with the U1 snRNP, was proposed to comprise part of a very early intermediate that presumably plays an important role in defining the 5'-SS [284]. Thus, the observed recruitment of the U1 snRNP and the tri-snRNP to chromosomal loops in the absence of the U2 snRNP might reflect the formation and stalling of this early intermediate form on nascent transcripts. The second one is coming from the development over the last decade of a different model for spliceosome assembly. A large RNP complex, named the penta-snRNP, containing all five splicing snRNPs in equal stoichiometric abundance and at least 13 other proteins, was purified in yeast [285], and

a similar complex was found in mammals [44]. The penta-snRNP forms in absence of a pre-mRNA template and, thus, challenges the canonical view of step-wise assembly of the spliceosome. Importantly, when supplemented with a snRNP depleted extract, the penta-snRNP was competent to splice synthetic substrates as a unitary particle, providing evidence for a preassembly model of splicing wherein all five snRNPs engage the pre-mRNA in one step as a single complex [285]. Therefore, another interpretation of the U1 snRNP and the tri-snRNP association with chromosomal loops in absence of splicing is that snRNPs are recruited to the nascent transcripts as part of a pre-assembled complex. In that case, however, one would have to assume that such complex could be formed and recruited to the transcriptional units without the U2 snRNP. Interestingly, a model in which the splicing machinery is staged directly on the transcriptional unit implies some level of pre-assembly of the splicing machinery before or directly onto the nascent RNP fibrils. Importantly, such a paradigm does not antagonize the canonical view of an ordered assembly process of the spliceosome onto intronic sequences, as the various spliceosomal intermediates could form by recruitment of the splicing factors already associated with nascent transcripts onto the cis-acting RNA elements during transcription elongation.

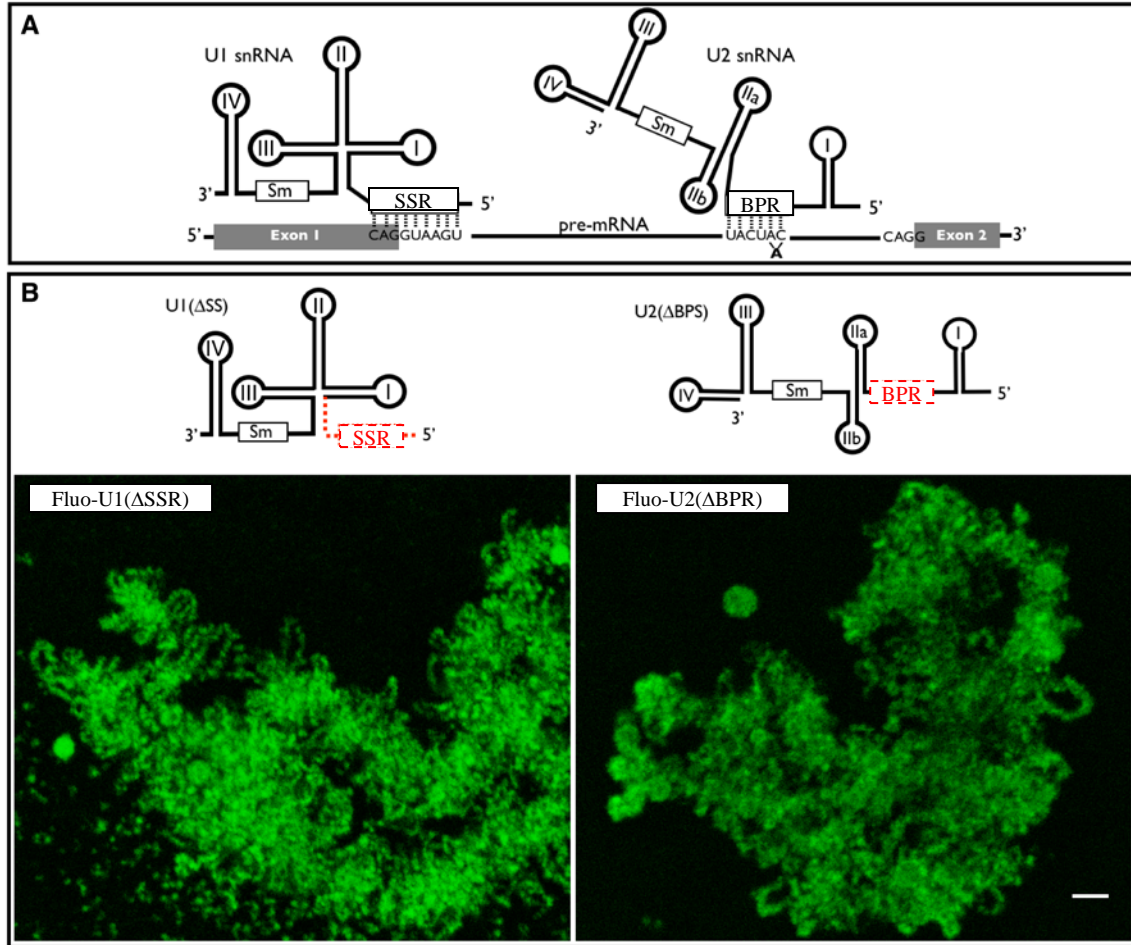


**Figure 11. Mutant U1 and U2 snRNAs that cannot engage splicing are still recruited to active transcriptional units.** U1( $\Delta$ SSR) and U2( $\Delta$ BPR) snRNAs (green) were injected into the cytoplasm of stage V oocytes, and nuclear spreads were prepared 18 hours later. **A)** Diagram shows the regions of the U1 and U2 snRNAs involved in interacting with pre-mRNA. **B)** Diagram shows the regions deleted (in red dashed lines) in the mutant U1( $\Delta$ SSR) and U2( $\Delta$ BPR) snRNAs. Laser scanning confocal images showing the association of U1( $\Delta$ SSR) and U2( $\Delta$ BPR) snRNPs with the nascent transcripts of the chromosomal loops. Scale bar is 5  $\mu$ m.

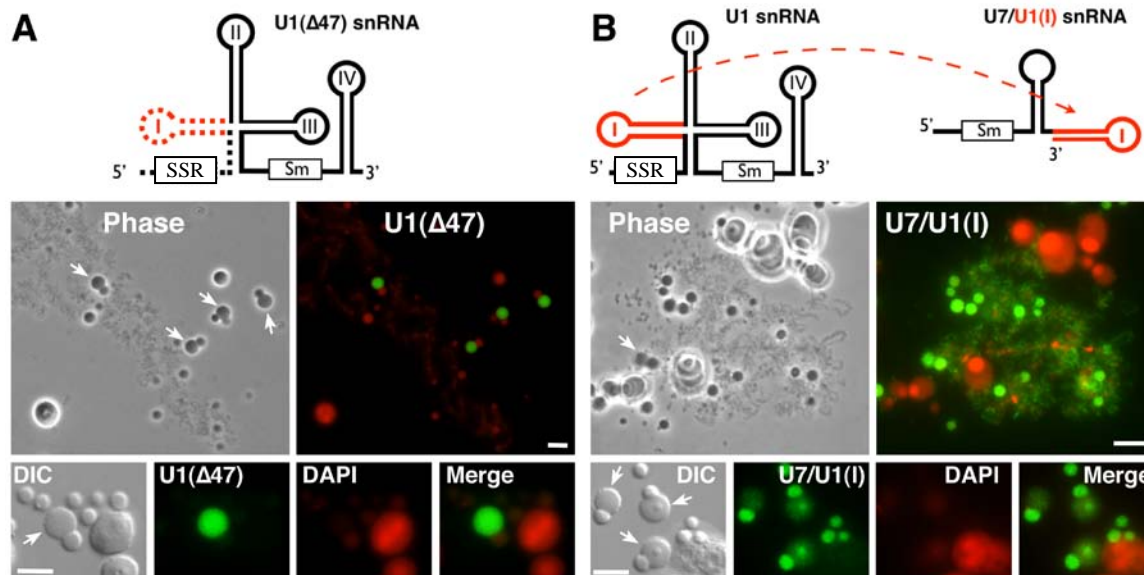


**Figure 12. The first stem loop of the U1 snRNA is necessary and sufficient for its association with SFCs and nascent RNP fibrils.** Phase contrast, or DIC, and corresponding fluorescent micrographs of nuclear spreads from oocytes injected 18 hours earlier with either (A) mutant U1( $\Delta$ 47) RNA or (B) chimeric U7/U1(I) RNA (green). A diagram above each panel indicates the structure of the corresponding RNAs. The deleted residues in U1( $\Delta$ 47) are indicated in a dashed line. Stem loop I is colored in red. The newly assembled U1( $\Delta$ 47) snRNP targets CBs (arrows) but fails to associate with chromosomal loops and SFCs. In contrast, the U7/U1(I) snRNP associates with nascent RNP fibrils and SFCs in addition to CBs. A group of CBs, SFCs, and nucleoli are presented at a higher magnification in both cases. Note that the signal resulting from the association of U7/U1(I) snRNP with CBs is very weak. Dapi (pseudocolored in red) was used here to counterstain nucleoli and chromosomal axes. Note that SFCs are weakly labeled due to their high RNA content. Scale bars are 10  $\mu$ m.



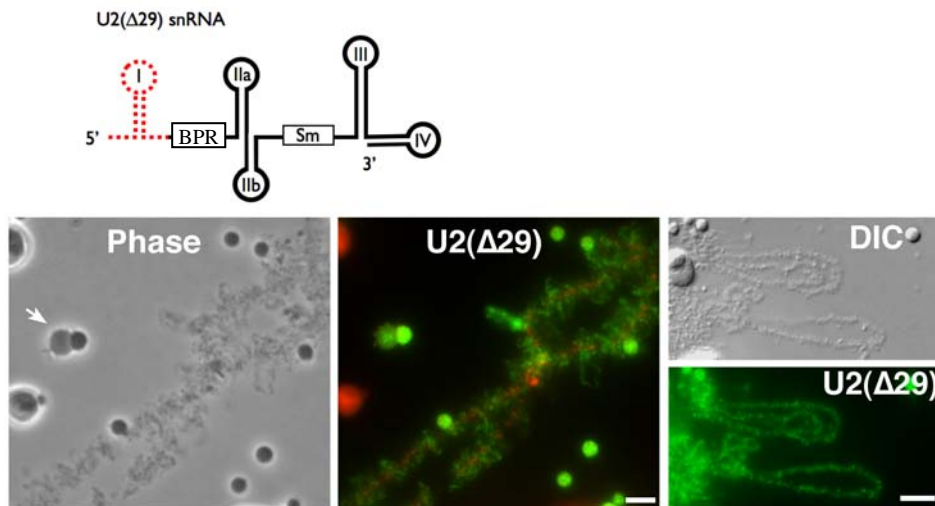


**Figure 13. A non-functional U2 snRNP targets nascent RNP fibrils.** Phase contrast, or DIC, and corresponding fluorescent micrographs of nuclear spreads from an oocyte injected 18 hours earlier with fluorescent U2( $\Delta$ 29) snRNA (green). The newly assembled U2( $\Delta$ 29) snRNP is recruited to CBs (arrows), SFCs and the chromosomal loops. Note that the labeling of CBs is dramatically reduced when compared to full length U2 snRNA (see Figure 6). Chromosomal axes and nucleoli were counterstained with DAPI (pseudo-colored in red). Scale bars are 5  $\mu$ m. The diagram shows (dashed red line) the deleted region of U2 snRNAs.

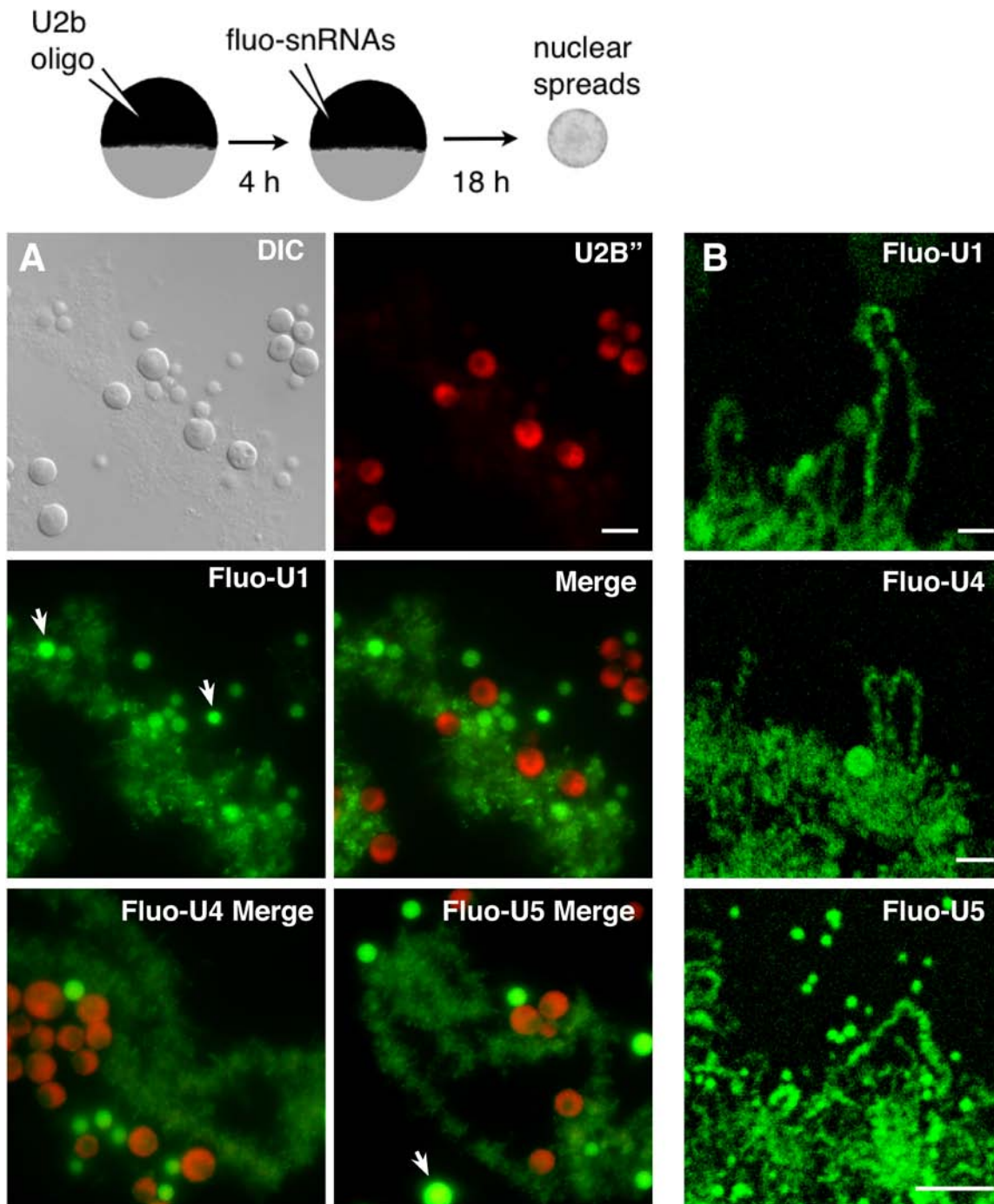


Figure 14 (cont. on next page)

---

**Figure 14. Spliceosomal U1, U4, and U5 snRNPs target LBC loops in the absence of splicing.** Fluorescent U1, U4, or U5 snRNAs were injected into the cytoplasm of stage V oocytes previously depleted of their endogenous U2 snRNA. Nuclear spreads were prepared 18 hours later and the distribution of the newly assembled snRNPs (green) determined by fluorescence microscopy. **A)** In all three cases, a signal was associated with the chromosomal loops as well as with CBs (arrows) and SFCs. Thus, the targeting of the U1 snRNP and the U4/U6.U5 tri-snRNP to nascent transcripts does not require the presence of the U2 snRNP. U2B'' (red) is detected using mAb 4G8 and is found accumulated in the granular region of nucleoli, which is indicative of an efficient U2 snRNA depletion. Scale bar is 10  $\mu\text{m}$ . **B)** Magnified views (laser scanning microscopy) of particularly extended chromosomal loops that illustrate the association of newly assembled snRNPs with nascent transcripts. Scale bars are 1  $\mu\text{m}$ .

---

## CHAPTER IV

### LIVE IMAGES OF RNA POLYMERASE II TRANSCRIPTIONAL UNITS

#### **Introduction**

Contrary to our initial belief that DNA is static and lifeless, the nuclear genome, in the context of assembled chromatin, takes center stage today as perhaps the most complex structure in the cell being capable of extraordinary conformational plasticity, dynamic exchanges with the soluble nucleoplasm, and serving as nucleolar organizers. Indeed, a variety of metabolic processes occurs directly on chromatin itself and changes with external stimuli or during the cell cycle. These processes include DNA replication, recombination, and repair, as well as RNA transcription and processing and sister chromatid cohesion and separation. In turn, they are regulated, at least partially, by the dynamic architecture of chromatin. The study of these processes in live cells is of great interest, but efforts have been hampered by the difficulty in ascertaining the localization of fluorescent molecules to chromatin, rather than the surrounding nucleoplasmic background. Second, somatic systems do not offer the spatial resolution to examine chromatin by light microscopy. In contrast, the giant lampbrush chromosomes (LBCs) of amphibian oocytes can be as large as 100 $\mu\text{m}$  in length and the transcriptionally active lateral loops can be as long as 5 $\mu\text{m}$  along their contour (excellently reviewed in [236]). Each chromosomal loop corresponds to a DNA axis actively transcribed by RNAPII and surrounded by tightly packed nascent RNP fibrils. However, until now, they have only been visualized on fixed nuclear spread preparations or in thin sections of the oocyte. The standard preparation of nuclear spreads to visualize LBCs, however, results in a complete loss of the nucleoplasm and, thus, prevents *in vivo* studies of the LBCs and associated loops. The large size of amphibian

oocytes (0.8-1.2mm diameter) and their abundance of cytoplasmic pigment compromise the working distance of the microscope objective and present a barrier to the penetration of light, respectively, and, thus, cannot be used for high-resolution live cell microscopy.

The breakthrough came with the simple yet effective finding that nuclei isolated in mineral oil can be flattened between a microscope slide and a cover glass to permit a direct *in vivo* observation of the nuclear organelles by light microscopy [52]. Oil-isolated nuclei maintain their structures and functions for many hours [286, 287]. In particular, the structural integrity of the nuclear bodies and the nuclear pore complexes (NPCs) is maintained as determined by electron and light microscopy. In addition, these nuclei are active in transcription, recombination, and pre-mRNA splicing. Furthermore, when supplemented with cytoplasmic extract, their nuclear envelope supports nucleo-cytoplasmic exchanges. They were used to study the steady-state dynamics of several components of the CB [52, 235, 288], a nuclear organelle implicated in the transcription and processing of all nuclear RNAs (reviewed in [289]). Furthermore, the physical structure of CBs and two other organelles, nucleoli and SFCs, were also analyzed [290]. While all the nuclear organelles were readily identifiable, LBCs remained elusive.

During our previous studies on spliceosomal snRNP trafficking, we often left oil-isolated nuclei in an 18°C incubator overnight and examined them again the next day. On one such occasion, we found structures that bore striking resemblance to bivalent chromosomes without lateral loops. This observation came as quite a surprise since LBCs were not supposed to be visible under these conditions. It was speculated that the refractive index of LBCs was very close to mineral oil and would not refract light.

Here, we show that the apparent lack of LBCs from oil-isolated nuclei is due to their extensive damage during sample preparation. We also detail an improved preparation method that preserves chromosomal integrity, and we use it to present the very first images of LBCs in intact, unfixed nuclei. We show that these chromosomes are morphologically identical to those observed in nuclear spread preparations. Remarkably, their lateral loops are readily observable by difference interference contrast (DIC) microscopy, which represents the very first visualization of RNAPII transcription units in a live nucleus.

## **Results**

### ***The isolation of nuclei in oil does not modify nuclear structure.***

When oil-isolated nuclei are directly flattened under a cover glass for observation by light microscopy as described [52], organelles such as CBs, nucleoli, and SFCs display normal morphology (Figure 15). In contrast, we find that LBCs are difficult to observe because of extensive physical damage. Indeed, LBCs are stretched beyond their elasticity limit, resulting in many breaks and the anomalous presence of very thin chromatin fibers (Figure 15A), which can be labeled with DNA dyes such as DAPI. We further demonstrate that this dramatic structural change is due to the apposition of the cover glass rather than the isolation of the nucleus in mineral oil itself. Oil-isolated nuclei from stage V oocytes were left in oil at 18°C for several hours and subsequently recovered into a physiological buffer for nuclear spread preparations. Figure 15B shows that LBCs from these nuclei display a normal architecture. In particular, the lateral loops are readily distinguishable over the entire length of both homologues, and there is no obvious alteration of the chromosomal axes, highlighted here by DAPI staining.

### ***Visualization of LBCs in oil-isolated nuclei.***

These findings prompted us to alter the flattening step during sample preparation to prevent mechanical disruption of the LBCs. We find that a very effective modification is the insertion of a spacer of ~20  $\mu\text{m}$  between the microscope slide and the cover glass as shown schematically in Figure 16A. Stages IV and VI oocytes were injected with 100 pg of DAPI in water, and nuclei were isolated in mineral oil 30 minutes later. In all cases, chromosomes could readily be identified as bivalent structures using fluorescence microscopy (Figure 16A and B). LBCs from stage IV oocytes were considerably more extended than the LBCs from stage VI oocytes. This difference in chromatin organization is correlated with the reduced transcriptional activity of the nucleus within the late stages of oogenesis and is also observed on conventional nuclear spreads. We also observed that a higher concentration of DAPI such as 20 ng/oocyte has a dramatic effect on the physiology of the chromosomes. Under this condition, LBCs appear very condensed (Figure 16A), and the absence of chromosomal loops indicates that RNA transcription is totally inhibited. While it is not clear how DAPI influences LBC architecture, its effect does not depend on UV irradiation and occurs within minutes after injection (our unpublished data). The amount of 100 pg of DAPI/oocyte was thus determined experimentally to permit a rapid identification of LBCs in oil-isolated nuclei without any obvious effect on their physiology. Surprisingly, LBCs are consistently found all grouped within one limited region of the large nucleoplasmic volume. This remarkable organization suggests that LBCs are not free to diffuse away from each other.

### ***RNAPII transcription units.***

One of the most obvious characteristics of LBCs on nuclear spreads is the presence of numerous lateral loops, which are active RNAPII transcription units. We are pleased to report that the same organization is exhibited by LBCs in oil-isolated nuclei. The DIC image of one such LBC is presented in Figure 17. The two homologues, still attached at chiasmata (indicated by arrowheads), are readily distinguished from the nucleoplasm. Importantly, numerous loops are projected away from each chromosomal axis. Unlike in nuclear spread preparations, however, the loops are not brought into the two-dimensional plane of the microscope slide surface by centrifugation. Rather the loops are distributed radially from the chromosomal axes, which makes it difficult to image them all in the same focal plan. A magnified view of two sets of loops is also presented in Figure 17 to further demonstrate that the bases of these loops are tethered to a chromosomal axis, which is defined here using DAPI fluorescence. We then tested whether these loops were sensitive to the transcription inhibitor actinomycin D (AMD). It is well known from previous studies using nuclear spread preparations that treatment of oocytes with AMD, or other transcriptional inhibitors, induces a dramatic retraction of the loops and an overall condensation of LBCs. Figure 18 shows LBCs of oil-isolated nuclei from AMD-treated oocytes. After 1 h of treatment, LBCs still display an extended shape but, unlike in control oocytes, the lateral loops are missing. With longer times of exposure to the AMD treatment, LBCs shorten and chromosomal axes are now shaped into linear arrays of immediately adjacent condensed chromatin domains.

In summary, it is now possible to study LBCs in an isolated and fully functional nucleus where their overall dynamic architecture is essentially identical to that previously defined on nuclear spreads [236].



### ***Toward the study of steady-state dynamics of LBC components.***

The highly extended form of LBCs and the very large nucleoplasmic volume of the oocyte nucleus permit chromatin structures to be distinguished from the nucleoplasm and other nuclear structures unambiguously using a light microscope. Oil-isolated nuclei thus represent a powerful system to study the *in vivo* steady-state dynamics of chromosomal factors. Figure 19 is presented here to demonstrate that it is now possible to monitor the dynamic exchanges of a chromosomal factor between LBCs and the nucleoplasm. The protein MCD1 (mitotic chromosome determinant 1) is a subunit of the cohesin complex, which regulates sister chromatid cohesion (reviewed in [291]). When expressed in fusion with YFP in stage IV–VI oocytes, YFP-MCD1 associates specifically with chromosomal axes (each formed of two paired sister chromatids) where it co-localizes with other members of the cohesin complex (our unpublished data). The fluorescence recovery of YFP-MCD1 on chromosomal axes after photobleaching is presented in Figure 19. The fact that the fluorescent signal was recovered within minutes highlights the dynamic behavior of chromosomal MCD1.

## **Discussion**

### ***A renewal of the lampbrush chromosome?***

Every major cell biology textbook, such as *Molecular Biology of the Cell* (Alberts *et al.* 2002), shows a micrograph of LBCs in support of the well-accepted hypothesis that somatic chromatin organizes into looped domains in all eukaryotes. LBCs were also used in early chromosome-stretching experiments [292] to pioneer the idea that they are extensible and elastic structures. Finally, DNase treatments of LBCs were used to demonstrate that each chromatid contains a single DNA molecule [293, 294]. Despite such a distinguished legacy, very little work

is currently being done using LBCs to tackle current questions on chromatin organization. Here, we present a new method for visualizing LBCs in oil-isolated nuclei, which we hope will renew interest in using them to study fundamental aspects of chromatin dynamics *in vivo*. We find that in such nuclei LBCs display the overall architecture of actively transcribing bivalent chromosomes, as seen on nuclear spreads. Such organization was expected since it was previously shown that an oil-isolated nucleus maintains all its activities for several hours [287]. In particular, transcription is still very active and accordingly we observe the presence of numerous chromosomal loops that are sensitive to AMD. Importantly, our data demonstrate that the conventional method for nuclear spread preparation does not alter LBC physiology.

While DAPI is used here to rapidly identify LBCs within the large nucleoplasmic volume of an oocyte nucleus, it is not required. Indeed, with practice one can distinguish LBCs from other nuclear structures simply using DIC. Another strategy to unambiguously identify chromosomal axes without compromising the functional integrity of LBCs is to induce the expression of a fluorescently tagged chromosomal protein in oocytes prior the isolation of nuclei. A good example is provided in Figure 19 by the protein YFP-MCD1.

### ***LBC clusters?***

In oil-isolated nuclei, LBCs are very often found all grouped into a limited nuclear domain. Interestingly, a similar aggregation of LBCs in the middle of the nucleus was previously reported in specific developmental stages of the axolotl oocyte [295]. While it is not clear why LBCs do not distribute throughout the nucleoplasmic volume, it suggests the interesting possibility that they are tethered among each other. Over the years, evidence that DNA-containing filaments connect mitotic chromosomes has been obtained (see [295-297] for

reviews), and it was proposed recently that satellite DNA-containing bridges could link metaphase chromosomes [298]. Whether similar chromatin bridges tether the meiotic diplotene LBCs together is an interesting question that will require further investigation.

### ***Studying functional LBCs.***

The fact that LBCs can be observed in an oil-isolated nucleus, an essentially *in vivo* condition, represents a unique opportunity to study chromosome structure and function. We present here a brief qualitative FRAP analysis of the chromosomal YFP-MCD1 dynamics as an example. It is important to note that the bleached region can be precisely defined. In this case, only a small domain of one of the two homologous axes was photobleached. The other axis conveniently served as an internal control to monitor changes of fluorescence signals due to data acquisition. Such a level of spatial resolution simply cannot be achieved with any other system. Because the chromosomal loops are also easily distinguishable in oil-isolated nuclei, one of the most exciting future developments of the present work will be to use similar approaches to that used for MCD1 to tackle fundamental questions regarding the dynamic organization of the transcription unit.

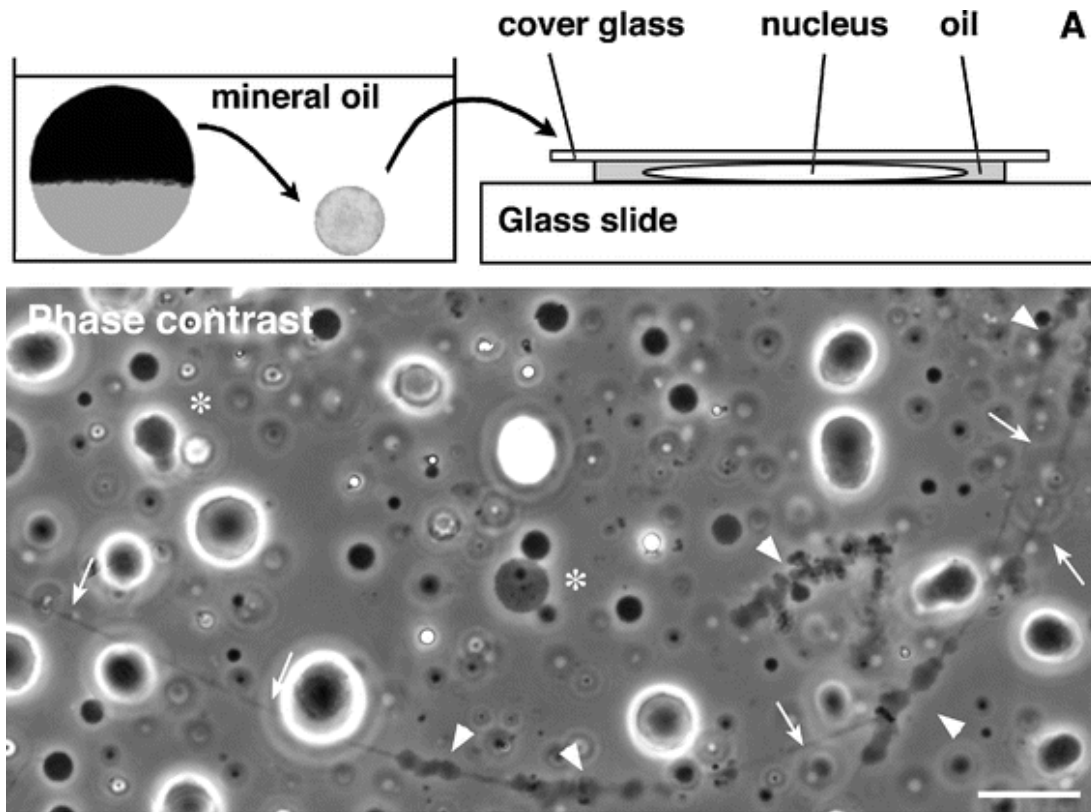


**Figure 15: The oil-isolation procedure does not affect chromosome architecture.** (A) Phase-contrast micrograph showing one disrupted LBC within a small nucleoplasmic region of an oil-isolated nucleus. The chromosomal axes display an abnormal structure that consists of extensively stretched chromatin fibers (arrows) interspaced with small regions of more condensed chromatin (arrowheads). Note that lateral loops are absent. The nucleus was prepared using the method described in [52], which is also schematically represented here. Two Cajal bodies (\*) are readily distinguished from the other organelles. Scale bar is 10 $\mu$ m.

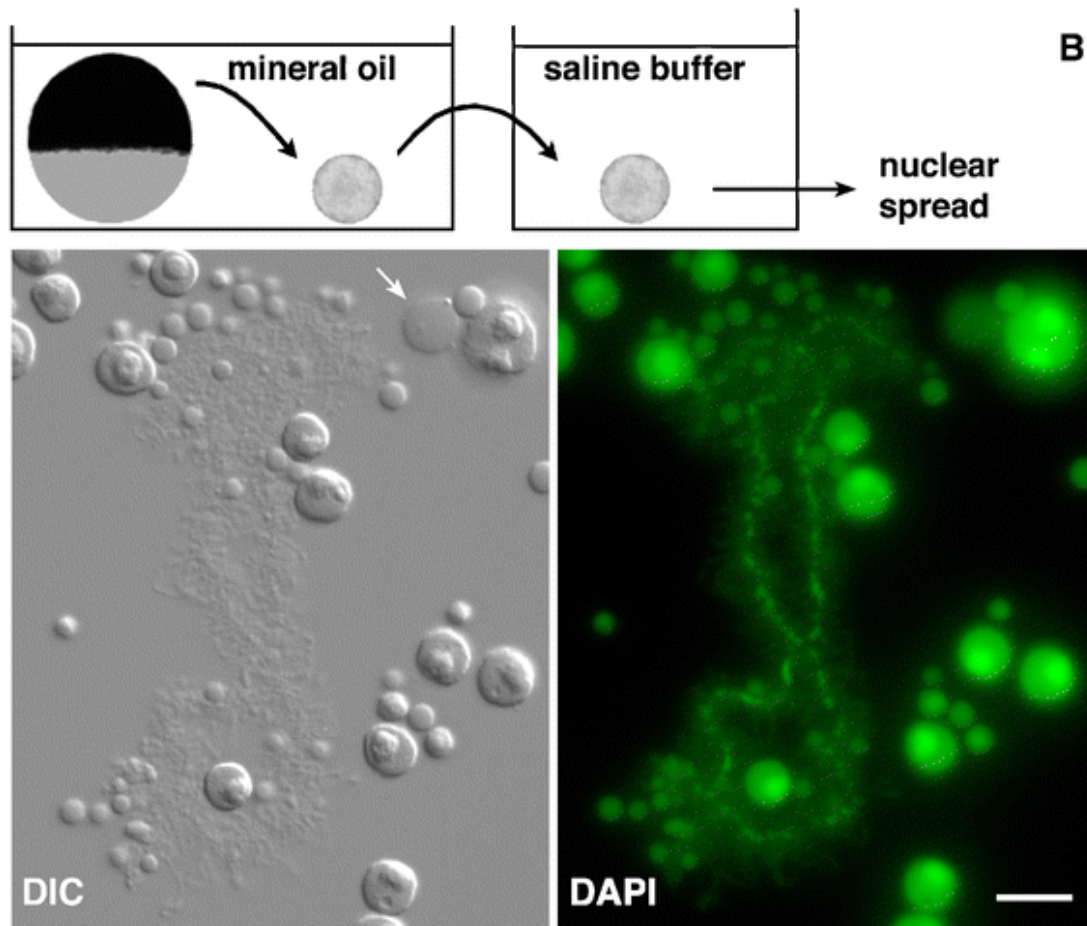


**Figure 15 (cont.): (B)** A differential interference contrast (DIC) image showing one LBC surrounded by several organelles on a nuclear spread. As indicated schematically, the nucleus was isolated and maintained in mineral oil for 5 h before transferring it to the saline buffer for nuclear spread preparation. Both LBCs and organelles were found to exhibit normal structures. In particular, chromosomes displayed numerous lateral loops. Both chromosomal axes as well as Nucleoli were well labeled with DAPI. Notice that chromosomal loops, SFCs, and CBs are weakly labeled (most likely because of their high RNA content). Scale bar is 10  $\mu$ m.

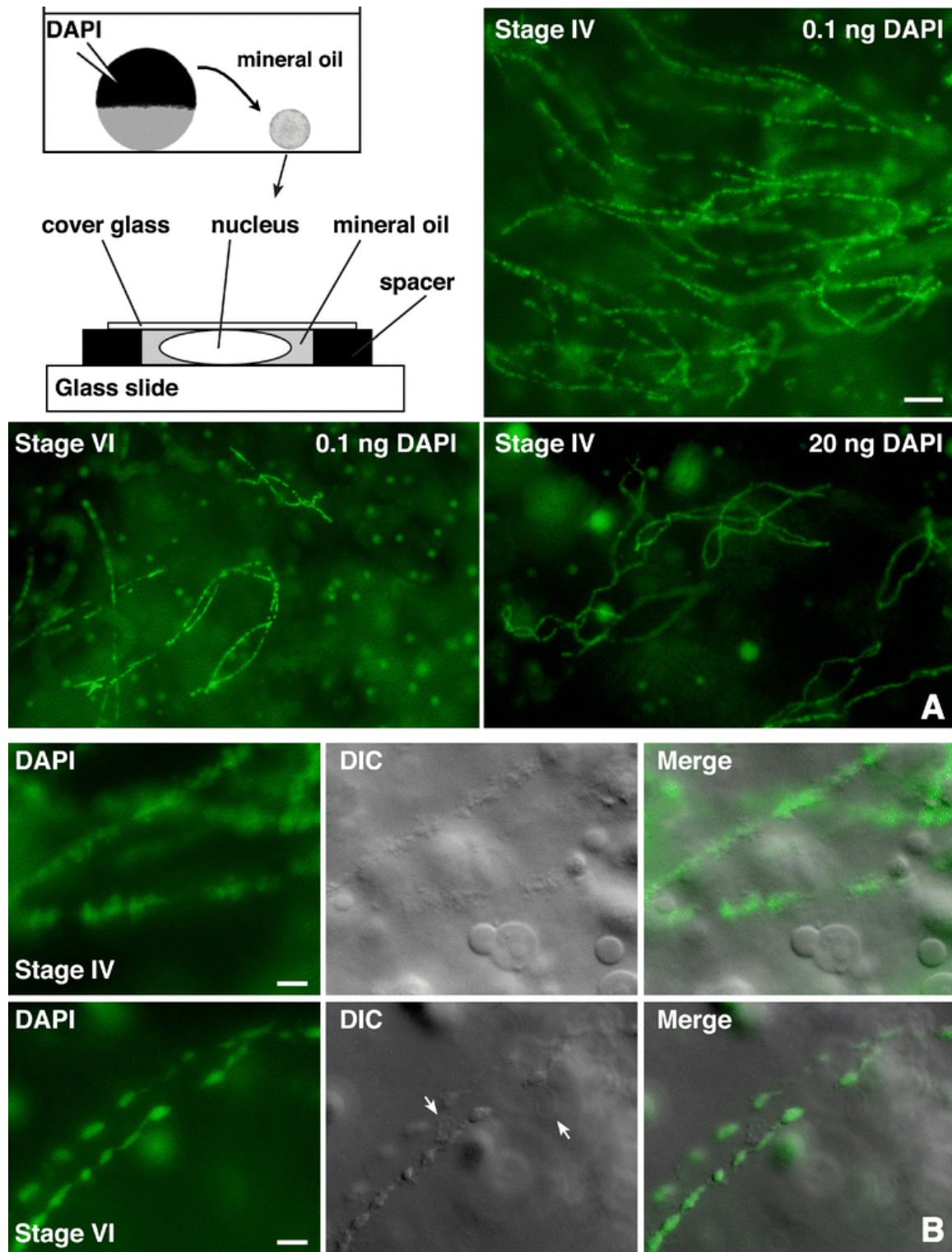
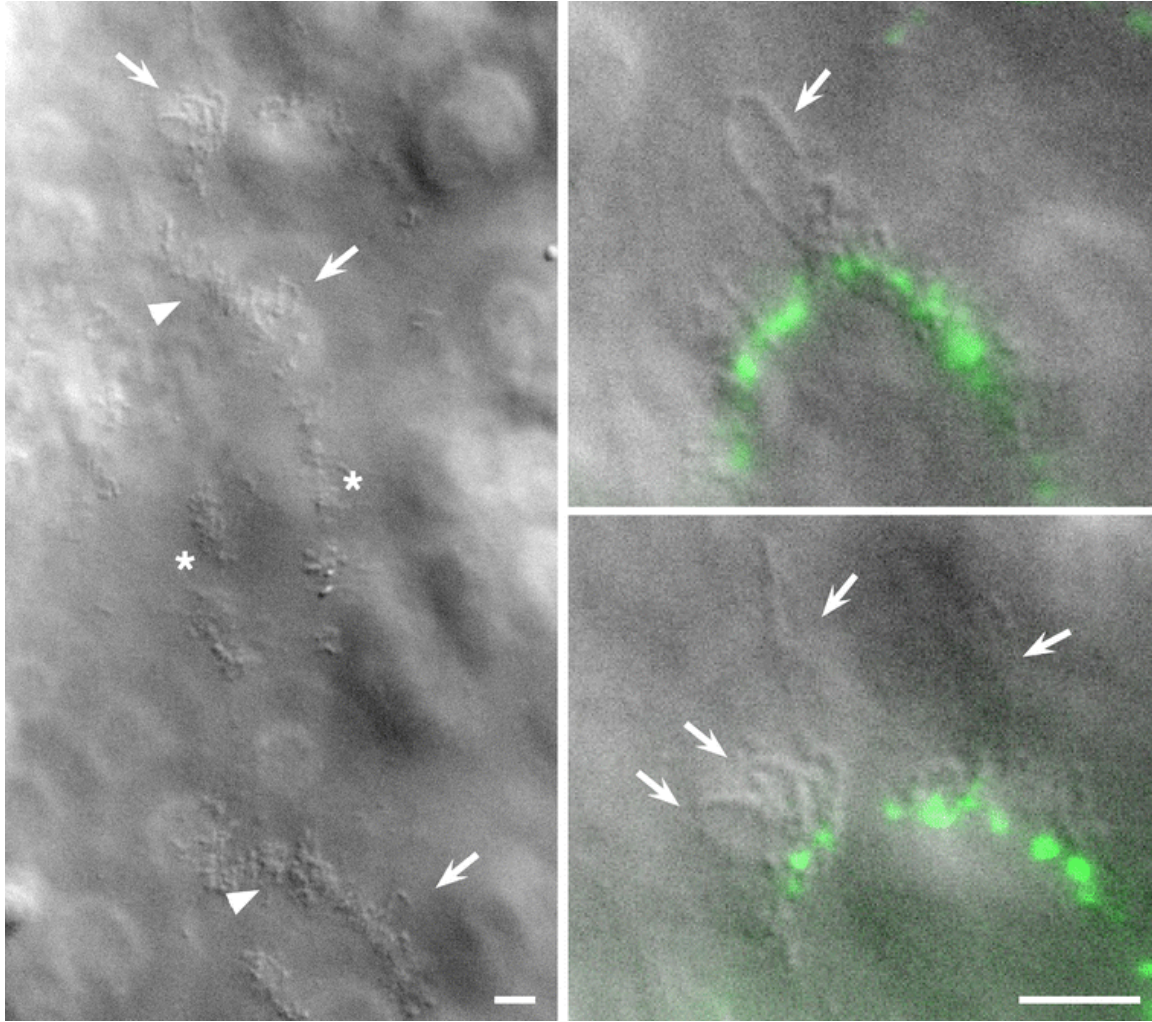


Figure 16 (cont. on next page)

---

**Figure 16; Lampbrush chromosomes in oil-isolated nuclei.** (A) Fluorescent micrographs of oil-isolated nuclei from stage IV and VI oocytes. As indicated schematically, oocytes were injected with DAPI (0.1 ng) before nuclear isolation. In agreement with their respective transcriptional activities, stage IV oocytes have LBCs that are consistently more extended than the one from stage VI oocytes. At high concentration, such as 20 ng/oocyte, DAPI inhibits transcription efficiently, which results in very condensed LBCs. Scale bar is 10  $\mu\text{m}$ . (B) Magnified views of chromosomal axes are presented together with their corresponding DIC images. Stage IV axes are visible by DIC primarily because of the numerous lateral loops. In contrast, stage VI axes appear as linear arrays of condensed chromatin domain from which fewer/smaller loops are projected. Arrows indicate several large loops. DAPI labeling was pseudo-colored in green. Scale bar is 5  $\mu\text{m}$ .

---



---

**Figure 17: DIC images of individual RNAPII transcription units in oil-isolated nuclei.** DIC micrograph of an LBC in oil-isolated nucleus from a stage IV oocyte (left panel). The two homologues (indicated by \*) are still paired at chiasmata (arrowheads). Arrows indicate particularly extended loops. Magnified views of chosen sets of loops are also presented. There, DAPI staining is merged (pseudo-colored in green) to indicate the position of chromosomal axes. Scale bars are 5  $\mu\text{m}$ .

---



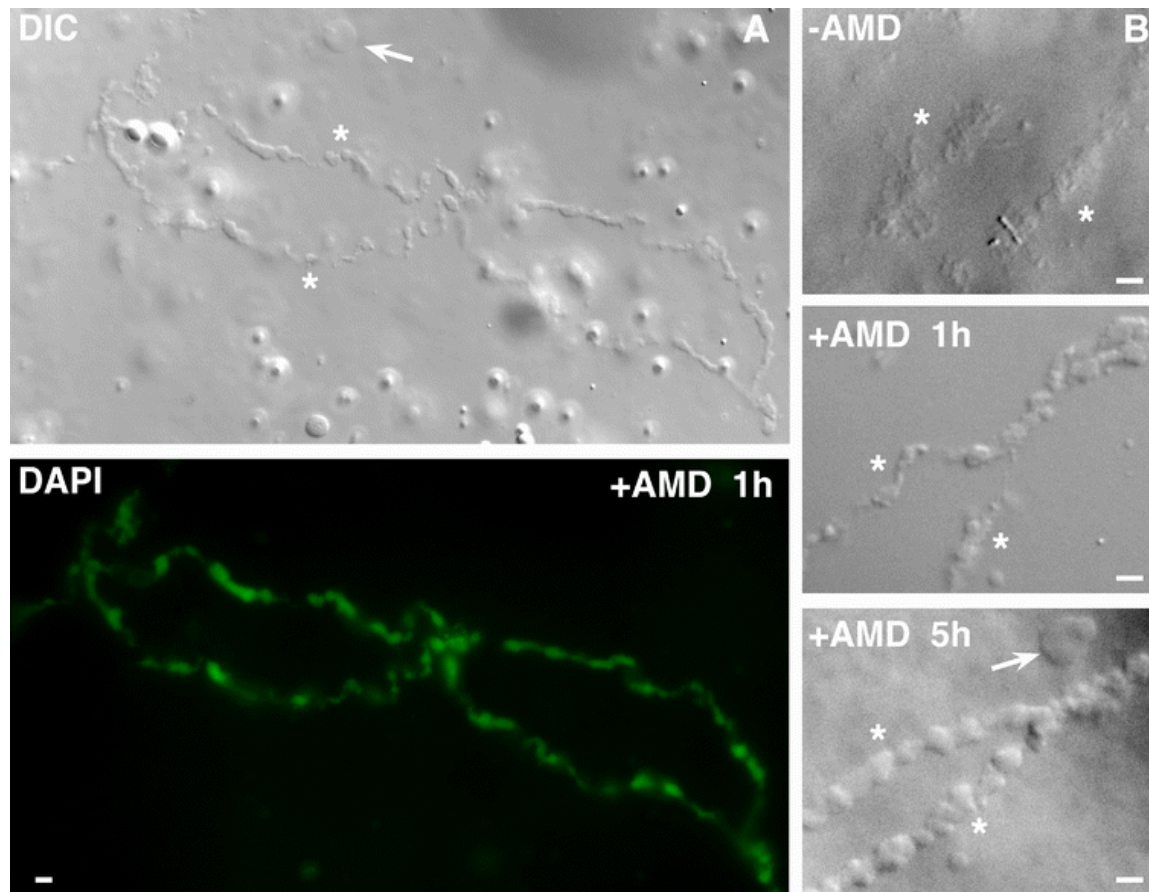


**Figure 18: LBC structure in oil-isolated nuclei after actinomycin D treatment.** (A) DIC micrograph and its corresponding fluorescent image (DAPI) of one LBC in a live nucleus. A stage IV oocyte was treated with actinomycin D (AMD) for 1 h before the isolation of its nucleus in mineral oil. Chromosomal axes, which are well labeled with DAPI, are also readily identified by DIC. As expected, the lateral loops, which are active sites of transcription for RNAPII, are absent. (B) DIC images showing the effect of AMD over time on the architecture of LBCs. Only a small chromosomal region is shown in each panel. LBCs from control stage IV oocytes display extended axes, organized in repeats of loop clusters (-AMD). Inhibition of transcription by AMD rapidly (+AMD 1 h) results in the loss of the lateral loops and a thickening of the chromosomal axes. Over time (+AMD 5 h), chromosomes shorten and the axes appear as linear arrays of tightly packed chromatin domains. In all images, the two homologues of the same LBC are indicated by \*. Arrows indicate CBs. Scale bars are 5  $\mu$ m.

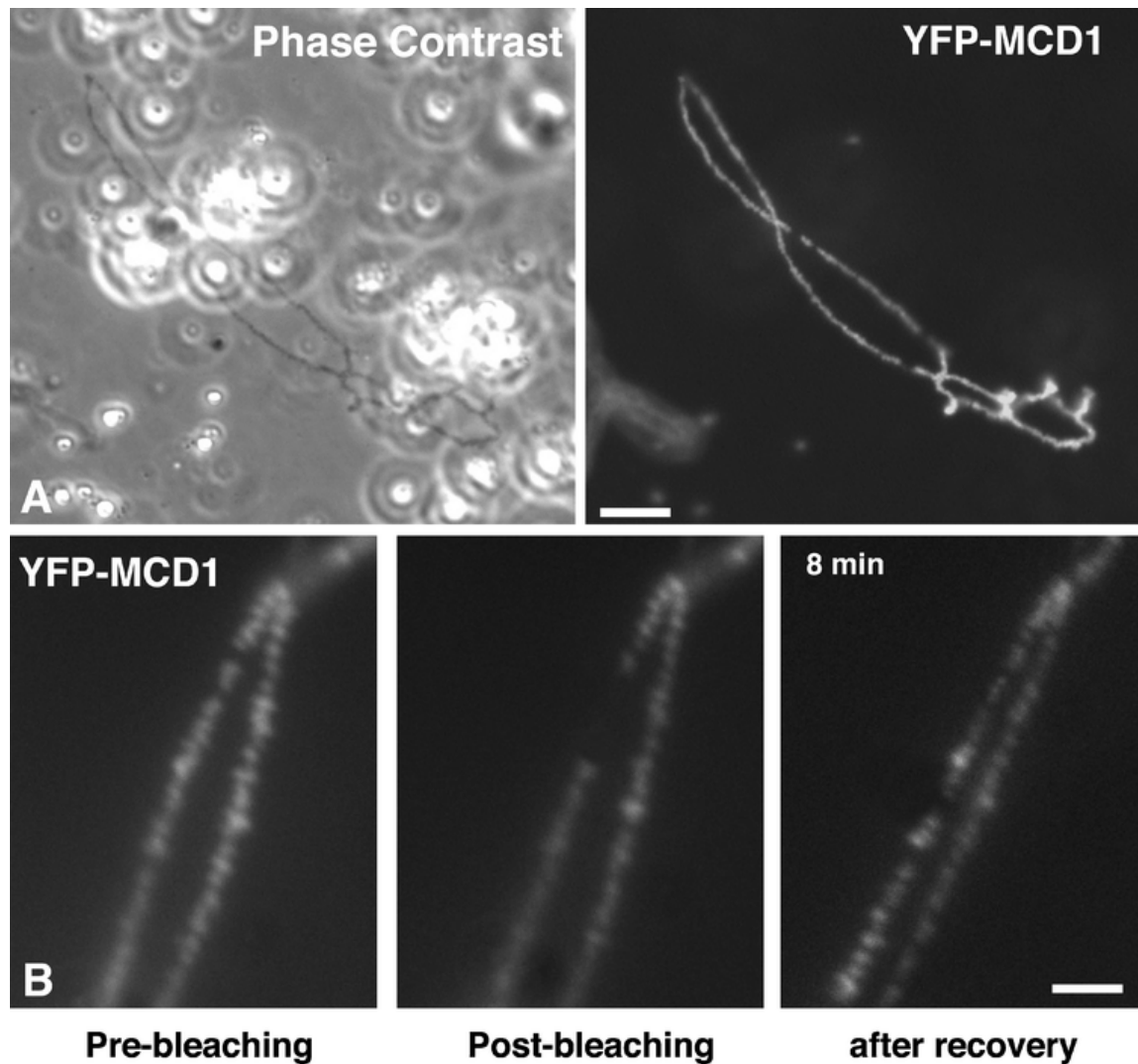


**Figure 19: Steady-state dynamics of chromosomal YFP-MCD1.** (A) A phase-contrast image and its corresponding fluorescent micrograph showing the chromosomal distribution of the newly expressed YFP-MCD1 in an oil-isolated nucleus from a stage VI oocyte. As expected for a member of the cohesin complex, MCD1 associates with chromosomal axes where sister chromatid cohesion is occurring. Scale bar is 10  $\mu\text{m}$ . (B) Fluorescence bleaching and recovery of chromosomal YFP-MCD1. A narrow region of one of the two homologues forming an LBC was photobleached (“post-bleaching” panel) and recovery of fluorescence was monitored over time. Scale bar is 5  $\mu\text{m}$ .

CHAPTER V  
EXPERIMENTAL PROCEDURES

**In Vitro Transcription and Labeling of RNA**

The templates for the transcription of fluorescein-labeled splicing snRNAs and their deletion mutants and chimeras were amplified with the high fidelity Deep Vent<sub>R</sub><sup>®</sup> DNA Polymerase (New England BioLabs, Ipswich, MA). The templates for the transcription of fluorescein-labeled FISH probes and [<sup>32</sup>P]-labeled Northern hybridization probes were amplified with GoTaq<sup>®</sup> DNA Polymerase (Promega, Madison, WI).

The ΔBPR xIU2 snRNA template was produced by two-step PCR, where the first step deletes the BPS recognition sequence and two residues on each side (residues 31-40 of the xIU2 snRNA) and the second step introduces the T3 promoter. The xIU1sII-xIU7 chimeric RNA template was produced by two-step PCR, where the first step adds the xIU1 snRNA stem loop I sequence (residues 21-47) to the 5' end of the xIU7 snRNA sequence and the second step introduces a T3 promoter. The BS-xIU1Sm and BS-xIU1Sm-xIU1sII chimeric templates were amplified with a 3' primer that adds the xIU1 snRNA Sm site with two surrounding residues. The primer for the latter construct also introduces the xIU1 snRNA stem loop I sequence downstream of the xIU1 snRNA Sm site.

The appropriate primer pairs (Integrated DNA Technologies, Coralville, IA) and templates for PCR are indicated below. The PCR products were gel purified by placing the excised band in a 0.45μm cellulose acetate Spin-X<sup>®</sup> Plastic Centrifuge Tube Filter (Corning Inc., Corning, NY) and spinning at 20,000xg for 10min at ambient temperature.

The template for the transcription of the xIU7 snRNA and the AdML splicing reporter was prepared by linearizing the pUC9-T7/xIU7 snRNA vector with PvuII (Invitrogen Corp., Carlsbad, CA) and the pSP64-AdML vector with HincII (Invitrogen Corp., Carlsbad, CA), respectively, and purifying by phenol:chloroform:isoamyl alcohol (25:24:1, pH 8.0, Sigma, St. Louis, MO) extraction.

**PCR Product:** Template, and 5' and 3' Primers are shown below. Sp6, T3, or T7 bacteriophage promoters are underlined. The Sm site and its two surrounding residues are italicized.

*Wild-type U snRNAs*

**T3/hsU1:** pCR2.1/hsU1 snRNA

5' GCA ATT AAC CCT CAC TAA AGG GAT ACT TAC CTG GCA GGG GAG

3' CAG GGG AAA GCG CGA ACG CAG TCC CCC AC

**T3/xIU2:** pCR2.1/xIU2 snRNA

5' GCA ATT AAC CCT CAC TAA AGG GAT CCT TTC GCC TTT GC

3' AAG TGC ACC GGT CCT GGA GGT ACT GC

**T3/ggU4B:** pUC9/ggU4B snRNA

5' CGA ATT AAC CCT CAC TAA AGG GAG CTT TGC GCA GTG GCA GTA TC

3' CAG TCT CCG TAG AGA CTG TCA

**T3/xIU5:** pUC19/xIU5 snRNA

5' CGG AAT TCA ATT AAC CCT CAC TAA AGG G

3' ATA CCT GGT GTG AAC CAG GCT TC

**T3/xtU6:** pUC19/xtU6

5' CGG AAT TCA ATT AAC CCT CAC TAA AGG G

3' TAA AAT ATG GAA CGC TTC ACG

*Deletion Mutant U snRNAs*

**T3/Δ5'-20 hsU1:** pCR2.1/hsU1 snRNA

5' GCA ATT AAC CCT CAC TAA AGG GAT ACC ATG ATC ATG AAG

3' CAG GGG AAA GCG CGA ACG CAG TCC CCC AC

**T7/Δ5'-47 hsU1:** pCR2.1/hsU1 snRNA

5' CGT AAT ACG ACT CAC TAT AGG CAG GGC CAG GCT CAG CC

3' CAG GGG AAA GCG CGA ACG CAG TCC CCC AC

**T3/Δ5'-90 hsU1:** pCR2.1/hsU1 snRNA

5' GCA ATT AAC CCT CAC TAA AGG GGC GAT TTC CCC AAA TGT G

3' CAG GGG AAA GCG CGA ACG CAG TCC CCC AC

**T3/Δ5'-122 hsU1:** pCR2.1/hsU1 snRNA

5' GCA ATT AAC CCT CAC TAA AGG GAT AAT TTG TGG TAG TGG G

3' CAG GGG AAA GCG CGA ACG CAG TCC CCC AC

**T3/Δ3'-139 hsU1:** pCR2.1/hsU1 snRNA

5' GCA ATT AAC CCT CAC TAA AGG GAT ACT TAC CTG GCA GGG GAG

3' CAC TAC CAC AAA TTA TGC

**T3/Δ5'-29 xIU2:** pCR2.1/hsU2 snRNA

5' CGA ATT AAC CCT CAC TAA AGG GAG TGT AGT ATC TGT TCT TAT C

3' AAG TGC ACC GGT CCT GGA GGT ACT GC

**T3/Δ5'-42 xIU2:** pCR2.1/xIU2 snRNA

5' CGA ATT AAC CCT CAC TAA AGG GTT CTT ATC AGT TTA ATA TCT GAT

3' AAG TGC ACC GGT CCT GGA GGT ACT GC

**T3/ $\Delta$ 5'-65 xIU2:** pCR2.1/xIU2 snRNA

**5'** CGA ATT AAC CCT CAC TAA AGG GAC GTC CCC TAT CTG GGG

**3'** AAG TGC ACC GGT CCT GGA GGT ACT GC

**T3/ $\Delta$ 3'-111 xIU2:** pCR2.1/xIU2 snRNA

**5'** GCA ATT AAC CCT CAC TAA AGG GAT CCT TTC GCC TTT GC

**3'** TGT TCC AAA AAT CCA TTT AAT AT

**T3/ $\Delta$ 3'-146 xIU2:** pCR2.1/xIU2 snRNA

**5'** GCA ATT AAC CCT CAC TAA AGG GAT CCT TTC GCC TTT GC

**3'** TGG AGT GGA CAG AGC AAG

**T3/ $\Delta$ BPR xIU2**

Step 1 -  **$\Delta$ BPR xIU2:** pCR2.1/xIU2 snRNA

**5'** ATC GCT TCT CGG CCT TTT GGC TAA GAT CAA TGT TCT TAT CAG TTT

AAT ATC TG

**3'** AAG TGC ACC GGT CCT GGA GGT ACT GC

Step 2 - **T3/ $\Delta$ BPR xIU2:** gel purified  $\Delta$ BPR xIU2

**5'** GCA ATT AAC CCT CAC TAA AGG GAT CCT TTC GCC TTT GC

**3'** AAG TGC ACC GGT CCT GGA GGT ACT GC

*Chimeric RNAs*

**T3/xIU1sII-xIU7**

Step 1 - **xIU1sII-xIU7:** pUC9/xIU7 snRNA

**5'** ATA CCA TGA TCA TGA AGG TGG TTC TCC AAG TGT TAC AGC TC

**3'** TGT GGC TCC TAC AGA G

Step 2 – **T3/xIU1sII-xIU7:** gel purified xIU1sII-xIU7

**5'** GCA ATT AAC CCT CAC TAA AGG GAT ACC ATG ATC ATG AAG

**3'** TGT GGC TCC TAC AGA G

**T7/BS-xlU1sm:** pBluescriptII K/S +/-

**5'** TAA TAC GAC TCA CTA TAG G

**3'** TAC CAG AAA TTT GCT GGG TAC CGG G

**T7/BS-xlU1sm-xlU1slI:** pBluescriptII K/S +/-

**5'** TAA TAC GAC TCA CTA TAG G

**3'** GGA GAA CCA CCT TCG TGA TCA TGG TAT TAC CAG AAA TTT GCT GGG

TAC CGG G

*Anti-sense Probes*

**T7/anti-hsU1:** pCR2.1/xlU1 snRNA

**5'** CGT AAT ACG ACT CAC TAT AGG GCA GGG GAA AGC GCG AAC G

**3'** ATA CTT ACC TGG CAG GGG AG

**T7/anti-xlU2:** pCR2.1/xlU2 snRNA (Bellini & Gall, 1998)

**5'** CGT AAT ACG ACT CAC TAT AGG GAA GTG CAC CGG TCC TGG AG

**3'** ATC GCT TCT CGG CCT TTT GG

**T7/anti-ggU4B:** pUC9/ggU4B snRNA

**5'** CGT AAT ACG ACT CAC TAT AGG GCA GTC TCC GTA GAG ACT G

**3'** AGC TTT GCG CAG TGG CAG

**T7/anti-xlU5:** pUC19/xlU5 snRNA

**5'** CGT AAT ACG ACT CAC TAT AGG GTA CCT GGT GTG AAC CAG GCT T

**3'** ATA CTC TGG TTT CTC TTC AAA TTC

**T7/anti-xtU6:** pUC19/xtU6

5' CGT AAT ACG ACT CAC TAT AGG GAA AAT ATG GAA CGC TTC ACG AAT

3' GTG CTT GCT TCG GCA GCA

*Histone gene probes*

**Sp6/anti-xIH2A, T7/anti-xIH2B, T7/anti-xIH3, T7/anti-xIH4:** pBluntII-TOPO/xIH2A,

pBluntII-TOPO/xIH2B, pBluntII-TOPO/xIH3, pBluntII-TOPO/xIH4

T AAT ACG ACT CAC TAT AGG G

ATT TAG GTG ACA CTA TAG

***Vectors.***

pCR2.1/hsU1 snRNA (Gall, J. G., et. al., 1999)

pCR2.1/xIU2 snRNA (Gall, J. G., et. al., 1999)

pUC9/ggU4B snRNA (Gerbi, S. A., et. al., 2003)

pUC19/xIU5 snRNA (Gall, J. G., et. al., 1999)

pUC19/xtU6 snRNA (Gall, J. G., et. al., 1999)

pUC9/xIU7 snRNA (Bellini and Gall, 1998)

pBluescriptII K/S +/- (Stratagene, La Jolla, CA)

pBluntII-TOPO/xIH2A (Bellini)

pBluntII-TOPO/xIH2B (Bellini)

pBluntII-TOPO/xIH3 (Bellini)

pBluntII-TOPO/xIH4 (Bellini)

pSP64-AdML (Yu, Y., et. al., 1998)



All templates were ethanol precipitated and washed prior to transcription. RNAs were transcribed in the presence of 1.0U/ $\mu$ L of T3, T7, or Sp6 RNA polymerase (Stratagene, La Jolla, CA), depending on the promoter.

- Fluorescein-labeled snRNAs and their deletion mutants and chimeras were transcribed in the presence of 125nM ATP, 62.5nM GTP, 125nM CTP, 125nM 62.5nM UTP, 25nM ChromaTide<sup>®</sup> fluorescein-12-UTP (Invitrogen Corp., Carlsbad, CA) and 125nM m<sup>7</sup>G(5')ppp(5')G cap analog (GE Healthcare Bio-Sciences Corp., Piscataway, NJ).
- Fluorescein-labeled FISH probes were transcribed in the presence of 125nM ATP, 125nM GTP, 125nM CTP, 125nM 62.5nM UTP, 25nM ChromaTide<sup>®</sup> fluorescein-12-UTP.
- The [<sup>32</sup>P]-labeled Northern hybridization probes were transcribed in the presence of 125nM ATP, 125nM GTP, 125nM CTP, 50 $\mu$ Ci  $\alpha$ -[<sup>32</sup>P]-UTP (GE Healthcare Bio-Sciences Corp., Piscataway, NJ).
- The [<sup>32</sup>P]-labeled AdML splicing reporter was transcribed in the presence of 125nM ATP, 62.5nM GTP, 125nM CTP, 125nM m<sup>7</sup>G(5')ppp(5')G cap analog, and 50 $\mu$ Ci  $\alpha$ -[<sup>32</sup>P]-UTP.

Recombinant RNasin<sup>®</sup> Ribonuclease Inhibitor (Promega Corp., Madison, WI) was present at 1.0U/ $\mu$ L in all transcription reactions. After a 2hr incubation at 37°C, 1.0U of RQ1 RNase-free DNase (Promega Corp., Madison, WI) was added to the transcription reaction and incubated for 15 minutes at 37°C to digest the DNA template. The RNA was purified using NucAway Spin Columns (Ambion Inc., Austin, TX) equilibrated with water.

### **Northern Hybridization Probe Quantitation**

To measure the radioactivity of Northern hybridization probes, 1  $\mu$ L of purified probe was transferred to a vial containing 5mL of 30% ScintiSafe™ scintillation fluid (Fischer Scientific Co., Hanover Park, IL), and  $^{32}$ P cpm/ $\mu$ L were determined using the LS6500 Multipurpose Scintillation Counter (Beckman Coulter, Inc., Fullerton, CA).

### **Ovarian Biopsy**

To surgically isolate a fragment of ovary, a sexually mature *Xenopus laevis* female frog (NASCO, Fort Atkinson, WI) was first submerged and maintained in an anesthetic chamber containing 0.15% methanesulfonate salt of 3-aminobenzoic acid ethyl ether (tricane methane sulfonate, MS222, Sigma, St. Louis, MO). The animal was periodically tested for the riding reflex to monitor the consciousness of the animal. Typically, the frog fails to display the reflex after 8-10min and is ready for surgery. The frog was then removed from the anesthetic chamber and placed in supine position on ice. An incision was made with surgical scissors to the lower right or left quadrant of the abdomen to expose the ovarian tissue. A small fragment of the ovary measuring approximately 5mL was extracted with forceps, cut free with surgical scissors, placed in a Petri dish containing the physiological saline buffer OR2 (82.5mM NaCl, 2.5mM KCl, 1mM CaCl<sub>2</sub>, 1mM MgCl<sub>2</sub>, 1mm Na<sub>2</sub>HPO<sub>4</sub>, 5mM HEPES, 100mg/mL streptomycin, pH 7.4), and stored at 18°C.

To complete the surgery, the incision was doubly sutured, and the anesthetic was rinsed off of the frog with frog water (tap water purified by reverse osmosis). The frog was placed in a damp chamber until it regained consciousness, which is typically 30-45min after surgery. At this

time, it was transferred to a post-surgical tank, where it was deprived of food and closely monitored for three days. After recovery was complete, the frog was placed back in its original tank and provided with its usual dietary regimen.

### **Defolliculation**

To remove the follicular tissue surrounding the oocytes, the fragment of ovary was broken into smaller pieces with jeweler's forceps and gently rocked on a rotator for approximately 2hrs at ambient temperature in OR2 containing 0.2% collagenase from *Clostridium histolyticum*, Type II (Sigma, St. Louis, MO). These defolliculated oocytes were then extensively washed with OR2 to remove the collagenase and stored at 18°C in an OR2 containing Petri dish until needed. In some experiments, actinomycin D (Sigma) was used at 10 µg/ml in OR2 to inhibit RNA transcription.

### **Oocyte Microinjection**

Stage IV-V oocytes (0.9-1.1mm diameter) were selected for injection DNA oligonucleotides used in depletion studies or fluorescein-labeled RNAs used in targeting studies. AdML splicing substrate was injected directly into mineral oil isolated nuclei for splicing assays. Glass needles were prepared with 3.5'' Drummond #3-000-203-G/X Tubes (Drummond Scientific Co, Broomall, PA) using a horizontal pipette puller P-97 (Sutter Instrument, Novato, CA). All injections were performed under a S6 Leica dissecting microscope (Leica Microsystems, Inc., Bannockburn, IL) using a Nanojet II Automatic Nanoliter Injector (Drummond Scientific Co., Broomall, PA).

DAPI was also used in oil-isolated nuclei to identify LBCs. In this case, oocytes were injected into the cytoplasm (20 nl of a 5 ng/μl solution of DAPI in water).

### **Antisense DNA Oligonucleotide Design and U snRNA Depletion Assay**

DNA oligonucleotides complementary to the U snRNAs were designed to direct the RNase H mediated degradation of the endogenous U snRNAs. The “H” in RNase H is for hybrid, as it degrades the RNA component of RNA:DNA hybrid duplexes. As the Sm site on the U snRNAs are well protected by the Sm proteins, other regions were chosen for DNA oligonucleotide-directed RNase H targeting. The sequences for DNA oligonucleotides and the corresponding regions of complementarity on the U snRNA are indicated in Table 2. A schematic of the U snRNAs in their secondary structure representation and complementary oligonucleotides are shown in Figure 20.

The effects of injecting the C oligo, U2b oligo, and U1a oligo were characterized previously in the oocyte [299]. Importantly, after injection of any oligo, the chromosomes contract, the transcriptionally active loops retract, and transcription halts. After approximately 24hrs after injection, the chromosomes and loops returned even beyond their original length and transcription resumed. Thus, oligo injected oocytes were incubated at least 24hrs prior to examining chromosomal targeting. Also, the half-life of the DNA oligo is approximately 10min, thus, allowing for rescue experiments [184].

The C oligo has no sequence identity to any *Xenopus laevis* sequence and was used as a negative control for depletion [299]. The U2b oligo was shown to specifically deplete the xIU2 snRNA [299] and abolish splicing [184]. The U1a oligo was demonstrated to result in the formation of a stable, truncated xIU1 snRNA lacking the first ~15 residues and a failure of the

chromosome and loops to recover and transcription to resume [299]. The U4d and U6f oligos used in this study targeted similar regions as previously characterized oligos, which resulted in the depletion of the xIU4 and xIU6 snRNAs, respectively. The U7g oligo was demonstrated to deplete the xIU7 snRNA [300]. In the literature [214], there is no mention of a DNA oligo that completely depletes the U1 snRNA or of any oligo that truncates or depletes the U5 snRNA; thus, several were designed and tested.

After injection of 25nL of 2ng/nL DNA oligo, oocytes were incubated for 24hrs at 18°C. Total RNA from a single nucleus was isolated and gel fractionated. Northern blots were used to test for the depletion of specific U snRNAs.

### **Targeting Assay**

Fluorescein-labeled snRNAs and their mutants and chimeras were injected at a constant volume of 25nL and a concentration of 0.5-1fmol/nL into the cytoplasm of the oocyte. After various incubation times at 18°C, nuclear spreads were prepared, and the fluorescein epitope was probed with primary and secondary antibodies to amplify the fluorescein signal.

### **Splicing Assay**

An undefolliculated oocyte was dried on Whatman® paper and transferred to a Petri dish containing mineral oil (Sigma, St. Louis, MO). The presence of the follicular tissue here is critical as it stabilizes the plasma membrane. Defolliculated oocytes tend to lyse rapidly when placed on Whatman® paper. The nucleus was isolated in this medium with jeweler's forces and injected with 9nL of AdML splicing substrate at  $5 \times 10^6$ cpm. Nuclei isolated in mineral oil maintain *in vivo* architecture and retain all nuclear functions, including transcription and splicing

for over 24hrs [301]. After a 10min incubation at ambient temperature, total RNA was isolated and gel fractionated. Autoradiography was used for detection of previously characterized splicing intermediates and product [184].

### **RNA Isolation**

Nuclei were transferred to homogenization buffer (10mM Tris-HCl pH 7.4, 0.1% SDS) and vortexed for 1min. If nuclei were transferred from mineral oil, the sample was centrifuged for 2min at 20,000xg, and the aqueous phase was recovered. The RNA was isolated by phenol:chloroform (1:5, pH 4.7, Sigma, St. Louis, MO) extraction and concentrated by ethanol precipitation. The RNA pellet was washed in 70% ethanol and resuspended in 10 $\mu$ L of 8M urea/TBE (80mM Tris-borate 1mM EDTA, pH 8.0) for electrophoresis.

### **RNA Electrophoresis**

RNA was fractionated on an 8M urea, TBE, 8% polyacrylimide gel in TBE electrophoresis buffer using the Mini-PROTEAN 3 Electrophoresis System (Bio-Rad, Hercules, CA). The gel was used for Northern blotting for snRNA detection or autoradiography for splicing assays

### **Northern Blotting**

After gel fractionation, the RNA was electrophoretically transferred to a Zeta probe membrane (Bio-Rad, Hercules, CA) in TAE transfer buffer (40mM Tris-acetate, 1mM EDTA, pH 8.0) using a Mini Trans-Blot Cell (Bio-Rad, Hercules, CA). The RNA was UV crosslinked (12kJ/cm<sup>2</sup>) to the membrane using a Spectrolinker (Spectronics Corp, Lincoln, NE). The

membrane was blocked for 10min with hybridization buffer (171mM Na<sub>2</sub>HPO<sub>4</sub>, 79mM NaH<sub>2</sub>PO<sub>4</sub>, 1mM EDTA, pH 8.0, 7% SDS), probed overnight with [<sup>32</sup>P]-labeled antisense RNA at 10<sup>6</sup> cpm/mL in hybridization buffer, and washed twice for 30 minutes with wash buffer (13.7mM Na<sub>2</sub>HPO<sub>4</sub>, 6.3mM NaH<sub>2</sub>PO<sub>4</sub>, 1mM EDTA pH 8.0, 1% SDS). Blocking, hybridization, and washing were carried out at 65°C with rotation in a Fisher Isotemp Hybridization Incubator (Fischer Scientific, Hanover Park, IL). Autoradiography was used for detection.

### **Autoradiography**

To obtain radiographs, the gel or membrane was first wrapped in saran wrap. A phosphor screen was the exposed for 1-5hrs and scanned with the Cyclone Storage Phosphor System (PerkinElmer Life And Analytical Sciences, Inc., Wellesley, MA).

### **Microscope Slide Preparation**

Propper select<sup>®</sup> Microscope slides (Propper Manufacturing Co., Inc., Long Island City, NY) were first thoroughly cleaned by applying ES 7X<sup>®</sup> Cleaning Solution (MP Biomedicals, Inc., Aurora, OH) and allowing hot tap water, cold tap water, and deionized water to sequentially flow over the slides for 30min each. To facilitate adhesion of nuclear contents, the slides were briefly submerged in subbing solution (1g/L gelatin, 0.1g/L CrK(SO<sub>4</sub>)<sub>2</sub>\*12H<sub>2</sub>O) and placed in an 80°C oven overnight.

A 1:1 (m:m) ratio of petroleum and paraffin was combined in a beaker and allowed to melt and mix on a hotplate. A line of melted wax was placed 0.5in to the right and left of the center line on the microscope slide. A square with a central hole is placed on the slide such that the hole aligns with the center of the slide. The slide is then placed on the hotplate until the wax

melts again and spreads underneath the square. The layer of wax holds the square on the slide. The hole in the square and the slide together form a well in which the nuclear spreads are prepared and processed.

### **Protein expression and Western blot**

To express HA-tagged Y14, 25nL (0.5ng/nL) of HA-Y14 mRNA was injected into the cytoplasm of stage V oocytes. After a 50 hour incubation, 10 oocytes, cytoplasms, or nuclei were hand-isolated using jeweler's forceps and homogenized in 10mM Tris-HCl (pH8.0), 1mM EDTA, 0.2% SDS. The crude extract was centrifuged at 22,000xg at 4°C for 10min. The clarified extract was collected and fractionated on a 12% polyacrylimide gel using the Mini-PROTEAN 3 Electrophoresis System (Bio-Rad, Hercules, CA). Immunoblots were then performed as described in (Beenders et al. 2007) with the anti-HA antibody, mAb 3F10 (Hoffmann-La Roche Inc., Nutley, NJ), used at 50 ng/ml.

### **Nuclear Spreads**

Nuclei were isolated from oocytes using jeweler's forceps in 5:1 isolation medium (83mM KCl, 17mM NaCl, 6.5mM Na<sub>2</sub>HPO<sub>4</sub>, 3.5mM KH<sub>2</sub>PO<sub>4</sub>, 1mM MgCl<sub>2</sub>, 1mM dithiothreitol, pH 7.0). In this medium, the nucleoplasm becomes a gelatinous ball, presumably due to actin polymerization, which is critical for a later step in which the nucleoplasm must be transferred to a microscope slide without loss of contents. The yolk surrounding the nucleus was removed by pipeting the nucleus up and down very gently. Approximately 20-30sec after isolation, the nucleus was transferred to quarter strength dispersal medium (20.7mM KCl, 4.3mM NaCl, 1.6mM Na<sub>2</sub>HPO<sub>4</sub>, 0.9mM KH<sub>2</sub>PO<sub>4</sub>, 1mM MgCl<sub>2</sub>, 1mM dithiothreitol, 0.1% paraformaldehyde,



pH 7.0). The nuclear envelope was removed with jeweler's forces, and the gelatinous nucleoplasmic ball was transferred to the central well on the microscope slide, which also contains the dispersal medium. Within approximately 30sec, the contents of the nucleus begin to disperse onto the plane of the slide.

After approximately 10min, dispersion was typically complete, and the slide was spun at 4°C in a Sorvall® RC-5B Plus Superspeed Centrifuge (DuPont Sorvall® Product, Newton, CT) at 1krpm for 1min in a Sorvall® HS-4 rotor (DuPont Sorvall® Product, Newton, CT). The speed was increased in increments of 1krpm every minute until the speed reached 5krpm at which it was kept constant for the next 35min. Next, the slide is incubated in fixing solution (2% paraformaldehyde, 1mM MgCl<sub>2</sub>, PBS) for 1hr and rinsed in PBS. A razor blade was used as a wedge to remove the square. The wax that remained around the sample provided a hydrophobic barrier to retain a small amount of PBS over the sample. After this step, slides were used for immunofluorescence detection or fluorescence *in situ* hybridization.

### **Immunofluorescence Staining**

After drying residual PBS around the spread, 40µL of blocking buffer (0.45% Cold fish gelatin, 0.5% bovine serum albumin, 100µg/mL streptomycin, PBS) was placed on the sample and incubated for 5min to reduce nonspecific staining. The blocking buffer was rinsed away in PBS. Primary and secondary antibodies indicated below were diluted 1:50 and 1:800, respectively, in blocking buffer. The anti-fluorescein antibody was the only primary antibody diluted 1:500. The Alexa 488 mouse anti-fluorescein IgG (Millipore, Billerica MA) was used at 1 µg/mL. The anti-coilin antibody, mAb H1, was used at 500 ng/mL. The anti-RPC53 is a purified rabbit polyclonal serum and was used at a dilution of 1:50,000.

After applying 10 $\mu$ L of the antibody to the specimen, incubation was conducted for 1hr. The slides were incubated in three changes of PBS for 10min each to wash away unbound antibody after primary and after secondary antibody incubations. All steps were carried out at ambient temperature.

***Primary Antibodies.***

anti-fluorescein/Oregon Green®, rabbit IgG fraction , Alexa Fluor® 488 conjugate (Invitrogen Corp., Carlsbad, CA)

anti-fluorescein mouse IgG fraction , Alexa Fluor® 488 conjugate

H14 mouse monoclonal anti-RPB1 Ser5-P CTD IgM cell supernatant

4G3 mouse monoclonal anti-xlU2B'' IgG cell supernatant

H1 mouse monoclonal anti-xlcoilin IgG cell supernatant

Y12 mouse monoclonal anti-Sm IgG cell supernatant

K121 mouse monoclonal anti-TMG IgG cell supernatant

anti-RPC53 rabbit polyclonal serum

***Secondary Antibodies.*** (Invitrogen Corp., Carlsbad, CA)

Alexa Fluor® 488 goat anti-rabbit IgG (H+L)

Alexa Fluor® 594 goat anti-mouse IgG (H+L)

Alexa Fluor® 350 goat anti-mouse IgM ( $\mu$  chain)

### **Fluorescence *In Situ* Hybridization**

A 1:5 dilution of the FISH probe in hybridization buffer (40% formamide, 4X SSC, 60mM Na<sub>2</sub>HPO<sub>4</sub>, 40mM KH<sub>2</sub>PO<sub>4</sub>, 300µg/mL *E. coli* RNA, and 300µg/mL *E. coli* DNA.) was prepared. After adding 20µL of the probe to the sample, an 18mm X 18mm cover slip was placed over the sample, and the slide was incubated at 42°C for 4 to 16 hrs in a hybridization oven. Next, the cover slip was gently removed, and the slide was incubated at 45°C with three changes of wash buffer (50% formamide and 2X SSC) for 10min each. Finally, the slide was rinsed in PBS and either mounted for microscopic examination or used for immunofluorescence staining.

### **Counter-staining and Mounting Slides**

Prior to counter-staining or mounting with a cover slip, the slides were dried around the sample. Depending on the desired counter stain, 10µL of either 1µM Syto 61 (Invitrogen Corp., Carlsbad, CA) or 1µM YOYO-1 (Invitrogen Corp., Carlsbad, CA) in PBS was placed on the spread preparation, allowed to incubate at ambient temperature for 20min, and briefly rinsed away in PBS. If 4, 6-diamidino-2-phenylindole (DAPI) was used as the counter-stain, then it was included in the mounting medium at 1µg/mL. To mount slides for microscopy, an 8µL drop of mounting media (0.1mg/mL phenylenediamine in PBS pH 9, 50% glycerol) was placed on the sample, and a 22mm X 22mm cover slip was gently pressed over the sample. The slides were stored at -20°C until they were ready for microscopy to prevent photobleaching.

### **Oil-isolation of nuclei and preparation for microscopy**

The isolation of nuclei in mineral oil (Sigma) is performed as described [287]. When needed, isolated nuclei were transferred into a small oil-containing plastic Petri dish and maintained at 18°C. The wax spacer needed for imaging LBCs is produced directly onto microscope slides using the following method: 20 mg of a 1:1 mixture of petroleum–paraffin wax is melted onto a microscope slide under a 25 mm acrylic square containing a circular hole (5 mm in diameter) in its center, using a hotplate (~80°C). After the homogeneous spreading of the melted wax between the acrylic square and the slide, the wax is allowed to re-solidify by letting the slide cool slowly. Once the wax has hardened (5 min.), the acrylic square is removed using a razor blade and a thin layer of wax (~25–30 µm in thickness) with a hole in its center is left imprinted on the slide. An oil-isolated nucleus can then be deposited together with ~8 µl of oil in the central shallow well. Finally, an 18 mm square coverslip (Corning Inc., Corning, NY, USA) is apposed gently onto the specimen, which is then ready for microscopy.

### **Transferring a nucleus from mineral oil to an aqueous saline buffer**

The method was developed by Dr. Joseph Gall and is as follows. A small drop of oil is deposited at the bottom of a plastic Petri dish containing the 5:1 buffer (83 mM KCl, 17 mM NaCl, 6.5 mM Na<sub>2</sub>HPO<sub>4</sub>, 3.5 mM KH<sub>2</sub>PO<sub>4</sub>, 1 mM MgCl<sub>2</sub>, 1 mM DTT) where cohesive forces maintain it in place. Oil-isolated nuclei are then directly pipetted in the oil drop. Using fine tweezers, nuclei are pushed one by one to the oil–buffer interface. The first nucleus is totally disrupted, presumably because of tension at the surface of the oil drop. Its content is not lost in the buffer, however, but rather appears to coat the surface of the oil drop. Importantly, such a in

conditioned surface lets the other nuclei pass intact from oil to the aqueous buffer. Nuclear spreads can then be prepared.

### **Microscopy**

Nuclear spreads were examined using an upright Leica DMR (Leica Microsystems, Inc., Bannockburn, IL) and imaged with a monochrome Spot RT Charge-Coupled Device (CCD) camera for phase contrast, differential interference contrast, and fluorescence images. Confocal microscopy using the Zeiss LSM 510 Laser Scanning Microscope (Carl Zeiss Microimaging, Inc., Thornwood, NY) was used for high resolution fluorescence images. When a comparison of staining between various preparations was desired, images were captured and processed identically.

All microscopy on oil-isolated nuclei was performed on an upright Leica DMR. Standard fluorescence microscopy was carried out using a PL Fluotar 40X oil objective (NA = 1.0) and a HCL FL Fluotar 100× oil objective (NA = 1.30). Images were captured using a monochrome Retiga EXI Charge-Coupled Device (CCD) camera (Qimaging, Surrey, BC, Canada) driven by the In vivo software (version 3.2.0, Media Cybernetics, Bethesda, MD, USA). All images were captured at room temperature. Figures were processed using Adobe Photoshop CS version 8.0 and assembled with Adobe InDesign CS version 3.0.

Fluorescence recovery after photobleaching (FRAP) was performed using the SRS NL100 MicroPoint Laser System (Photonic Instruments Inc., St. Charles, IL, USA) adapted to our DMR microscope. A 514 nm laser dye was used for the photobleaching of yellow fluorescent protein (YFP). Data acquisition was done using the In vivo software (version 3.2.0, Media

Cybernetics). The protein YFP-MCD1 was expressed by microinjection of its corresponding transcript using a strategy described.

<b>Oligo</b>	<b>Sequence</b>	<b>Complementarity</b>
C	TCC GGT ACC ACG ACG	None
U1a	CTC CCC TGC CAG GTA AGT AT	1-20 of xIU1
U1a'	AGC CGG AGT GCA ATG GCT	61-78 of xIU1
U1a''	GGG AAA TCG CAG GGG TCA GCA	80-100 of xIU1
U1a'''	AAA GCG CGA ACG CAG T	143-148 of xIU1
U2b	CAG ATA CTA CAC TTG	28-42 of xIU2
U4d	TAT TGG GAA AAG TTT	65-79 of hsU4
U5e	ATT GAA CGA AAC TCA	75-89 of xIU5
U5e'	CTT TAG TAA AAG GCG AAA G	33-51 of xIU5
U5e''	TAC CTG GTG TGA ACC AGG	99-116 of xIU5
U5e'''	TAC CTG GTG TGA ACC AGG	52-71 of xIU5
U6f	TCG TTC CAA TTT TAG	25-39 of xtU6
U7g	AAG AGC TGT AAC ACT T	1-16 of xIU7

**Table 2: Complementary DNA oligonucleotides for U snRNA depletion**

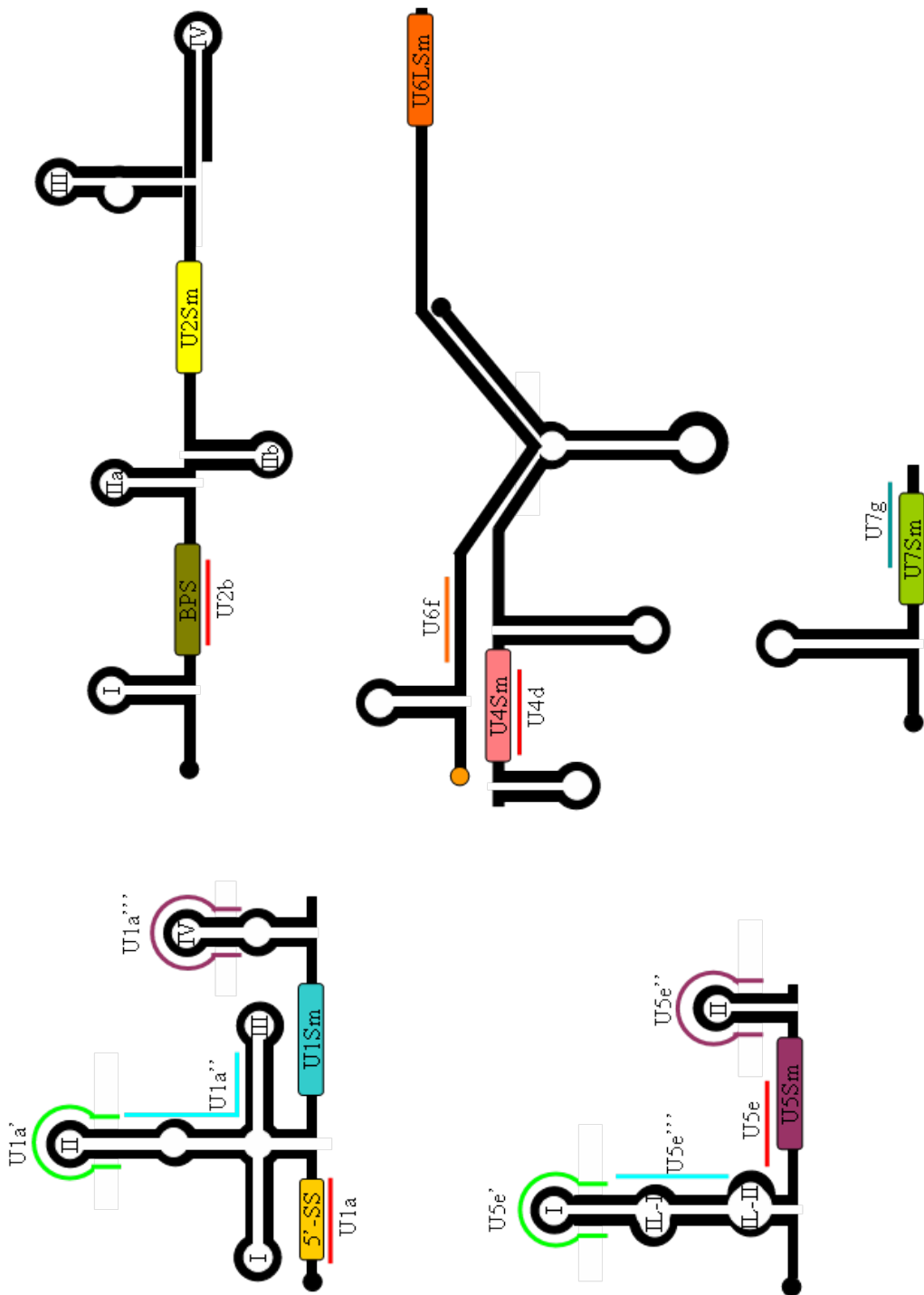


**Figure 20: U snRNA secondary structure and antisense oligonucleotides.**

CHAPTER VI  
CONCLUSIONS AND FUTURE DIRECTIONS

**Conclusions**

***The recruitment-loading model.***

The U1, U2, U4, U5, and U6 snRNPs are indispensable components of the spliceosome *in vivo*. Hence, understanding the trafficking and maturation of these five spliceosomal snRNPs is a critical step towards the understanding of pre-mRNA splicing. After entry into the nucleus, the core snRNP particle must traffic through several nuclear compartments to form a mature snRNP. Eventually, it must engage pre-mRNA transcripts to assemble into a spliceosome and catalyze the splicing reaction.

I demonstrated that fluorescent snRNPs are recruited to nascent pre-mRNAs associated with the loops of the lampbrush chromosome. While this may seem to be a trivial find given that fluorescent snRNPs can rescue splicing in oocytes depleted of the corresponding endogenous snRNPs and that splicing is believed to occur co-transcriptionally, several other groups that have examined the trafficking of fluorescent snRNPs in *Xenopus* oocytes were unsuccessful in demonstrating targeting to chromosomes. Our prediction that spliceosomal snRNPs are indeed recruited but at such a low concentration that it escapes detection was borne true when we were able to observe a specific signal with primary and secondary amplification. Importantly, while others have investigated snRNP recruitment to select transgenes, we are now able to examine the same phenomenon on a genome wide scale. Notably, we are not simply examining the binding of snRNPs to pre-mRNA, rather our assay examines recruitment, an event that is the culmination of snRNP trafficking and maturation in the living cell.



In addition, while much evidence exists to support co-transcriptional splicing<sup>25</sup> in metazoans, most is either indirect or dependent on the choice of the transgene. I have shown, using a vertebrate system, that the majority of pre-mRNAs are spliced co-transcriptionally, as indicated by the loading of Y14, an EJC component, onto nascent RNP fibrils. This conclusion was based on a previous demonstration that Y14 is loaded only after exon-exon ligation (i.e. the completion of splicing).

Using our novel snRNP recruitment assay, I began to address which characteristics of snRNPs are required for their targeting to nascent pre-mRNAs. We demonstrate that neither the 5'-SS recognition sequence on the U1 snRNA nor the BPS recognition sequence on the U2 snRNA is required to recruit the corresponding mutant snRNPs *in vivo*. Furthermore, SLI of the U1 snRNA was shown to be both necessary and sufficient for its association with nascent pre-mRNA. As SLI does not interact directly with pre-mRNA, the association is likely mediated through either the U1-70K or U1-C proteins. Our data suggests that the snRNP proteins, not the snRNA, are responsible for initial interaction with pre-mRNA. This came to us as quite a surprise given that current dogma states that the hybridization of the snRNA moieties of snRNPs and cis-acting sequences on pre-mRNA represents the first interaction with pre-mRNA.

Since snRNPs that cannot participate in splicing were recruited to elongating pre-mRNAs, a natural question was whether splicing itself was required to recruit snRNPs. To this effect, the U2 snRNA was depleted to inhibit splicing. While the fact that the U1 snRNA was still recruited came as no surprise since the canonical model predicts that it is the first to load, the recruitment of the U4 snRNP and U5 snRNP was quite intriguing. Given that the U2 snRNP is

---

<sup>25</sup> In yeast, most pre-mRNAs are spliced post-transcriptionally, even though snRNPs are recruited co-transcriptionally.

required for the integration of the U4/U6.U5 tri-snRNP into a spliceosome, the recruitment of the U4 and U5 snRNPs cannot be in the context of a functional spliceosome.

The covalent modifications of the cap proximal 29 residues of the U2 snRNA were shown to be absolutely required for splicing. Thus, it was surprising that our mutant U2 snRNA,  $\Delta 29$ U2 snRNA, which cannot participate in splicing, was still recruited to nascent transcripts. This finding indicates that the initial interaction of snRNPs with pre-mRNA does not depend on their role in splicing.

On the basis of our mutagenesis studies and splicing inhibition experiments, we proposed a two-step recruitment-loading model (Figure 21). In such a model, snRNPs are first recruited to nascent transcripts through an indirect interaction via heterogeneous nuclear RNPs (hnRNPs) or snRNP proteins. Only after cis-acting sequences are exposed on elongating pre-mRNAs do the snRNPs load directly onto pre-mRNA. The recruitment phase may be important for two, non-mutually exclusive reasons. First, the recruitment may increase the local concentration of spliceosomal snRNPs in the vicinity of cis-acting elements on the pre-mRNA. Second, an initial recruitment may serve to activate snRNPs prior to engaging in their roles in recognition and/or catalysis.

### ***Trafficking through nuclear domains.***

One important point regarding the trafficking of fluorescent snRNPs is that their distribution does not parallel that of endogenous snRNPs. In particular, they accumulate strongly in CBs, whereas endogenous snRNPs are only weakly present in CBs. Furthermore, their presence in SFCs is only modest in comparison to endogenous snRNPs. Given the role of CBs in snRNP maturation and SFCs in the storage of mature snRNPs, it is likely that some

fluorescent snRNPs did not fully mature during the time course of our studies. The failure of some fluorescent snRNPs to completely mature must be the result of an inability to acquire snRNP specific proteins, rather than the result of an inability to acquire covalent modifications, since pseudouridylation and 2'-O-methylation were shown to be complete by 16hrs.

Consistently, the distribution of the fluorescent U2 snRNP closely resembled that of the endogenous U2 snRNP when the latter was depleted. This strongly suggests that the maturation of fluorescent U2 snRNPs is greatly accelerated upon the depletion of the endogenous U2 snRNA. Since mature endogenous U2 is unlikely to compete with nascent fluorescent U2 for the modification guide RNAs as they are already covalently modified, it must compete for snRNP-specific proteins. The simplest explanation is that the depletion of the endogenous U2 snRNA must have liberated U2 snRNP specific proteins, which may then be incorporated into the fluorescent U2 snRNPs in CBs and allowing them to complete maturation and to continue along their trafficking pathway to SFCs.

#### ***A system for examining snRNP interactions with nascent RNA in vivo***

While studying the trafficking of spliceosomal snRNP we injected fluorescent snRNAs into the cytoplasm and prepared oil-isolated nuclei. The objective was to examine the kinetics of snRNP trafficking through CBs and SFCs over time. We had also intended to use FRAP to examine the kinetics of snRNP association of CBs. Unfortunately, due to the high nucleoplasmic level of fluorescent snRNPs, we did not achieve significant contrast to examine specific labeling of nuclear bodies.

During one such set of experiments, we observed structures that resembled bivalent chromosomes by light microscopy. This was a remarkable breakthrough since they were never

observed in oil-isolated preparations previously. Indeed, it was believed that they were impossible to visualize by light microscopy because the chromosomes were believed to have an optical density identical to mineral oil and, thus, would not refract light. After many attempts to repeat our observation, we discovered that the LBCs were frequently damaged during the standard preparation. A change in the preparation that limited the compression of the nucleus made all the difference. With our simple modification, we are now able to examine LBCs and their RNAPII transcriptional units in the live nucleus. We have shown that these preparations can be used to examine the dynamics of a subunit of the cohesion complex on the chromosomal axis. While similar experiments are not possible with fluorescent snRNPs due to the high nucleoplasmic background, in the next section we discuss how we may circumvent this problem.

### **Future directions**

Given that fluorescent snRNPs can be recruited to nascent transcripts in the absence of the U2 snRNP, it would be interesting to examine recruitment in the absence of other snRNPs. Unfortunately, the U1a oligo which is complementary the 5'-SS recognition region of the U1 snRNA results in its truncation and the irreversible inhibition of transcription. My attempts to deplete the U1 snRNA with other oligos and the U5 snRNA were unsuccessful. However, oligos that successfully target the human U1 and U5 snRNAs have been determined and similar oligos should be designed against *Xenopus* U5 snRNAs and tested for their ability to direct RNase H mediated degradation. I have shown that the U4 and U6 snRNAs can be depleted with reversible transcriptional shutdown like that of U2 snRNA depletion.

Several links between transcription and splicing have been made. Interestingly, the U1 snRNA plays a direct role in transcription initiation. This may provide the basis for the

irreversible transcriptional shutdown upon U1a oligo directed truncation of the U1 snRNA. It will be interesting to determine whether injection of full length U1 snRNA is able to rescue transcriptional activity (loss of function) or if injection of a truncated U1 snRNA is able to inhibit transcription (dominant negative). Furthermore, complete depletions of the U1 snRNA should be attempted. Failure to irreversibly inhibit transcription, in this case, would strongly suggest a dominant negative effect.

Studies on snRNP recruitment to intronless genes have resulted in conflicting results. While *in vitro* assembled intronless viral mRNPs are able to bind to snRNPs, intronless  $\beta$ -globin transgenes failed to recruit splicing factor SC35 and the U2B'' proteins. These differences may be due to *in vitro* and *in vivo* differences or mRNA differences. While I showed that intronless RNAs transcribed by RNAPIII fail to recruit snRNPs, it would be interesting to determine whether naturally occurring intronless RNAPII genes, such as the heat shock, snRNA, and histone genes, recruit splicing snRNPs in our system.

It has been proposed that the targeting of snRNP and coilin to CBs are interdependent. Others, however, have shown that snRNPs accumulate in "residual" CBs in coilin knock out mice. My preliminary studies show that depletion of the U2, U4, U6, and U7 snRNAs does not perturb the localization of coilin to CBs. We have devised an approach for performing the complementary experiment where coilin is "depleted." Injecting anti-coilin coated beads into the oocyte cytoplasm should trap coilin in the cytoplasm since it is a shuttling protein. Afterwards, we can ask whether the snRNPs still target CBs. Alternatively, our preliminary studies show that dominant negative mutants of coilin are able to perturb the targeting of U7 and U2 snRNPs to CBs. Since CBs are the sites of snRNP maturation, it would be interesting to determine if inhibiting CB targeting disrupts the recruitment of fluorescent snRNPs to LBC loops and pre-

mRNA splicing. To further address the role of CBs in snRNP maturation, it would be interesting to determine if mature fluorescent snRNPs target CBs or go directly to SFCs or LBC loops. Immature fluorescent U2 snRNPs should not be able to rescue LBC targeting of U2B'' when CB targeting is inhibited; however, mature fluorescent U2 snRNPs should be equally functional in presence of dominant negative coilin mutants.

Fluorouridine labeled U2 snRNAs were shown to inhibit the pseudouridylation of the U2 snRNA. It would be interesting to see if nascent fluorescent U2 snRNA continues its trafficking pathway to SFCs and LBCs when its modification in CBs is inhibited. Alternatively, it would be interesting to see whether mature fluorescent U2 snRNPs. Since mature fluorescent U2 snRNP are already modified, their distribution should not be influenced by fluorouridine U2 snRNAs.

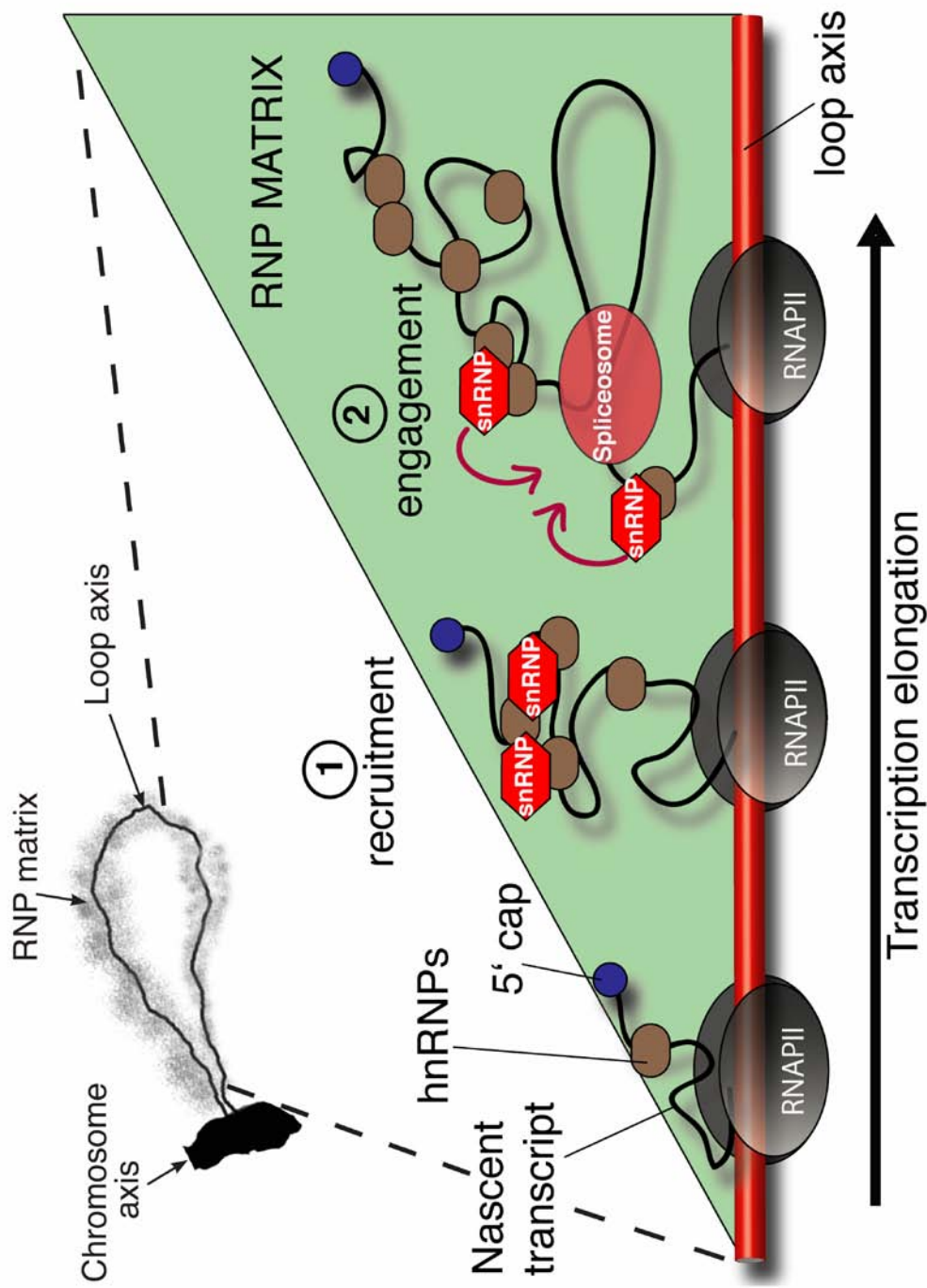


**Figure 21: The recruitment-loading model.** The splicing snRNPs are first recruited to nascent transcripts through indirect contact with other factors (hnRNPs for example). When cis-acting elements emerge from the actively transcribing RNAPII, snRNPs are loaded (engagement) directly onto the nascent RNA.

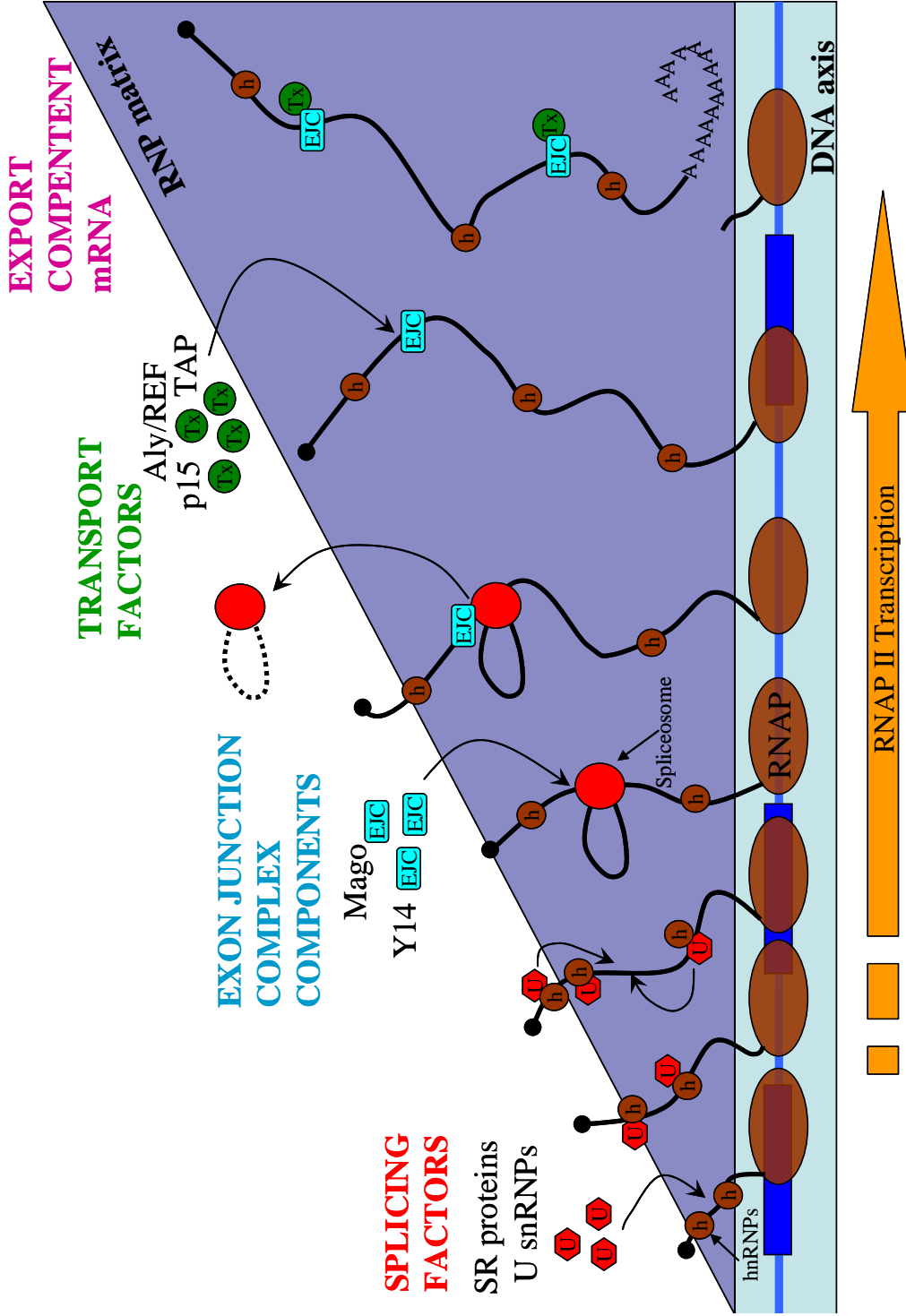
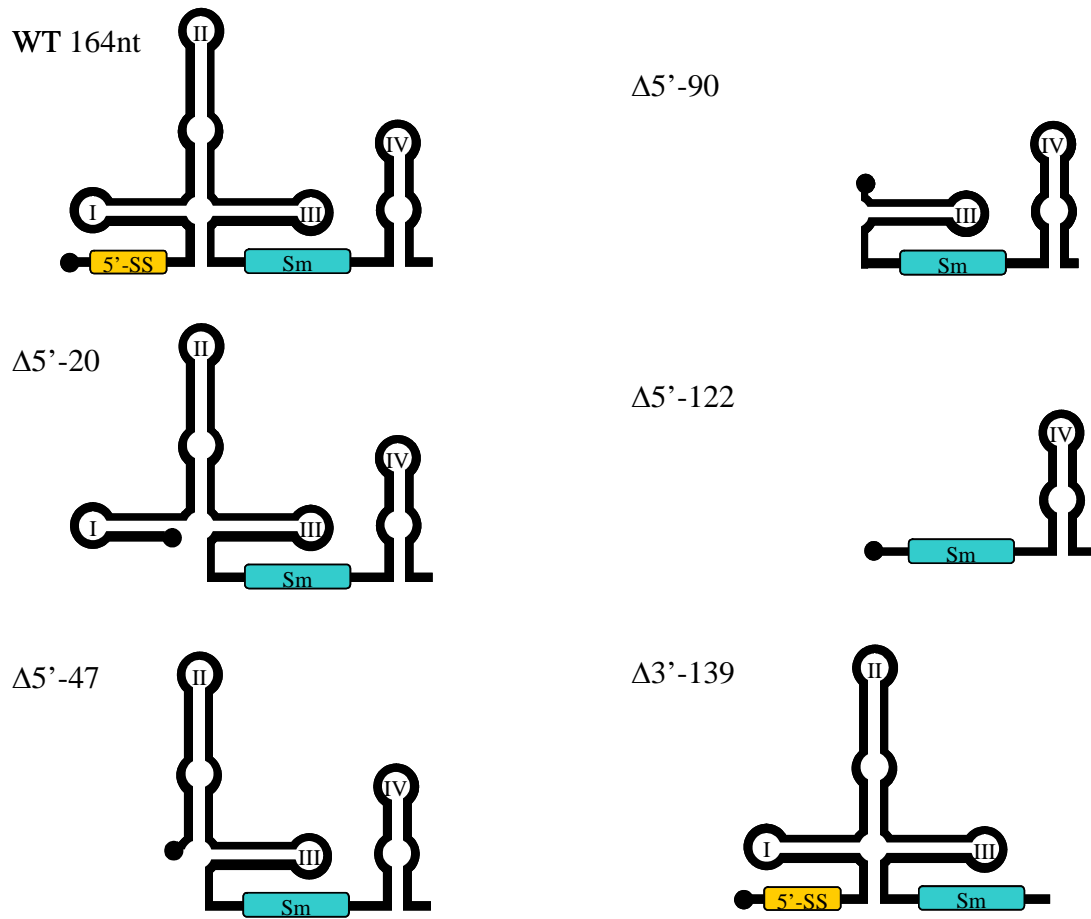


**Figure 22: Co-transcriptional assembly of an export competent mRNP.** As nascent pre-mRNAs are extended by RNAPII they rapidly and sequentially associate with factors involved in their packaging (hnRNPs), processing (splicing snRNPs, SR proteins), stability (Mago, Y14), and export to the cytoplasm (Aly/REF, p15, TAP).






---

**Figure 23: Deletion mutants of the U1 snRNA.** Stemloops are indicated by roman numerals. Sm site shown as blue box, and 5'-SS recognition sequence shown as yellow box. 5' mutants are deleted to indicated residue. 3' mutants are deleted at indicated residue

---

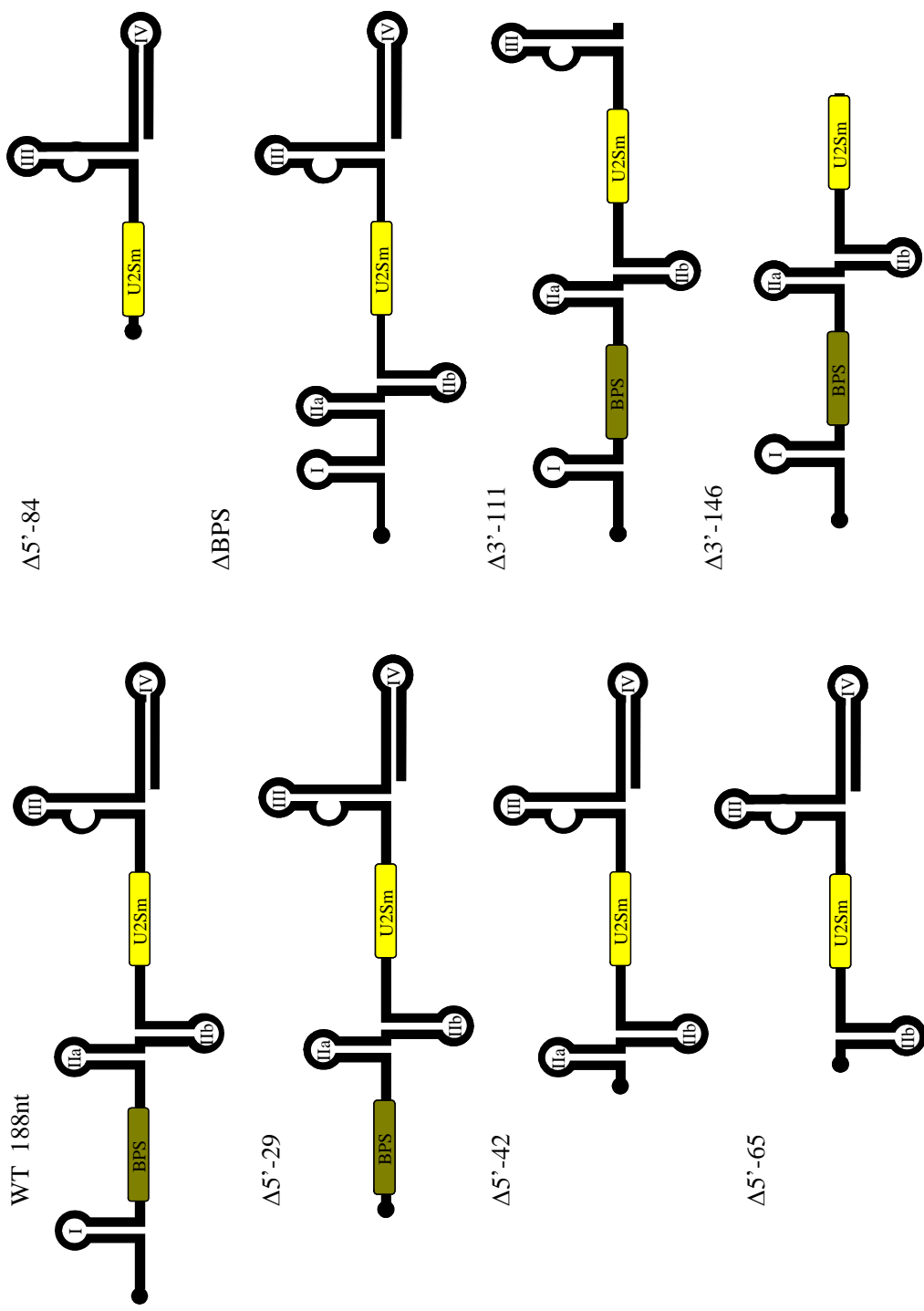


**Figure 24: Deletion mutants of the U2 snRNA.** Stemloops are indicated by roman numerals. Sm site shown as yellow box, and BPS recognition sequence shown as green box. 5' mutants are deleted to indicated residue. 3' mutants are deleted at inated residue onward.

## REFERENCES

1. Witkowski, J.A., *The discovery of 'split' genes: a scientific revolution*. Trends Biochem Sci, 1988. **13**(3): p. 110-3.
2. Sharp, P.A., *The discovery of split genes and RNA splicing*. Trends Biochem Sci, 2005. **30**(6): p. 279-81.
3. Sharp, P.A., *Split genes and RNA splicing*. Cell, 1994. **77**(6): p. 805-15.
4. Crick, F., *Split genes and RNA splicing*. Science, 1979. **204**(4390): p. 264-71.
5. Roberts, R.J., *How restriction enzymes became the workhorses of molecular biology*. Proc Natl Acad Sci U S A, 2005. **102**(17): p. 5905-8.
6. Blencowe, B.J., *Alternative splicing: new insights from global analyses*. Cell, 2006. **126**(1): p. 37-47.
7. Fedorova, L. and A. Fedorov, *Introns in gene evolution*. Genetica, 2003. **118**(2-3): p. 123-31.
8. Kiss, T., *SnoRNP biogenesis meets Pre-mRNA splicing*. Mol Cell, 2006. **23**(6): p. 775-6.
9. Johansen, S.D., P. Haugen, and H. Nielsen, *Expression of protein-coding genes embedded in ribosomal DNA*. Biol Chem, 2007. **388**(7): p. 679-86.
10. Ng, B., et al., *Reverse transcriptases: intron-encoded proteins found in thermophilic bacteria*. Gene, 2007. **393**(1-2): p. 137-44.
11. Schmidt, E.E. and C.J. Davies, *The origins of polypeptide domains*. Bioessays, 2007. **29**(3): p. 262-70.
12. Liu, M. and A. Grigoriev, *Protein domains correlate strongly with exons in multiple eukaryotic genomes--evidence of exon shuffling?* Trends Genet, 2004. **20**(9): p. 399-403.
13. Novoyatleva, T., et al., *Pre-mRNA missplicing as a cause of human disease*. Prog Mol Subcell Biol, 2006. **44**: p. 27-46.
14. Philips, A.V. and T.A. Cooper, *RNA processing and human disease*. Cell Mol Life Sci, 2000. **57**(2): p. 235-49.
15. Saleh, L. and F.B. Perler, *Protein splicing in cis and in trans*. Chem Rec, 2006. **6**(4): p. 183-93.
16. Haugen, P., D.M. Simon, and D. Bhattacharya, *The natural history of group I introns*. Trends Genet, 2005. **21**(2): p. 111-9.
17. Patel, A.A. and J.A. Steitz, *Splicing double: insights from the second spliceosome*. Nat Rev Mol Cell Biol, 2003. **4**(12): p. 960-70.
18. Mayer, M.G. and L.M. Floeter-Winter, *Pre-mRNA trans-splicing: from kinetoplastids to mammals, an easy language for life diversity*. Mem Inst Oswaldo Cruz, 2005. **100**(5): p. 501-13.
19. Jurica, M.S. and M.J. Moore, *Pre-mRNA splicing: awash in a sea of proteins*. Mol Cell, 2003. **12**(1): p. 5-14.
20. Nagai, K., et al., *Structure and assembly of the spliceosomal snRNPs*. Novartis Medal Lecture. Biochem Soc Trans, 2001. **29**(Pt 2): p. 15-26.
21. Fabrizio, P., et al., *Isolation of *S. cerevisiae* snRNPs: comparison of U1 and U4/U6.U5 to their human counterparts*. Science, 1994. **264**(5156): p. 261-5.
22. Stanek, D. and K.M. Neugebauer, *The Cajal body: a meeting place for spliceosomal snRNPs in the nuclear maze*. Chromosoma, 2006. **115**(5): p. 343-54.

23. Branlant, C., et al., *U2 RNA shares a structural domain with U1, U4, and U5 RNAs*. *Embo J*, 1982. **1**(10): p. 1259-65.
24. Singh, R. and R. Reddy, *Gamma-monomethyl phosphate: a cap structure in spliceosomal U6 small nuclear RNA*. *Proc Natl Acad Sci U S A*, 1989. **86**(21): p. 8280-3.
25. Achsel, T., et al., *A doughnut-shaped heteromer of human Sm-like proteins binds to the 3'-end of U6 snRNA, thereby facilitating U4/U6 duplex formation in vitro*. *Embo J*, 1999. **18**(20): p. 5789-802.
26. Vidal, V.P., et al., *Characterization of U6 snRNA-protein interactions*. *Rna*, 1999. **5**(11): p. 1470-81.
27. Mayes, A.E., et al., *Characterization of Sm-like proteins in yeast and their association with U6 snRNA*. *Embo J*, 1999. **18**(15): p. 4321-31.
28. Salgado-Garrido, J., et al., *Sm and Sm-like proteins assemble in two related complexes of deep evolutionary origin*. *Embo J*, 1999. **18**(12): p. 3451-62.
29. Donahue, W.F. and K.A. Jarrell, *A BLAST from the past: ancient origin of human Sm proteins*. *Mol Cell*, 2002. **9**(1): p. 7-8.
30. Wilusz, C.J. and J. Wilusz, *Eukaryotic Lsm proteins: lessons from bacteria*. *Nat Struct Mol Biol*, 2005. **12**(12): p. 1031-6.
31. Sun, X., I. Zhulin, and R.M. Wartell, *Predicted structure and phyletic distribution of the RNA-binding protein Hfq*. *Nucleic Acids Res*, 2002. **30**(17): p. 3662-71.
32. Arluison, V., et al., *Three-dimensional structures of fibrillar Sm proteins: Hfq and other Sm-like proteins*. *J Mol Biol*, 2006. **356**(1): p. 86-96.
33. Chu, J.L. and K.B. Elkon, *The small nuclear ribonucleoproteins, SmB and B', are products of a single gene*. *Gene*, 1991. **97**(2): p. 311-2.
34. Elkon, K.B., et al., *Epitope mapping of recombinant HeLa SmB and B' peptides obtained by the polymerase chain reaction*. *J Immunol*, 1990. **145**(2): p. 636-43.
35. van Dam, A., et al., *Cloned human snRNP proteins B and B' differ only in their carboxy-terminal part*. *Embo J*, 1989. **8**(12): p. 3853-60.
36. Gray, T.A., et al., *Concerted regulation and molecular evolution of the duplicated SNRPB/B and SNRPN loci*. *Nucleic Acids Res*, 1999. **27**(23): p. 4577-84.
37. Huntriss, J.D., D.S. Latchman, and D.G. Williams, *The snRNP core protein SmB and tissue-specific SmN protein are differentially distributed between snRNP particles*. *Nucleic Acids Res*, 1993. **21**(17): p. 4047-53.
38. Tkacz, I.D., et al., *Identification of novel snRNA-specific Sm proteins that bind selectively to U2 and U4 snRNAs in Trypanosoma brucei*. *Rna*, 2007. **13**(1): p. 30-43.
39. Liu, S., et al., *The network of protein-protein interactions within the human U4/U6.U5 tri-snRNP*. *Rna*, 2006. **12**(7): p. 1418-30.
40. Behrens, S.E. and R. Luhrmann, *Immunoaffinity purification of a [U4/U6.U5] tri-snRNP from human cells*. *Genes Dev*, 1991. **5**(8): p. 1439-52.
41. Schneider, C., et al., *Human U4/U6.U5 and U4atac/U6atac.U5 tri-snRNPs exhibit similar protein compositions*. *Mol Cell Biol*, 2002. **22**(10): p. 3219-29.
42. Will, C.L., et al., *The human 18S U11/U12 snRNP contains a set of novel proteins not found in the U2-dependent spliceosome*. *Rna*, 2004. **10**(6): p. 929-41.
43. Wassarman, K.M. and J.A. Steitz, *The low-abundance U11 and U12 small nuclear ribonucleoproteins (snRNPs) interact to form a two-snRNP complex*. *Mol Cell Biol*, 1992. **12**(3): p. 1276-85.

44. Malca, H., N. Shomron, and G. Ast, *The U1 snRNP base pairs with the 5' splice site within a penta-snRNP complex*. Mol Cell Biol, 2003. **23**(10): p. 3442-55.
45. Stevens, S.W., et al., *Composition and functional characterization of the yeast spliceosomal penta-snRNP*. Mol Cell, 2002. **9**(1): p. 31-44.
46. Nilsen, T.W., *The spliceosome: no assembly required?* Mol Cell, 2002. **9**(1): p. 8-9.
47. Behzadnia, N., et al., *Functional spliceosomal A complexes can be assembled in vitro in the absence of a penta-snRNP*. Rna, 2006. **12**(9): p. 1738-46.
48. Patel, S.B., N. Novikova, and M. Bellini, *Splicing-independent recruitment of spliceosomal small nuclear RNPs to nascent RNA polymerase II transcripts*. J Cell Biol, 2007. **178**(6): p. 937-49.
49. Nilsen, T.W., *The spliceosome: the most complex macromolecular machine in the cell?* Bioessays, 2003. **25**(12): p. 1147-9.
50. Kiss, T., *Biogenesis of small nuclear RNPs*. J Cell Sci, 2004. **117**(Pt 25): p. 5949-51.
51. Will, C.L. and R. Luhrmann, *Spliceosomal UsnRNP biogenesis, structure and function*. Curr Opin Cell Biol, 2001. **13**(3): p. 290-301.
52. Handwerger, K.E., C. Murphy, and J.G. Gall, *Steady-state dynamics of Cajal body components in the Xenopus germinal vesicle*. J Cell Biol, 2003. **160**(4): p. 495-504.
53. Abbott, J., W.F. Marzluff, and J.G. Gall, *The stem-loop binding protein (SLBPI) is present in coiled bodies of the Xenopus germinal vesicle*. Mol Biol Cell, 1999. **10**(2): p. 487-99.
54. Cioce, M. and A.I. Lamond, *Cajal bodies: a long history of discovery*. Annu Rev Cell Dev Biol, 2005. **21**: p. 105-31.
55. Gall, J.G., *[A role for Cajal bodies in assembly of the nuclear transcription machinery]*. Tsitologiya, 2003. **45**(10): p. 971-5.
56. Matera, A.G., *Cajal bodies*. Curr Biol, 2003. **13**(13): p. R503.
57. Filipowicz, W. and V. Pogacic, *Biogenesis of small nucleolar ribonucleoproteins*. Curr Opin Cell Biol, 2002. **14**(3): p. 319-27.
58. Lamond, A.I. and D.L. Spector, *Nuclear speckles: a model for nuclear organelles*. Nat Rev Mol Cell Biol, 2003. **4**(8): p. 605-12.
59. Handwerger, K.E. and J.G. Gall, *Subnuclear organelles: new insights into form and function*. Trends Cell Biol, 2006. **16**(1): p. 19-26.
60. Dirks, R.W., et al., *Synthesis, processing, and transport of RNA within the three-dimensional context of the cell nucleus*. Crit Rev Eukaryot Gene Expr, 1999. **9**(3-4): p. 191-201.
61. Gerbi, S.A., A.V. Borovjagin, and T.S. Lange, *The nucleolus: a site of ribonucleoprotein maturation*. Curr Opin Cell Biol, 2003. **15**(3): p. 318-25.
62. Olson, M.O., K. Hingorani, and A. Szebeni, *Conventional and nonconventional roles of the nucleolus*. Int Rev Cytol, 2002. **219**: p. 199-266.
63. Liu, J.L. and J.G. Gall, *U bodies are cytoplasmic structures that contain uridine-rich small nuclear ribonucleoproteins and associate with P bodies*. Proc Natl Acad Sci U S A, 2007. **104**(28): p. 11655-9.
64. Paule, M.R. and R.J. White, *Survey and summary: transcription by RNA polymerases I and III*. Nucleic Acids Res, 2000. **28**(6): p. 1283-98.
65. Krol, A., et al., *Xenopus tropicalis U6 snRNA genes transcribed by Pol III contain the upstream promoter elements used by Pol II dependent U snRNA genes*. Nucleic Acids Res, 1987. **15**(6): p. 2463-78.

66. Dahlberg, J.E. and E. Lund, *Structure and expression of U-snRNA genes*. Mol Biol Rep, 1987. **12**(3): p. 139-43.
67. Datta, B. and A.M. Weiner, *The phylogenetically invariant ACAGAGA and AGC sequences of U6 small nuclear RNA are more tolerant of mutation in human cells than in Saccharomyces cerevisiae*. Mol Cell Biol, 1993. **13**(9): p. 5377-82.
68. Liao, D., et al., *Concerted evolution of the tandemly repeated genes encoding human U2 snRNA (the RNU2 locus) involves rapid intrachromosomal homogenization and rare interchromosomal gene conversion*. Embo J, 1997. **16**(3): p. 588-98.
69. Van Arsdell, S.W. and A.M. Weiner, *Human genes for U2 small nuclear RNA are tandemly repeated*. Mol Cell Biol, 1984. **4**(3): p. 492-9.
70. Lund, E. and J.E. Dahlberg, *True genes for human U1 small nuclear RNA. Copy number, polymorphism, and methylation*. J Biol Chem, 1984. **259**(3): p. 2013-21.
71. Bark, C., et al., *Genes for human U4 small nuclear RNA*. Gene, 1986. **50**(1-3): p. 333-44.
72. Domitrovich, A.M. and G.R. Kunkel, *Multiple, dispersed human U6 small nuclear RNA genes with varied transcriptional efficiencies*. Nucleic Acids Res, 2003. **31**(9): p. 2344-52.
73. Eliceiri, G.L. and M.S. Sayavedra, *Small RNAs in the nucleus and cytoplasm of HeLa cells*. Biochem Biophys Res Commun, 1976. **72**(2): p. 507-12.
74. Wieben, E.D., J.M. Nenner, and T. Pederson, *Ribonucleoprotein organization of eukaryotic RNA. XXXII. U2 small nuclear RNA precursors and their accurate 3' processing in vitro as ribonucleoprotein particles*. J Mol Biol, 1985. **183**(1): p. 69-78.
75. Visa, N., et al., *A nuclear cap-binding complex binds Balbiani ring pre-mRNA cotranscriptionally and accompanies the ribonucleoprotein particle during nuclear export*. J Cell Biol, 1996. **133**(1): p. 5-14.
76. Gornemann, J., et al., *Cotranscriptional spliceosome assembly occurs in a stepwise fashion and requires the cap binding complex*. Mol Cell, 2005. **19**(1): p. 53-63.
77. Ford, E., M. Strubin, and N. Hernandez, *The Oct-1 POU domain activates snRNA gene transcription by contacting a region in the SNAPc largest subunit that bears sequence similarities to the Oct-1 coactivator OBF-1*. Genes Dev, 1998. **12**(22): p. 3528-40.
78. Wendelburg, B.J. and W.F. Marzluff, *Two promoter elements are necessary and sufficient for expression of the sea urchin U1 snRNA gene*. Nucleic Acids Res, 1992. **20**(14): p. 3743-51.
79. Ma, B. and N. Hernandez, *A map of protein-protein contacts within the small nuclear RNA-activating protein complex SNAPc*. J Biol Chem, 2001. **276**(7): p. 5027-35.
80. Mittal, V., et al., *The Oct-1 POU-specific domain can stimulate small nuclear RNA gene transcription by stabilizing the basal transcription complex SNAPc*. Mol Cell Biol, 1996. **16**(5): p. 1955-65.
81. Janson, L. and U. Pettersson, *Transcription factor requirements for U2 snRNA-encoding gene activation in B lymphoid cells*. Gene, 1991. **109**(2): p. 297-301.
82. Forsberg, M., et al., *Activation functions of transcription factor Sp1 at U2 snRNA and TATA box promoters*. Biol Chem Hoppe Seyler, 1995. **376**(11): p. 661-9.
83. Korf, G.M., I.W. Botros, and W.E. Stumph, *Developmental and tissue-specific expression of U4 small nuclear RNA genes*. Mol Cell Biol, 1988. **8**(12): p. 5566-9.
84. Caceres, J.F., et al., *Control of mouse U1a and U1b snRNA gene expression by differential transcription*. Nucleic Acids Res, 1992. **20**(16): p. 4247-54.

85. Howard, E.F., et al., *Functional, developmentally expressed genes for mouse U1a and U1b snRNAs contain both conserved and non-conserved transcription signals*. Nucleic Acids Res, 1986. **14**(24): p. 9811-25.
86. Cuello, P., et al., *Transcription of the human U2 snRNA genes continues beyond the 3' box in vivo*. Embo J, 1999. **18**(10): p. 2867-77.
87. Hernandez, N. and A.M. Weiner, *Formation of the 3' end of U1 snRNA requires compatible snRNA promoter elements*. Cell, 1986. **47**(2): p. 249-58.
88. Hernandez, N. and R. Lucito, *Elements required for transcription initiation of the human U2 snRNA gene coincide with elements required for snRNA 3' end formation*. Embo J, 1988. **7**(10): p. 3125-34.
89. Mattaj, I.W. and R. Zeller, *Xenopus laevis U2 snRNA genes: tandemly repeated transcription units sharing 5' and 3' flanking homology with other RNA polymerase II transcribed genes*. Embo J, 1983. **2**(11): p. 1883-91.
90. Hernandez, N., *Formation of the 3' end of U1 snRNA is directed by a conserved sequence located downstream of the coding region*. Embo J, 1985. **4**(7): p. 1827-37.
91. Yuo, C.Y., M. Ares, Jr., and A.M. Weiner, *Sequences required for 3' end formation of human U2 small nuclear RNA*. Cell, 1985. **42**(1): p. 193-202.
92. Baillat, D., et al., *Integrator, a multiprotein mediator of small nuclear RNA processing, associates with the C-terminal repeat of RNA polymerase II*. Cell, 2005. **123**(2): p. 265-76.
93. Jacobs, E.Y., I. Ogiwara, and A.M. Weiner, *Role of the C-terminal domain of RNA polymerase II in U2 snRNA transcription and 3' processing*. Mol Cell Biol, 2004. **24**(2): p. 846-55.
94. Uguen, P. and S. Murphy, *The 3' ends of human pre-snRNAs are produced by RNA polymerase II CTD-dependent RNA processing*. Embo J, 2003. **22**(17): p. 4544-54.
95. Medlin, J.E., et al., *The C-terminal domain of pol II and a DRB-sensitive kinase are required for 3' processing of U2 snRNA*. Embo J, 2003. **22**(4): p. 925-34.
96. Egloff, S., et al., *Serine-7 of the RNA polymerase II CTD is specifically required for snRNA gene expression*. Science, 2007. **318**(5857): p. 1777-9.
97. Gall, J.G., et al., *Histone genes are located at the sphere loci of newt lampbrush chromosomes*. Chromosoma, 1981. **84**(2): p. 159-71.
98. Callan, H.G., J.G. Gall, and C. Murphy, *Histone genes are located at the sphere loci of Xenopus lampbrush chromosomes*. Chromosoma, 1991. **101**(4): p. 245-51.
99. Frey, M.R. and A.G. Matera, *Coiled bodies contain U7 small nuclear RNA and associate with specific DNA sequences in interphase human cells*. Proc Natl Acad Sci U S A, 1995. **92**(13): p. 5915-9.
100. Liu, J.L., et al., *The Drosophila melanogaster Cajal body*. J Cell Biol, 2006. **172**(6): p. 875-84.
101. Schul, W., et al., *Coiled bodies are predisposed to a spatial association with genes that contain snoRNA sequences in their introns*. J Cell Biochem, 1999. **75**(3): p. 393-403.
102. Gao, L., M.R. Frey, and A.G. Matera, *Human genes encoding U3 snRNA associate with coiled bodies in interphase cells and are clustered on chromosome 17p11.2 in a complex inverted repeat structure*. Nucleic Acids Res, 1997. **25**(23): p. 4740-7.
103. Matera, A.G. and D.C. Ward, *Nucleoplasmic organization of small nuclear ribonucleoproteins in cultured human cells*. J Cell Biol, 1993. **121**(4): p. 715-27.

104. Smith, K.P. and J.B. Lawrence, *Interactions of U2 gene loci and their nuclear transcripts with Cajal (coiled) bodies: evidence for PreU2 within Cajal bodies*. Mol Biol Cell, 2000. **11**(9): p. 2987-98.
105. Jacobs, E.Y., et al., *Coiled bodies preferentially associate with U4, U11, and U12 small nuclear RNA genes in interphase HeLa cells but not with U6 and U7 genes*. Mol Biol Cell, 1999. **10**(5): p. 1653-63.
106. Dimario, P.J., *Cell and molecular biology of nucleolar assembly and disassembly*. Int Rev Cytol, 2004. **239**: p. 99-178.
107. Raska, I., et al., *Association between the nucleolus and the coiled body*. J Struct Biol, 1990. **104**(1-3): p. 120-7.
108. Frey, M.R. and A.G. Matera, *RNA-mediated interaction of Cajal bodies and U2 snRNA genes*. J Cell Biol, 2001. **154**(3): p. 499-509.
109. Frey, M.R., et al., *Association of snRNA genes with coiled bodies is mediated by nascent snRNA transcripts*. Curr Biol, 1999. **9**(3): p. 126-35.
110. Marzluff, W.F., *Metazoan replication-dependent histone mRNAs: a distinct set of RNA polymerase II transcripts*. Curr Opin Cell Biol, 2005. **17**(3): p. 274-80.
111. Shopland, L.S., et al., *Replication-dependent histone gene expression is related to Cajal body (CB) association but does not require sustained CB contact*. Mol Biol Cell, 2001. **12**(3): p. 565-76.
112. Schul, W., R. van Driel, and L. de Jong, *Coiled bodies and U2 snRNA genes adjacent to coiled bodies are enriched in factors required for snRNA transcription*. Mol Biol Cell, 1998. **9**(5): p. 1025-36.
113. Rodriguez, M.S., C. Dargemont, and F. Stutz, *Nuclear export of RNA*. Biol Cell, 2004. **96**(8): p. 639-55.
114. Izaurralde, E., et al., *A cap-binding protein complex mediating U snRNA export*. Nature, 1995. **376**(6542): p. 709-12.
115. Izaurralde, E., et al., *A cap binding protein that may mediate nuclear export of RNA polymerase II-transcribed RNAs*. J Cell Biol, 1992. **118**(6): p. 1287-95.
116. Segref, A., I.W. Mattaj, and M. Ohno, *The evolutionarily conserved region of the U snRNA export mediator PHAX is a novel RNA-binding domain that is essential for U snRNA export*. Rna, 2001. **7**(3): p. 351-60.
117. Ohno, M., et al., *PHAX, a mediator of U snRNA nuclear export whose activity is regulated by phosphorylation*. Cell, 2000. **101**(2): p. 187-98.
118. Lemm, I., et al., *Ongoing U snRNP biogenesis is required for the integrity of Cajal bodies*. Mol Biol Cell, 2006. **17**(7): p. 3221-31.
119. Watkins, N.J., et al., *Assembly and maturation of the U3 snoRNP in the nucleoplasm in a large dynamic multiprotein complex*. Mol Cell, 2004. **16**(5): p. 789-98.
120. Boulon, S., et al., *PHAX and CRM1 are required sequentially to transport U3 snoRNA to nucleoli*. Mol Cell, 2004. **16**(5): p. 777-87.
121. Yu, Y.T., et al., *Internal modification of U2 small nuclear (sn)RNA occurs in nucleoli of Xenopus oocytes*. J Cell Biol, 2001. **152**(6): p. 1279-88.
122. Callan, H.G. and J.G. Gall, *Association of RNA with the B and C snurposomes of Xenopus oocyte nuclei*. Chromosoma, 1991. **101**(2): p. 69-82.
123. Zieve, G.W., R.A. Sauterer, and R.J. Feeney, *Newly synthesized small nuclear RNAs appear transiently in the cytoplasm*. J Mol Biol, 1988. **199**(2): p. 259-67.



124. Kohler, A. and E. Hurt, *Exporting RNA from the nucleus to the cytoplasm*. Nat Rev Mol Cell Biol, 2007. **8**(10): p. 761-73.
125. Eliceiri, G.L., *Short-lived, small RNAs in the cytoplasm of HeLa cells*. Cell, 1974. **3**(1): p. 11-4.
126. Eliceiri, G.L. and T. Gurney, Jr., *Subcellular location of precursors to small nuclear RNA species C and D and of newly synthesized 5 S RNA in HeLa cells*. Biochem Biophys Res Commun, 1978. **81**(3): p. 915-9.
127. Kitao, S., et al., *A compartmentalized phosphorylation/dephosphorylation system that regulates U snRNA export from the nucleus*. Mol Cell Biol, 2007.
128. Kolb, S.J., D.J. Battle, and G. Dreyfuss, *Molecular functions of the SMN complex*. J Child Neurol, 2007. **22**(8): p. 990-4.
129. Battle, D.J., et al., *The SMN complex: an assembly machine for RNPs*. Cold Spring Harb Symp Quant Biol, 2006. **71**: p. 313-20.
130. Matera, A.G. and K.B. Shpargel, *Pumping RNA: nuclear bodybuilding along the RNP pipeline*. Curr Opin Cell Biol, 2006. **18**(3): p. 317-24.
131. Pellizzoni, L., *Chaperoning ribonucleoprotein biogenesis in health and disease*. EMBO Rep, 2007. **8**(4): p. 340-5.
132. Carrel, T.L., et al., *Survival motor neuron function in motor axons is independent of functions required for small nuclear ribonucleoprotein biogenesis*. J Neurosci, 2006. **26**(43): p. 11014-22.
133. Sumner, C.J., *Molecular mechanisms of spinal muscular atrophy*. J Child Neurol, 2007. **22**(8): p. 979-89.
134. Massenet, S., et al., *The SMN complex is associated with snRNPs throughout their cytoplasmic assembly pathway*. Mol Cell Biol, 2002. **22**(18): p. 6533-41.
135. Narayanan, U., et al., *SMN, the spinal muscular atrophy protein, forms a pre-import snRNP complex with snurportin1 and importin beta*. Hum Mol Genet, 2002. **11**(15): p. 1785-95.
136. Raker, V.A., G. Plessel, and R. Luhrmann, *The snRNP core assembly pathway: identification of stable core protein heteromeric complexes and an snRNP subcore particle in vitro*. Embo J, 1996. **15**(9): p. 2256-69.
137. Peng, R. and D. Gallwitz, *Multiple SNARE interactions of an SM protein: Sed5p/Sly1p binding is dispensable for transport*. Embo J, 2004. **23**(20): p. 3939-49.
138. Pellizzoni, L., J. Yong, and G. Dreyfuss, *Essential role for the SMN complex in the specificity of snRNP assembly*. Science, 2002. **298**(5599): p. 1775-9.
139. Battle, D.J., et al., *The Gemin5 protein of the SMN complex identifies snRNAs*. Mol Cell, 2006. **23**(2): p. 273-9.
140. Yong, J., L. Pellizzoni, and G. Dreyfuss, *Sequence-specific interaction of U1 snRNA with the SMN complex*. Embo J, 2002. **21**(5): p. 1188-96.
141. Cote, J. and S. Richard, *Tudor domains bind symmetrical dimethylated arginines*. J Biol Chem, 2005. **280**(31): p. 28476-83.
142. Selenko, P., et al., *SMN tudor domain structure and its interaction with the Sm proteins*. Nat Struct Biol, 2001. **8**(1): p. 27-31.
143. Sprangers, R., et al., *High-resolution X-ray and NMR structures of the SMN Tudor domain: conformational variation in the binding site for symmetrically dimethylated arginine residues*. J Mol Biol, 2003. **327**(2): p. 507-20.

144. Sprangers, R., et al., *Definition of domain boundaries and crystallization of the SMN Tudor domain*. Acta Crystallogr D Biol Crystallogr, 2003. **59**(Pt 2): p. 366-8.
145. Wang, J. and G. Dreyfuss, *Characterization of functional domains of the SMN protein in vivo*. J Biol Chem, 2001. **276**(48): p. 45387-93.
146. Ma, Y., et al., *The Gemin6-Gemin7 heterodimer from the survival of motor neurons complex has an Sm protein-like structure*. Structure, 2005. **13**(6): p. 883-92.
147. Otter, S., et al., *A comprehensive interaction map of the human survival of motor neuron (SMN) complex*. J Biol Chem, 2007. **282**(8): p. 5825-33.
148. Meister, G., et al., *Methylation of Sm proteins by a complex containing PRMT5 and the putative U snRNP assembly factor pICln*. Curr Biol, 2001. **11**(24): p. 1990-4.
149. Friesen, W.J., et al., *The methylosome, a 20S complex containing JBP1 and pICln, produces dimethylarginine-modified Sm proteins*. Mol Cell Biol, 2001. **21**(24): p. 8289-300.
150. Branscombe, T.L., et al., *PRMT5 (Janus kinase-binding protein 1) catalyzes the formation of symmetric dimethylarginine residues in proteins*. J Biol Chem, 2001. **276**(35): p. 32971-6.
151. Gonsalvez, G.B., et al., *The Sm-protein methyltransferase, dart5, is essential for germ-cell specification and maintenance*. Curr Biol, 2006. **16**(11): p. 1077-89.
152. Gonsalvez, G.B., et al., *Two distinct arginine methyltransferases are required for biogenesis of Sm-class ribonucleoproteins*. J Cell Biol, 2007. **178**(5): p. 733-40.
153. Lee, J.H., et al., *PRMT7, a new protein arginine methyltransferase that synthesizes symmetric dimethylarginine*. J Biol Chem, 2005. **280**(5): p. 3656-64.
154. Cook, J.R., et al., *FBXO11/PRMT9, a new protein arginine methyltransferase, symmetrically dimethylates arginine residues*. Biochem Biophys Res Commun, 2006. **342**(2): p. 472-81.
155. Miranda, T.B., et al., *Spliceosome Sm proteins D1, D3, and B/B' are asymmetrically dimethylated at arginine residues in the nucleus*. Biochem Biophys Res Commun, 2004. **323**(2): p. 382-7.
156. Cheng, D., et al., *The arginine methyltransferase CARM1 regulates the coupling of transcription and mRNA processing*. Mol Cell, 2007. **25**(1): p. 71-83.
157. Brahm, H., et al., *Symmetrical dimethylation of arginine residues in spliceosomal Sm protein B/B' and the Sm-like protein LSm4, and their interaction with the SMN protein*. Rna, 2001. **7**(11): p. 1531-42.
158. Khusial, P.R., K. Vaidya, and G.W. Zieve, *The symmetrical dimethylarginine post-translational modification of the SmD3 protein is not required for snRNP assembly and nuclear transport*. Biochem Biophys Res Commun, 2005. **337**(4): p. 1119-24.
159. Mouaikel, J., et al., *Interaction between the small-nuclear-RNA cap hypermethylase and the spinal muscular atrophy protein, survival of motor neuron*. EMBO Rep, 2003. **4**(6): p. 616-22.
160. Plessel, G., U. Fischer, and R. Luhrmann, *m3G cap hypermethylation of U1 small nuclear ribonucleoprotein (snRNP) in vitro: evidence that the U1 small nuclear RNA-(guanosine-N2)-methyltransferase is a non-snRNP cytoplasmic protein that requires a binding site on the Sm core domain*. Mol Cell Biol, 1994. **14**(6): p. 4160-72.
161. Jady, B.E., et al., *Modification of Sm small nuclear RNAs occurs in the nucleoplasmic Cajal body following import from the cytoplasm*. Embo J, 2003. **22**(8): p. 1878-88.

162. Seipelt, R.L., et al., *U1 snRNA is cleaved by RNase III and processed through an Sm site-dependent pathway*. Nucleic Acids Res, 1999. **27**(2): p. 587-95.
163. Huang, Q. and T. Pederson, *A human U2 RNA mutant stalled in 3' end processing is impaired in nuclear import*. Nucleic Acids Res, 1999. **27**(4): p. 1025-31.
164. Kleinschmidt, A.M. and T. Pederson, *Accurate and efficient 3' processing of U2 small nuclear RNA precursor in a fractionated cytoplasmic extract*. Mol Cell Biol, 1987. **7**(9): p. 3131-7.
165. Mattaj, I.W. and E.M. De Robertis, *Nuclear segregation of U2 snRNA requires binding of specific snRNP proteins*. Cell, 1985. **40**(1): p. 111-8.
166. Madore, S.J., et al., *Precursors of U4 small nuclear RNA*. J Cell Biol, 1984. **99**(3): p. 1140-4.
167. Madore, S.J., E.D. Wieben, and T. Pederson, *Intracellular site of U1 small nuclear RNA processing and ribonucleoprotein assembly*. J Cell Biol, 1984. **98**(1): p. 188-92.
168. van Hoof, A., P. Lennertz, and R. Parker, *Yeast exosome mutants accumulate 3'-extended polyadenylated forms of U4 small nuclear RNA and small nucleolar RNAs*. Mol Cell Biol, 2000. **20**(2): p. 441-52.
169. Zhou, D., D. Frendewey, and S.M. Lobo Ruppert, *Pac1p, an RNase III homolog, is required for formation of the 3' end of U2 snRNA in Schizosaccharomyces pombe*. Rna, 1999. **5**(8): p. 1083-98.
170. Huang, Q., M.R. Jacobson, and T. Pederson, *3' processing of human pre-U2 small nuclear RNA: a base-pairing interaction between the 3' extension of the precursor and an internal region*. Mol Cell Biol, 1997. **17**(12): p. 7178-85.
171. Yang, H., et al., *Nuclear processing of the 3'-terminal nucleotides of pre-U1 RNA in Xenopus laevis oocytes*. Mol Cell Biol, 1992. **12**(4): p. 1553-60.
172. Espert, L., et al., *The exonuclease ISG20 mainly localizes in the nucleolus and the Cajal (Coiled) bodies and is associated with nuclear SMN protein-containing complexes*. J Cell Biochem, 2006. **98**(5): p. 1320-33.
173. Marshallsay, C., et al., *In vitro and in vivo evidence that protein and U1 snRNP nuclear import in somatic cells differ in their requirement for GTP-hydrolysis, Ran/TC4 and RCC1*. Nucleic Acids Res, 1996. **24**(10): p. 1829-36.
174. Fischer, U., et al., *Nucleo-cytoplasmic transport of U snRNPs: definition of a nuclear location signal in the Sm core domain that binds a transport receptor independently of the m3G cap*. Embo J, 1993. **12**(2): p. 573-83.
175. Palacios, I., et al., *Nuclear import of U snRNPs requires importin beta*. Embo J, 1997. **16**(22): p. 6783-92.
176. Rollenhagen, C. and N. Pante, *Nuclear import of spliceosomal snRNPs*. Can J Physiol Pharmacol, 2006. **84**(3-4): p. 367-76.
177. Wohlwend, D., et al., *Structural basis for RanGTP independent entry of spliceosomal U snRNPs into the nucleus*. J Mol Biol, 2007. **374**(4): p. 1129-38.
178. Huber, J., A. Dickmanns, and R. Luhrmann, *The importin-beta binding domain of snurportin1 is responsible for the Ran- and energy-independent nuclear import of spliceosomal U snRNPs in vitro*. J Cell Biol, 2002. **156**(3): p. 467-79.
179. Narayanan, U., et al., *Coupled in vitro import of U snRNPs and SMN, the spinal muscular atrophy protein*. Mol Cell, 2004. **16**(2): p. 223-34.
180. Hebert, M.D., et al., *Coilin forms the bridge between Cajal bodies and SMN, the spinal muscular atrophy protein*. Genes Dev, 2001. **15**(20): p. 2720-9.

181. Bellini, M. and J.G. Gall, *Coilin shuttles between the nucleus and cytoplasm in Xenopus oocytes*. Mol Biol Cell, 1999. **10**(10): p. 3425-34.
182. Bauer, D.W. and J.G. Gall, *Coiled bodies without coilin*. Mol Biol Cell, 1997. **8**(1): p. 73-82.
183. Tucker, K.E., et al., *Residual Cajal bodies in coilin knockout mice fail to recruit Sm snRNPs and SMN, the spinal muscular atrophy gene product*. J Cell Biol, 2001. **154**(2): p. 293-307.
184. Yu, Y.T., M.D. Shu, and J.A. Steitz, *Modifications of U2 snRNA are required for snRNP assembly and pre-mRNA splicing*. Embo J, 1998. **17**(19): p. 5783-95.
185. Zhao, X., et al., *An H/ACA guide RNA directs U2 pseudouridylation at two different sites in the branchpoint recognition region in Xenopus oocytes*. Rna, 2002. **8**(12): p. 1515-25.
186. Nesic, D., G. Tanackovic, and A. Kramer, *A role for Cajal bodies in the final steps of U2 snRNP biogenesis*. J Cell Sci, 2004. **117**(Pt 19): p. 4423-33.
187. Schaffert, N., et al., *RNAi knockdown of hPrp31 leads to an accumulation of U4/U6 di-snRNPs in Cajal bodies*. Embo J, 2004. **23**(15): p. 3000-9.
188. Stanek, D., et al., *Targeting of U4/U6 small nuclear RNP assembly factor SART3/p110 to Cajal bodies*. J Cell Biol, 2003. **160**(4): p. 505-16.
189. Klingauf, M., D. Stanek, and K.M. Neugebauer, *Enhancement of U4/U6 small nuclear ribonucleoprotein particle association in Cajal bodies predicted by mathematical modeling*. Mol Biol Cell, 2006. **17**(12): p. 4972-81.
190. Mattaj, I.W., et al., *Changing the RNA polymerase specificity of U snRNA gene promoters*. Cell, 1988. **55**(3): p. 435-42.
191. Lobo, S.M. and N. Hernandez, *A 7 bp mutation converts a human RNA polymerase II snRNA promoter into an RNA polymerase III promoter*. Cell, 1989. **58**(1): p. 55-67.
192. Lescure, A., P. Carbon, and A. Krol, *The different positioning of the proximal sequence element in the Xenopus RNA polymerase II and III snRNA promoters is a key determinant which confers RNA polymerase III specificity*. Nucleic Acids Res, 1991. **19**(3): p. 435-41.
193. Bernues, J., et al., *Common and unique transcription factor requirements of human U1 and U6 snRNA genes*. Embo J, 1993. **12**(9): p. 3573-85.
194. Cabart, P. and S. Murphy, *BRFU, a TFIIB-like factor, is directly recruited to the TATA-box of polymerase III small nuclear RNA gene promoters through its interaction with TATA-binding protein*. J Biol Chem, 2001. **276**(46): p. 43056-64.
195. Geiduschek, E.P. and G.A. Kassavetis, *Comparing transcriptional initiation by RNA polymerases I and III*. Curr Opin Cell Biol, 1995. **7**(3): p. 344-51.
196. Olson, B.L. and P.G. Siliciano, *A diverse set of nuclear RNAs transfer between nuclei of yeast heterokaryons*. Yeast, 2003. **20**(10): p. 893-903.
197. Fury, M.G. and G.W. Zieve, *U6 snRNA maturation and stability*. Exp Cell Res, 1996. **228**(1): p. 160-3.
198. Bhattacharya, R., et al., *Methylphosphate cap structure in small RNAs reduces the affinity of RNAs to La protein*. Gene Expr, 2002. **10**(5-6): p. 243-53.
199. Dong, G., et al., *Structure of the La motif: a winged helix domain mediates RNA binding via a conserved aromatic patch*. Embo J, 2004. **23**(5): p. 1000-7.
200. Wolin, S.L. and T. Cedervall, *The La protein*. Annu Rev Biochem, 2002. **71**: p. 375-403.
201. Trippe, R., et al., *Identification, cloning, and functional analysis of the human U6 snRNA-specific terminal uridylyl transferase*. Rna, 2006. **12**(8): p. 1494-504.

202. Trippe, R., H. Richly, and B.J. Benecke, *Biochemical characterization of a U6 small nuclear RNA-specific terminal uridylyltransferase*. Eur J Biochem, 2003. **270**(5): p. 971-80.
203. Trippe, R., B. Sandrock, and B.J. Benecke, *A highly specific terminal uridylyl transferase modifies the 3'-end of U6 small nuclear RNA*. Nucleic Acids Res, 1998. **26**(13): p. 3119-26.
204. Booth, B.L., Jr. and B.F. Pugh, *Identification and characterization of a nuclease specific for the 3' end of the U6 small nuclear RNA*. J Biol Chem, 1997. **272**(2): p. 984-91.
205. Gu, J., et al., *Formation of 2',3'-cyclic phosphates at the 3' end of human U6 small nuclear RNA in vitro. Identification of 2',3'-cyclic phosphates at the 3' ends of human signal recognition particle and mitochondrial RNA processing RNAs*. J Biol Chem, 1997. **272**(35): p. 21989-93.
206. Shimba, S. and R. Reddy, *Purification of human U6 small nuclear RNA capping enzyme. Evidence for a common capping enzyme for gamma-monomethyl-capped small RNAs*. J Biol Chem, 1994. **269**(17): p. 12419-23.
207. Terns, M.P., E. Lund, and J.E. Dahlberg, *3'-end-dependent formation of U6 small nuclear ribonucleoprotein particles in Xenopus laevis oocyte nuclei*. Mol Cell Biol, 1992. **12**(7): p. 3032-40.
208. Tycowski, K.T., et al., *Modification of U6 spliceosomal RNA is guided by other small RNAs*. Mol Cell, 1998. **2**(5): p. 629-38.
209. Ganot, P., et al., *Nucleolar factors direct the 2'-O-ribose methylation and pseudouridylation of U6 spliceosomal RNA*. Mol Cell Biol, 1999. **19**(10): p. 6906-17.
210. Lange, T.S. and S.A. Gerbi, *Transient nucleolar localization Of U6 small nuclear RNA in Xenopus Laevis oocytes*. Mol Biol Cell, 2000. **11**(7): p. 2419-28.
211. Nottrott, S., H. Urlaub, and R. Luhrmann, *Hierarchical, clustered protein interactions with U4/U6 snRNA: a biochemical role for U4/U6 proteins*. Embo J, 2002. **21**(20): p. 5527-38.
212. Bell, M., et al., *p110, a novel human U6 snRNP protein and U4/U6 snRNP recycling factor*. Embo J, 2002. **21**(11): p. 2724-35.
213. Rader, S.D. and C. Guthrie, *A conserved Lsm-interaction motif in Prp24 required for efficient U4/U6 di-snRNP formation*. Rna, 2002. **8**(11): p. 1378-92.
214. Gerbi, S.A. and T.S. Lange, *All small nuclear RNAs (snRNAs) of the [U4/U6.U5] Tri-snRNP localize to nucleoli; Identification of the nucleolar localization element of U6 snRNA*. Mol Biol Cell, 2002. **13**(9): p. 3123-37.
215. Gall, J.G., et al., *Assembly of the nuclear transcription and processing machinery: Cajal bodies (coiled bodies) and transcriptosomes*. Mol Biol Cell, 1999. **10**(12): p. 4385-402.
216. Collins, C.A. and C. Guthrie, *The question remains: is the spliceosome a ribozyme?* Nat Struct Biol, 2000. **7**(10): p. 850-4.
217. Valadkhan, S., *snRNAs as the catalysts of pre-mRNA splicing*. Curr Opin Chem Biol, 2005. **9**(6): p. 603-8.
218. Valadkhan, S., *The spliceosome: caught in a web of shifting interactions*. Curr Opin Struct Biol, 2007. **17**(3): p. 310-5.
219. Calvet, J.P., L.M. Meyer, and T. Pederson, *Small nuclear RNA U2 is base-paired to heterogeneous nuclear RNA*. Science, 1982. **217**(4558): p. 456-8.

220. Calvet, J.P. and T. Pederson, *Base-pairing interactions between small nuclear RNAs and nuclear RNA precursors as revealed by psoralen cross-linking in vivo*. Cell, 1981. **26**(3 Pt 1): p. 363-70.
221. Ast, G. and A.M. Weiner, *A novel U1/U5 interaction indicates proximity between U1 and U5 snRNAs during an early step of mRNA splicing*. Rna, 1997. **3**(4): p. 371-81.
222. Wassarman, D.A. and J.A. Steitz, *A base-pairing interaction between U2 and U6 small nuclear RNAs occurs in > 150S complexes in HeLa cell extracts: implications for the spliceosome assembly pathway*. Proc Natl Acad Sci U S A, 1993. **90**(15): p. 7139-43.
223. Wassarman, D.A. and J.A. Steitz, *Interactions of small nuclear RNA's with precursor messenger RNA during in vitro splicing*. Science, 1992. **257**(5078): p. 1918-25.
224. Datta, B. and A.M. Weiner, *Genetic evidence for base pairing between U2 and U6 snRNA in mammalian mRNA splicing*. Nature, 1991. **352**(6338): p. 821-4.
225. Hausner, T.P., L.M. Giglio, and A.M. Weiner, *Evidence for base-pairing between mammalian U2 and U6 small nuclear ribonucleoprotein particles*. Genes Dev, 1990. **4**(12A): p. 2146-56.
226. Rinke, J., et al., *Localization of a base-paired interaction between small nuclear RNAs U4 and U6 in intact U4/U6 ribonucleoprotein particles by psoralen cross-linking*. J Mol Biol, 1985. **185**(4): p. 721-31.
227. Donmez, G., K. Hartmuth, and R. Luhrmann, *Modified nucleotides at the 5' end of human U2 snRNA are required for spliceosomal E-complex formation*. Rna, 2004. **10**(12): p. 1925-33.
228. Azubel, M., et al., *Three-dimensional structure of the native spliceosome by cryo-electron microscopy*. Mol Cell, 2004. **15**(5): p. 833-9.
229. Neugebauer, K.M., *On the importance of being co-transcriptional*. J Cell Sci, 2002. **115**(Pt 20): p. 3865-71.
230. Bentley, D.L., *Rules of engagement: co-transcriptional recruitment of pre-mRNA processing factors*. Curr Opin Cell Biol, 2005. **17**(3): p. 251-6.
231. Reed, R., *Coupling transcription, splicing and mRNA export*. Curr Opin Cell Biol, 2003. **15**(3): p. 326-31.
232. Beyer, A.L. and Y.N. Osheim, *Visualization of RNA transcription and processing*. Semin Cell Biol, 1991. **2**(2): p. 131-40.
233. Fong, N., et al., *A 10 residue motif at the C-terminus of the RNA pol II CTD is required for transcription, splicing and 3' end processing*. Embo J, 2003. **22**(16): p. 4274-82.
234. Bossi, E., M.S. Fabbrini, and A. Ceriotti, *Exogenous protein expression in Xenopus oocytes: basic procedures*. Methods Mol Biol, 2007. **375**: p. 107-31.
235. Gall, J.G., et al., *Structure in the amphibian germinal vesicle*. Exp Cell Res, 2004. **296**(1): p. 28-34.
236. Morgan, G.T., *Lampbrush chromosomes and associated bodies: new insights into principles of nuclear structure and function*. Chromosome Res, 2002. **10**(3): p. 177-200.
237. Beenders, B., et al., *Distribution of XCAP-E and XCAP-D2 in the Xenopus oocyte nucleus*. Chromosome Res, 2003. **11**(6): p. 549-64.
238. Morgan, G.T., *Lampbrush chromosomes and associated bodies: new insights into principles of nuclear structure and function*. Chromosome Research: An International Journal On the Molecular, Supramolecular and Evolutionary Aspects of Chromosome Biology, 2002. **10**(3): p. 177-200.

239. Pan, Z.-Q. and C. Prives, *Assembly of functional U1 and U2 human-amphibian hybrid snRNPs in Xenopus laevis oocytes*. Science (Wash. DC), 1988. **241**: p. 1328-1331.
240. Yu, Y.T., M.D. Shu, and J.A. Steitz, *Modifications of U2 snRNA are required for snRNP assembly and pre-mRNA splicing*. Embo J, 1998. **17**(19): p. 5783-95.
241. Wu, Z., et al., *Small nuclear ribonucleoproteins and heterogeneous nuclear ribonucleoproteins in the amphibian germinal vesicle: loops, spheres, and snurposomes*. Journal of Cell Biology, 1991. **113**: p. 465-483.
242. Grimm, C., B. Stefanovic, and D. Schumperli, *The low abundance of U7 snRNA is partly determined by its Sm binding site*. EMBO J., 1993. **12**: p. 1229-1238.
243. Stefanovic, B., et al., *Assembly, nuclear import and function of U7 snRNPs studied by microinjection of synthetic U7 RNA into Xenopus oocytes*. Nucleic Acids Res., 1995. **23**: p. 3141-3151.
244. Wu, C.-H., Herbert, C. Murphy, and J. Gall, G, *The Sm binding site targets U7 snRNA to coiled bodies (spheres) of amphibian oocytes*. RNA, 1996. **8**: p. 811-23.
245. Bellini, M. and J.G. Gall, *Coilin can form a complex with the U7 small ribonucleoprotein*. Molecular Biology of the Cell, 1998. **9**: p. 2987-3001.
246. Birchmeier, C., et al., *3' editing of mRNAs: sequence requirements and involvement of a 60-nucleotide RNA in maturation of histone mRNA precursors*. Proc Natl Acad Sci U S A, 1984. **81**(4): p. 1057-61.
247. Mowry, K., L and J. Steitz, A, *Identification of the human U7 snRNP as one of several factors in the 3' end maturation of histone pre-messenger RNAs*. Science, 1987. **238**: p. 1682-1687.
248. Birnstiel, M.L. and F.J. Schaufele, *Structure and function of minor snRNPs*, in *Structure and Function of Major and Minor Small Nuclear Ribonucleoproteins*, M.L. Birnstiel, Editor. 1988, Springer-Verlag: Berlin. p. 155-182.
249. Scharl, E. and J. Steitz, *The site of 3' end formation of histone messenger RNA is a fixed distance from the downstream element recognized by the U7 snRNP*. EMBO J, 1994. **13**(10): p. 2432-40.
250. Dominski, Z., et al., *A novel zinc finger protein is associated with U7 snRNP and interacts with the stem-loop binding protein in the histone pre-mRNP to stimulate 3'-end processing*. Genes and Development, 2002. **16**(1): p. 58-71.
251. Murphy, C., et al., *RNA polymerase III in Cajal bodies and lampbrush chromosomes of the Xenopus oocyte nucleus*. Mol Biol Cell, 2002. **13**(10): p. 3466-76.
252. Aguilera, A., *Cotranscriptional mRNP assembly: from the DNA to the nuclear pore*. Curr Opin Cell Biol, 2005. **17**(3): p. 242-50.
253. Stroupe, M.E., et al., *The three-dimensional architecture of the EJC core*. J Mol Biol, 2006. **360**(4): p. 743-9.
254. Bono, F., et al., *The crystal structure of the exon junction complex reveals how it maintains a stable grip on mRNA*. Cell, 2006. **126**(4): p. 713-25.
255. Kataoka, N. and G. Dreyfuss, *A simple whole cell lysate system for in vitro splicing reveals a stepwise assembly of the exon-exon junction complex*. J Biol Chem, 2004. **279**(8): p. 7009-13.
256. Degot, S., et al., *Association of the breast cancer protein MLN51 with the exon junction complex via its speckle localizer and RNA binding module*. J Biol Chem, 2004. **279**(32): p. 33702-15.

257. Pan, Z.Q., et al., *Oligonucleotide-targeted degradation of U1 and U2 snRNAs reveals differential interactions of simian virus 40 pre-mRNAs with snRNPs*. Nucleic Acids Res, 1989. **17**(16): p. 6553-68.
258. Segault, V., et al., *In vitro reconstitution of mammalian U2 and U5 snRNPs active in splicing: Sm proteins are functionally interchangeable and are essential for the formation of functional U2 and U5 snRNPs*. Embo J, 1995. **14**(16): p. 4010-21.
259. Kramer, A., et al., *The 5' terminus of the RNA moiety of U1 small nuclear ribonucleoprotein particles is required for the splicing of messenger RNA precursors*. Cell, 1984. **38**(1): p. 299-307.
260. Parker, R., P.G. Siliciano, and C. Guthrie, *Recognition of the TACTAAC box during mRNA splicing in yeast involves base pairing to the U2-like snRNA*. Cell, 1987. **49**(2): p. 229-39.
261. Wu, J. and J.L. Manley, *Mammalian pre-mRNA branch site selection by U2 snRNP involves base pairing*. Genes Dev, 1989. **3**(10): p. 1553-61.
262. Zhuang, Y. and A.M. Weiner, *A compensatory base change in human U2 snRNA can suppress a branch site mutation*. Genes Dev, 1989. **3**(10): p. 1545-52.
263. Du, H. and M. Rosbash, *Yeast U1 snRNP-pre-mRNA complex formation without U1snRNA-pre-mRNA base pairing*. Rna, 2001. **7**(1): p. 133-42.
264. Lacadie, S.A. and M. Rosbash, *Cotranscriptional spliceosome assembly dynamics and the role of U1 snRNA:5'ss base pairing in yeast*. Mol Cell, 2005. **19**(1): p. 65-75.
265. Rossi, F., et al., *Involvement of U1 small nuclear ribonucleoproteins (snRNP) in 5' splice site-U1 snRNP interaction*. J Biol Chem, 1996. **271**(39): p. 23985-91.
266. Patel, A.A. and J.A. Steitz, *Splicing double: insights from the second spliceosome*. Nature Review Molecular Cell Biology, 2003. **4**(12): p. 960-70.
267. Nelissen, R.L., et al., *The association of the U1-specific 70K and C proteins with U1 snRNPs is mediated in part by common U snRNP proteins*. Embo J, 1994. **13**(17): p. 4113-25.
268. Surowy, C.S., et al., *Direct, sequence-specific binding of the human U1-70K ribonucleoprotein antigen protein to loop I of U1 small nuclear RNA*. Mol Cell Biol, 1989. **9**(10): p. 4179-86.
269. Du, H. and M. Rosbash, *The U1 snRNP protein U1C recognizes the 5' splice site in the absence of base pairing*. Nature, 2002. **419**(6902): p. 86-90.
270. Wu, C.-H.H. and J.G. Gall, *U7 small nuclear RNA in C snurposomes of the Xenopus germinal vesicle*. Proc. Natl. Acad. Sci. USA, 1993. **90**: p. 6257-6259.
271. Tsvetkov, A., et al., *Transcription on lampbrush chromosome loops in the absence of U2 snRNA*. Molecular Biology of the Cell, 1992. **3**: p. 249-261.
272. Crispino, J.D., B.J. Blencowe, and P.A. Sharp, *Complementation by SR proteins of pre-mRNA splicing reactions depleted of U1 snRNP*. Science, 1994. **265**(5180): p. 1866-9.
273. Crispino, J.D., et al., *Cis-acting elements distinct from the 5' splice site promote U1-independent pre-mRNA splicing*. Rna, 1996. **2**(7): p. 664-73.
274. Lund, M. and J. Kjems, *Defining a 5' splice site by functional selection in the presence and absence of U1 snRNA 5' end*. Rna, 2002. **8**(2): p. 166-79.
275. Wilk, H.E., et al., *U1 SnRNP association with HnRNP involves an initial non-specific splice-site independent interaction of U1 SnRNP protein with HnRNA*. Mol Cell Biochem, 1991. **106**(1): p. 55-66.



276. Takagaki, Y. and J.L. Manley, *A polyadenylation factor subunit is the human homologue of the Drosophila suppressor of forked protein*. Nature, 1994. **372**(6505): p. 471-4.
277. Gall, J.G., et al., *Assembly of the nuclear transcription and processing machinery: Cajal bodies (coiled bodies) and transcriptosomes*. Mol Biol Cell, 1999. **10**(12): p. 4385-402.
278. Huang, S. and D.L. Spector, *Intron-dependent recruitment of pre-mRNA splicing factors to sites of transcription*. J Cell Biol, 1996. **133**(4): p. 719-32.
279. Chen, J.Y., et al., *Specific alterations of U1-C protein or U1 small nuclear RNA can eliminate the requirement of Prp28p, an essential DEAD box splicing factor*. Mol Cell, 2001. **7**(1): p. 227-32.
280. Forch, P., et al., *The splicing regulator TIA-1 interacts with U1-C to promote U1 snRNP recruitment to 5' splice sites*. Embo J, 2002. **21**(24): p. 6882-92.
281. Saitoh, N., et al., *Proteomic analysis of interchromatin granule clusters*. Mol Biol Cell, 2004. **15**(8): p. 3876-90.
282. Konforti, B.B. and M.M. Konarska, *U4/U5/U6 snRNP recognizes the 5' splice site in the absence of U2 snRNP*. Genes Dev, 1994. **8**(16): p. 1962-73.
283. Wyatt, J.R., E.J. Sontheimer, and J.A. Steitz, *Site-specific cross-linking of mammalian U5 snRNP to the 5' splice site before the first step of pre-mRNA splicing*. Genes Dev, 1992. **6**(12B): p. 2542-53.
284. Maroney, P.A., C.M. Romfo, and T.W. Nilsen, *Functional recognition of 5' splice site by U4/U6.U5 tri-snRNP defines a novel ATP-dependent step in early spliceosome assembly*. Mol Cell, 2000. **6**(2): p. 317-28.
285. Stevens, S.W., et al., *Composition and functional characterization of the yeast spliceosomal penta-snRNP*. Molecular Cell, 2002. **9**(1): p. 31-44.
286. Lund, E. and P.L. Paine, *Nonaqueous isolation of transcriptionally active nuclei from Xenopus oocytes*. Methods Enzymol, 1990. **181**: p. 36-43.
287. Paine, P.L., et al., *The oocyte nucleus isolated in oil retains in vivo structure and functions*. Biotechniques, 1992. **13**(2): p. 238-46.
288. Deryusheva, S. and J.G. Gall, *Dynamics of coilin in Cajal bodies of the Xenopus germinal vesicle*. Proc Natl Acad Sci U S A, 2004. **101**(14): p. 4810-4.
289. Gall, J.G., *The centennial of the Cajal body*. Nat Rev Mol Cell Biol, 2003. **4**(12): p. 975-80.
290. Handwerger, K.E., J.A. Cordero, and J.G. Gall, *Cajal bodies, nucleoli, and speckles in the Xenopus oocyte nucleus have a low-density, sponge-like structure*. Mol Biol Cell, 2005. **16**(1): p. 202-11.
291. Guacci, V., *Sister chromatid cohesion: the cohesin cleavage model does not ring true*. Genes Cells, 2007. **12**(6): p. 693-708.
292. Callan, H.G. *Recent work on the structure of cell nuclei*. in *Fine Structure of Cells: Symposium of the VIIIth Congress in Cell Biology, Leiden 1954*. 1955: Noordhof, Groningen.
293. Callan, H.G. and H.C. Macgregor, *Action of deoxyribonuclease on lampbrush chromosomes*. Nature, 1958. **181**(4621): p. 1479-80.
294. Gall, J.G., *Kinetics of deoxyribonuclease action on chromosomes*. Nature, 1963. **198**: p. 36-8.
295. Callan, H.G., *Chromosomes and nucleoli of the axolotl, Ambystoma mexicanum*. J Cell Sci, 1966. **1**(1): p. 85-108.

296. Poirier, M.G. and J.F. Marko, *Micromechanical studies of mitotic chromosomes*. *Curr Top Dev Biol*, 2003. **55**: p. 75-141.
297. Poirier, M.G. and J.F. Marko, *Micromechanical studies of mitotic chromosomes*. *J Muscle Res Cell Motil*, 2002. **23**(5-6): p. 409-31.
298. Kuznetsova, I.S., et al., *Evidence for the existence of satellite DNA-containing connection between metaphase chromosomes*. *J Cell Biochem*, 2007. **101**(4): p. 1046-61.
299. Tsvetkov, A., et al., *Transcription on lampbrush chromosome loops in the absence of U2 snRNA*. *Mol Biol Cell*, 1992. **3**(3): p. 249-61.
300. Bellini, M. and J.G. Gall, *Coilin can form a complex with the U7 small nuclear ribonucleoprotein*. *Mol Biol Cell*, 1998. **9**(10): p. 2987-3001.
301. Paine, P.L., et al., *The oocyte nucleus isolated in oil retains in vivo structure and functions*. *BioTechniques*, 1992. **13**(2): p. 238-245.

## CURRICULUM VITAE

Snehal B. Patel

101 W Park St Apt 201, Urbana, IL 61801 ~ sbpatel@illinois.edu ~ 901-289-7833

### Education

- 1997-2001 Vanderbilt University, Nashville, TN  
Bachelor of Engineering, biomedical engineering/mathematics
- 2002-2011 University of Illinois, Urbana-Champaign, IL  
Doctor of Philosophy, biochemistry (expected graduation December 2010)  
Doctor of Medicine (expected graduation May 2011)

### Publications

- Patel, S.B., N. Novikova, M. Bellini. *Splicing-independent recruitment of spliceosomal small nuclear RNPs to nascent RNA polymerase II transcripts*. J. Cell Biol. 2007. **178**(6). p. 937-49.
- Patel, S.B., N. Novikova, B. Beenders, C. Austin, M. Bellini. *Live images of RNA polymerase II transcription units*. Chromosome Res. 2008. **16**(2). p. 223-32.
- Patel, S.B., M. Bellini. *The assembly of a spliceosomal small nuclear ribonucleoprotein particle*. Nucleic Acids Res. 2008. **36**(20). p. 6482-93.

### Selected Talks

- Patel, S.B., N. Novikova, M. Bellini. *Splicing-independent recruitment of spliceosomal snRNPs to nascent transcripts*. American Society of Cell Biology. December 2007 Conference.

### Selected Poster Presentations

- Patel, S.B., N. Novikova, M. Bellini. Co-transcriptional assembly of export competent pre-mRNPs. American Society of Cell Biology. December 2008 Conference.

### Teaching

- Fall 2004. Molecular Genetics. Grading.
- Fall 2005. Molecular Genetics. Discussion sections/grading
- Spring 2006. Cells, Tissues, and Development. Discussion sections/grading.

### Volunteer Work

2002. MSP Fall Retreat. poster session chair.
2003. MSP Fall Retreat. co-chair.
2004. MSP Fall Retreat. MC.
2005. Biochemistry Audio/Visual weekly seminar chair.
2006. Summer. Habitat for Humanity. Organizing donated material.
2010. Spring break. Center for you Health. Worked in clinic seeing patients.

### Awards

- 2002-2003 Biochemistry Departmental fellowship
- 2005 Teaching Award